NASA TECHNICAL NOTE

NASA TN D-6656
c.1

NASA TN D-6656

A WIND-TUNNEL EVALUATION OF ANALYTICAL TECHNIQUES FOR PREDICTING STATIC STABILITY AND CONTROL CHARACTERISTICS OF FLEXIBLE AIRCRAFT

by Irving Abel

Langley Research Center
Hampton, Va. 23365

NATIONAL AERONAUTICS AND SPACE ADMINISTRATION • WASHINGTON, D. C. • MARCH 1972

1. Report No.	2. Government Accession No.	3. Recipient's Catalog No.
NASA TN D-6656		

4. Title and Subtitle
A WIND-TUNNEL EVALUATION OF ANALYTICAL TECHNIQUES FOR PREDICTING STATIC STABILITY AND CONTROL CHARACTERISTICS OF FLEXIBLE AIRCRAFT

5. Report Date March 1972

6. Performing Organization Code

7. Author(s)
Irving Abel

8. Performing Organization Report No. L-8105

9. Performing Organization Name and Address
NASA Langley Research Center
Hampton, Va. 23365

10. Work Unit No. 136-14-02-02

11. Contract or Grant No.

12. Sponsoring Agency Name and Address
National Aeronautics and Space Administration
Washington, D.C. 20546

13. Type of Report and Period Covered Technical Note

14. Sponsoring Agency Code

15. Supplementary Notes

16. Abstract

An experimental evaluation of analytical techniques for predicting certain stability and control characteristics of a large flexible aircraft is presented. Analytical methods based on both the modal approach and flexibility influence coefficients are developed to predict the aerodynamic characteristics of a flexible airplane. These methods are then applied to a flexibly scaled model of a supersonic transport configuration. Comparisons of wind-tunnel data, calculations based on the modal approach, and flexibility influence coefficients are presented over the Mach number range from 0.6 to 2.7. An examination of the results obtained from this study indicates that both analytical techniques predict reasonably well the effect of flexibility on the basic longitudinal characteristics and that both techniques give generally comparable results.

17. Key Words (Suggested by Author(s))
Stability and control
Flexible aircraft
Static aeroelasticity

18. Distribution Statement
Unclassified – Unlimited

19. Security Classif. (of this report)	20. Security Classif. (of this page)	21. No. of Pages	22. Price*
Unclassified	Unclassified	68	$3.00

*For sale by the National Technical Information Service, Springfield, Virginia 22151

A WIND-TUNNEL EVALUATION OF ANALYTICAL TECHNIQUES FOR PREDICTING STATIC STABILITY AND CONTROL CHARACTERISTICS OF FLEXIBLE AIRCRAFT

By Irving Abel
Langley Research Center

SUMMARY

An experimental evaluation of analytical techniques for predicting certain stability and control characteristics of a large flexible aircraft is presented. Analytical methods based on both the modal approach and flexibility influence coefficients are developed to predict the aerodynamic characteristics of a flexible airplane. These methods are then applied to a flexibly scaled model of a supersonic transport configuration. Comparisons of wind-tunnel data, calculations based on the modal approach, and flexibility influence coefficients are presented over the Mach number range from 0.6 to 2.7. An examination of the results obtained from this study indicates that both analytical techniques predict reasonably well the effect of flexibility on the basic longitudinal characteristics and that both techniques give generally comparable results.

INTRODUCTION

Effects of aeroelasticity on aircraft design have been considered for many years. The aeroelastician has been primarily concerned with such problems as flutter, divergence, response to turbulence, and control effectiveness. The effect of flexibility on airplane stability has usually been relatively small and could be taken care of by empirical corrections to measured or calculated stability derivatives. The effect of aeroelasticity on the static aerodynamic characteristics, however, has become a major concern for large flexible aircraft that operate in both the transonic and supersonic flight regimes.

No thorough experimental evaluation of analytical approaches for predicting aeroelastic effects or stability characteristics is available. Recent papers by Roskam, Holgate, and Shimizu (ref. 1) and by Chevalier, Dornfeld, and Schwanz (ref. 2) present some comparisons between theory and experiment, but these are limited by the flexibility of the model investigated. Langley Research Center, therefore, in cooperation with The Boeing Company, undertook a program to provide a comparison of analytically determined and wind-tunnel-measured rigid and flexible aerodynamic characteristics of a proposed supersonic transport configuration. Two independent analytical approaches were used: a modal technique by NASA and a direct influence-coefficient technique by The Boeing Company. (The analytical approaches are described in appendixes A and B.) The experimental portion of the investigation was conducted over a Mach number range from 0.6 to 2.7 and utilized separate rigid and flexibly scaled models.

This paper provides a description of the wind-tunnel models (including the structural representations used for the flexible model), a description of the analytical techniques being evaluated, and a comparison of calculated and measured results. A brief overall view of this program is given in reference 3.

The experimental results presented are not directly applicable to a full-size airplane since they do not include inertia effects associated with deformation of the structure due to load factor. The results are, in effect, "massless airplane characteristics" since the model experiences a constant (n = 1) load factor and the ratio of gravitational forces to aerodynamic forces (Froude number) was not scaled. Both analytical approaches, however, can include these inertia loadings for the free-flight case.

SYMBOLS

The moment reference center is located at 45 percent of $\bar{c}$.

a speed of sound

$\lfloor A \rfloor$ aerodynamic influence-coefficient matrix

$[\bar{A}]$ matrix defining deflection on right wing due to a unit load on right wing

A_{ij} element of aerodynamic matrix $\lfloor A \rfloor$ which defines pressure coefficient at panel i due to a unit angle of attack at panel j

b wing span

$[\bar{B}]$ matrix defining deflection on right wing due to a unit load on left wing

c local chord length measured streamwise

$\bar{c}$ reference chord

C_L lift coefficient, $\frac{\text{Lift}}{qS}$

$C_{L,o}$ lift coefficient at $\alpha = 0^o$

C_{L_q} lift coefficient due to pitch rate, $\frac{\partial C_L}{\partial\left(\frac{\dot{\theta}\bar{c}}{2V}\right)}$

C_{L_α} lift-curve slope, $\left.\frac{\partial C_L}{\partial \alpha}\right|_{\alpha=0^o}$

$C_{L_{\delta_e}}$ elevator effectiveness in lift, $\frac{\partial C_L}{\partial \delta_e}$

C_l rolling-moment coefficient, $\frac{\text{Rolling moment}}{qSb}$

C_{l_β} effective dihedral parameter, $\frac{\partial C_l}{\partial \beta}$

$C_{l_{\delta_a}}$ aileron effectiveness derivative, $\frac{\partial C_l}{\partial \delta_a}$

C_m pitching-moment coefficient, $\frac{\text{Pitching moment}}{qS\bar{c}}$

$C_{m,o}$ pitching-moment coefficient at $\alpha = 0^o$

C_{m_q} pitching moment due to pitch rate, $\frac{\partial C_m}{\partial\left(\frac{\dot{\theta}\bar{c}}{2V}\right)}$

C_{m_α} static stability derivative, $\frac{\partial C_m}{\partial \alpha}$

$C_{m_{\delta_e}}$ elevator effectiveness in pitch, $\frac{\partial C_m}{\partial \delta_e}$

C_N normal-force coefficient, $\frac{\text{Normal force}}{qS}$

C_{N_α} normal-force curve slope, $\left.\frac{\partial C_N}{\partial \alpha}\right|_{\alpha=0^o}$

C_n yawing-moment coefficient, $\frac{\text{Yawing moment}}{qSb}$

C_{n_β} directional stability parameter, $\frac{\partial C_n}{\partial \beta}$

C_Y side-force coefficient, $\frac{\text{Side force}}{qS}$

C_{Y_β}	side-force parameter, $\frac{\partial C_Y}{\partial \beta}$
F	air load (see table II)
$\{F\}$	matrix defining total resultant force on each wing panel
g	acceleration due to gravity
$h_i(x,y)$	shape of ith vibration mode of model structure
$H(x,y)$	vertical displacement of point (x,y)
i,j	indices
I	mass moment of inertia in pitch
K_i	generalized stiffness of ith vibration mode
$\{L\}$	matrix defining lift on each wing panel
L	sum of $\{L\}$
L_i	element of matrix $\{L\}$ defining lift on ith panel
m	total number of modes including rigid-body pitch and plunge
$m(x,y)$	mass distribution of flexible model
Δm	known incremental mass
M	airplane total mass; Mach number
M_i	generalized mass of ith vibration mode
$\{\overline{M}\}$	matrix defining pitching moment about reference axis for each wing panel
$\overline{M}_i$	pitching moment per unit generalized coordinate

n	load factor, $\frac{\text{Lift}}{\text{Weight}}$
N_i	normal force per unit generalized coordinate
Δp	total lifting pressure over wing
Δp_i	pressure distribution due to downwash of ith mode per unit generalized coordinate
q	free-stream dynamic pressure, $\frac{1}{2}\rho V^2$
q_i	generalized coordinate of ith vibration mode
$\bar{q}_i$	generalized coordinate per unit angle of attack, $\frac{q_i}{\alpha}$
Q_i	ith mode generalized force
S	reference wing area
$\lceil S \rfloor$	matrix defining area of each wing panel
V	free-stream velocity
$w(x,y)$	downwash on wing
W	aircraft total weight
$\{W\}$	matrix defining weight of each wing panel
x,y,z	distances along coordinate axes
X,Y,Z	orthogonal coordinate system, body axes
$\lceil X \rfloor$	matrix defining distance from each panel to reference axis
X_{ac}	aerodynamic center defined by $\left(0.45 - \frac{\partial C_{m_\alpha}}{\partial C_{L_\alpha}}\right)\bar{c}$
ΔX_{ac}	change in aerodynamic center due to flexibility, $\left(X_{ac,rigid} - X_{ac,flex}\right)$

z_{mcl} coordinate of mean-camber line from wing reference plane, $\frac{z_{upper} + z_{lower}}{2}$

Z(x,y,t) force distribution in Z-direction (eq. (A1c))

α angle of attack measured from wing reference plane

$\{\alpha\}$ matrix defining angle of attack of each wing panel

α_r reference angle of attack

$\{\alpha_o\}$ matrix defining initial angle of attack at each wing panel due to camber, twist, or control deflection for wind off

$\{\Delta\alpha_{flex}\}$ matrix defining change in angle of attack at each panel due to aerodynamic loading

β angle of sideslip

δ deflection per unit load

δ_a wing trailing-edge control displacement in roll, positive for right aileron trailing edge down

δ_e wing trailing-edge control displacement in pitch, positive for trailing edge down

δx ratio of modal deflection at station x to deflection at the station for which generalized mass is desired

θ pitch angle

$[\Theta]$ structural flexibility influence-coefficient matrix

Θ_{ji} element of structural matrix $[\Theta]$ which defines the angle that panel j deflects due to a unit load on panel i

η nondimensional spanwise coordinate, $\frac{y}{b/2}$

ρ air density

ω_i frequency of ith structural mode

Subscripts:

A full-size airplane

flex flexible model

m model

rigid rigid model

sy symmetric

as antisymmetric

Matrix notation:

$[\ ]$ square matrix

$\lfloor\ \rfloor$ row matrix

$\{\ \}$ column matrix

$\lceil\ \rfloor$ square diagonal matrix

Dots above symbols indicate derivatives with respect to time.

DESCRIPTION OF MODELS

Rigid Model

The shape of the rigid model is dictated by performance and defined as the shape of the airplane "frozen" at the 1g cruise condition (M = 2.7). This shape was predetermined by preliminary wind-tunnel tests at the NASA Langley Research Center and was used as a basis for all wind-tunnel tests during this investigation. A drawing of the complete model configuration is shown in figure 1. Detailed geometric properties of the model are presented in table I. Both models were built to a geometric scale factor of 0.015. The solid steel (rigid) model incorporates a slender cambered body with a 74° swept-wing planform, four simulated flow-through engine nacelles, and two vertical tails mounted outboard on the wing. The swept-wing planform has a subsonic leading edge at the cruise Mach number except in the region of the tip where the leading-edge sweep is reduced to 65°.

Flexible Model

The 0.015-size flexibly scaled model was designed from the shape of the rigid model at cruise condition $\left(M = 2.7,\ C_L = 0.09,\ q_A = 25.855\ \text{kN/m}^2\right)$. This model was elastically scaled with a rigid forward fuselage and elastic wings and aft fuselage. The condition for model to aircraft similarity, according to reference 1, is

$$\left(\frac{q_m}{q_A}\right)\left(\frac{\delta_m}{\delta_A}\right)\left(\frac{S_m}{S_A}\right)^{1/2} = 1.0$$

where $\left(\delta_m/\delta_A\right)$ and $\left(S_m/S_A\right)$ are the ratios of model to airplane deflection per unit load and reference wing area, respectively. A dynamic-pressure ratio $\left(q_m/q_A\right)$ of 1.20 was arbitrarily selected. In order to simulate aerodynamic characteristics of the flexible airplane, it is necessary only to scale static load deflections; therefore, model weight was not scaled. A table of model scale factors is presented in table II.

The flexible model was built so that at the cruise point the shape of the rigid and flexible models is the same. In order to achieve this condition, the flexible model is constructed to a model jig shape that is defined as the shape of the model when aerodynamic loads at the cruise point are removed. (The model jig shape will differ from that of the airplane jig shape since neither airplane mass nor mass distribution is simulated.) Figure 2 shows typical comparisons of the mean-camber line between cruise shape and the corresponding jig shape at various span stations.

The flexible model was designed and constructed by The Boeing Company using a structural layout that would be quite similar to that of a full-size airplane. Structural ribs were fabricated from a balsa wood and fiber-glass sandwich with a thin aluminum cap. Plastic foam was used between structural spars to provide the proper wing contour. Finally, fiber-glass skins were bonded to the upper and lower surfaces to provide the properly scaled stiffnesses. Figure 3 shows a photograph of the flexible model during construction. A photograph of the complete flexible model prior to wind-tunnel testing is shown in figure 4.

Flexible-Model Properties

Because of the different structural representations required in the two analytical approaches, it was necessary to measure both a set of modal properties (mode shapes, frequencies, and generalized masses) and structural influence coefficients. Both sets of measurements were made for a sting-mounted model.

Modal Properties

As input to the modal analysis, it is necessary to determine a set of generalized masses, mode shapes, and natural frequencies of model vibration. For this model, the first five symmetric structural modes, generalized masses, and natural frequencies were all that could be measured.

Mode shapes and natural frequencies.- Vibration properties of the model were determined using the mode-shape measuring apparatus shown in figure 5. Two small electromagnetic shakers were positioned under the model to provide excitation for each of the first five symmetric modes. (Phasing between wing tips was checked for each mode to insure only symmetric response.) At each model frequency the displacement at 56 model control points was measured using a variable reluctance pickup. The locations of these points on the wing and fuselage are shown in figure 6. A reference pickup, located near the wing tip, provided a continuous record of model displacement which is required to phase and correct raw data. Measured frequencies and nondimensional modal displacements (normalized to 1.0 at point 56) at the control points are presented in table III.

Generalized masses.- In order to characterize the mass properties of the model, it is not necessary to know the mass distribution explicitly because in the analysis the mass always occurs in the form of an integral value over the structure; that is,

$$M_i = \iint m(x,y) h_i^2(x,y) dx\, dy$$

This integral can be evaluated for each mode by using either the known mass distribution and mode shape or by experimental methods. Since the mass distribution was not determined during construction, the direct experimental approach was used.

The experimental technique employed is described in reference 4. A brief description of this technique and its application follows:

The generalized stiffness of the ith vibration mode is defined as

$$K_i = M_i \omega_i^2$$

where ω_i is the natural frequency of the ith structural mode. If it is assumed that by adding a small known mass Δm, at station x, the generalized stiffness does not change, then

$$\bar{K}_i = \left(M_i + \Delta m\, \delta x^2\right) \overline{\omega}_i^2$$

where

δx ratio of modal deflection at station x to deflection at the station for which generalized mass is desired

$\overline{\omega}_i$ natural frequency of ith mode with added mass Δm

Therefore,

$$\left(M_i + \Delta m \, \delta x^2\right)\overline{\omega}_i^{\,2} = M_i \omega_i^{\,2}$$

or

$$M_i = \frac{\Delta m \, \delta x^2}{\left(\frac{\omega_i}{\overline{\omega}_i}\right)^2 - 1}$$

For each mode, Δm is known and δx, $\overline{\omega}_i$, and ω_i are measured. The generalized mass M_i can now be evaluated by the preceding equation. In practice, it is convenient to plot $\Delta m \, \delta x^2$ as a function of $\left(\frac{\omega_i}{\overline{\omega}_i}\right)^2 - 1$ for various values of Δm in order to insure that the mode has not been altered by the additional mass. If the mode has been altered, this plot will be nonlinear. The slope of this curve, evaluated near zero for the nonlinear case, is the generalized mass.

The application of this technique to the flexible model is presented in figure 7. Also presented are the approximate locations of the symmetric node lines for each mode. For each mode a minimum of three data points were obtained. All generalized masses are referenced to model control point 56.

Structural-Influence Coefficients

The required structural information for the influence-coefficient analysis is the matrix $\left[\Theta\right]$ (eq. (B3)). This matrix defines the slope at any point on the structure due to a unit load at every other point. The flexibility influence coefficients for the flexible model were experimentally determined by The Boeing Company.

The data required to define the flexibility influence coefficients were measured using the test setup shown in figure 8. The model was rigidly attached to a test fixture. Fifty-one electrical transducers were positioned over the right wing at preselected control points to monitor displacements. Figure 9 shows the paneling scheme and location of each control point. (Control points are at panel centroids.) The deflections at stations 1 through 10 were not measured since the model was essentially rigid in this region. A pneumatic cylinder was used to apply point loads.

In order to evaluate the flexibility matrix, it is necessary to make two measurements: (1) the deflection on the right wing due to a load on the right wing, and (2) the deflection on the right wing due to a load on the left wing. These measurements were made by applying a known load at each of the 51 stations and monitoring the resulting deformation at all stations due to this load. If we define these two measured quantities as

$\left[\bar{A}\right]$ matrix defining deflection on the right wing due to a unit load on the right wing

$\left[\bar{B}\right]$ matrix defining deflection on the right wing due to a unit load on the left wing

then the symmetric deflection matrix can be expressed as

$$\left[\delta_{sy}\right] = \left[\bar{A}\right] + \left[\bar{B}\right]$$

and the antisymmetric deflection matrix as

$$\left[\delta_{as}\right] = \left[\bar{A}\right] - \left[\bar{B}\right]$$

The matrix $\left[\delta\right]$ is now differentiated, by using a finite difference technique, to provide the required result $\left[\Theta\right]$; that is, the slope at a point due to a unit load at any point on the structure. Measured values of deflection per unit load used to define matrices $\left[\bar{A}\right]$ and $\left[\bar{B}\right]$ are given in table IV.

WIND-TUNNEL METHODS AND TEST CONDITIONS

The wind-tunnel studies were conducted in the Langley 8-foot transonic pressure tunnel and in the Langley Unitary Plan wind tunnel in order to obtain data at subsonic and supersonic speeds. The stagnation dewpoint temperature was maintained sufficiently low to avoid any significant condensation effects in either tunnel.

In order to insure a turbulent boundary-layer condition, all tests of both models were conducted with boundary-layer transition strips. These strips were composed of a band of No. 60 carborundum grit located 3.05 cm aft of the forebody apex and a band of No. 80 grit located 1.52 cm streamwise from the leading edge of all external surfaces and on the inside surface of the engine nacelles.

Aerodynamic forces and moments about the $0.45\bar{c}$ reference center were measured using a six-component strain-gage balance mounted within the models. Angle of attack was corrected for deflection of the sting and balance under aerodynamic load and for tunnel-flow angularity. Angle of attack was varied from about -10° to 5°, and sideslip angle was varied from -6° to 6°.

Wind-tunnel studies at $M = 0.6$, 0.9, and 1.2 over a range of dynamic pressures from 11.970 to 38.304 kN/m^2 were conducted in the Langley 8-foot transonic pressure tunnel. This tunnel is a variable-pressure, single-return facility having a slotted test section and is capable of producing velocities in the test section up to $M = 1.3$ without appreciable effects of choking and blockage. The nominal test conditions for this investigation are:

Mach number	Stagnation temperature, °C	Dynamic pressure, kN/m^2	Reynolds number per meter
Rigid model			
0.60	48.9	12.593	6.562×10^6
.90	48.9	17.093	6.562
1.20	48.9	19.966	6.562
Flexible model			
0.60	48.9	11.970	6.201×10^6
.60	↓	23.940	12.434
.60	↓	32.654	16.962
.90	↓	11.970	4.593
.90	↓	23.940	9.186
.90	↓	29.638	11.385
1.20	↓	11.970	3.937
1.20	↓	23.940	7.874
1.20	↓	38.304	12.598

Wind-tunnel studies at $M = 2.3$ and $M = 2.7$ over a range of dynamic pressures from 11.970 to 47.880 kN/m^2 were conducted in the Langley Unitary Plan wind tunnel. The nominal test conditions for this investigation are:

Mach number	Stagnation temperature, °C	Dynamic pressure, kN/m^2	Reynolds number per meter
Rigid model			
2.3	65.6	21.738	6.562×10^6
2.7	65.6	19.822	6.562
Flexible model			
2.3	65.6	11.970	3.642×10^6
2.3	↓	23.940	7.251
2.7	↓	11.970	3.970
2.7	↓	23.940	7.940
2.7	↓	31.122	10.335
2.7	↓	47.880	15.879

AEROELASTIC ANALYSIS

Analytical calculations for the rigid model as a function of Mach number and for the flexible model as a function of Mach number and dynamic pressure have been made employing the modal method (appendix A) and structural influence coefficients (appendix B). The calculations were made for a sting-mounted, "massless" model. The term massless is used to describe the case in which only aerodynamic loads are considered acting upon the structure; that is, inertia loads such as weight times load factor are assumed to be zero.

Modal Method

A digital computer program, using the approach discussed in appendix A, was developed to predict aeroelastic effects on longitudinal stability and control characteristics. Calculations were made for a sting-mounted model using the first five measured symmetric modes and generalized masses (see fig. 7 and table III).

The basic free-flight equations presented in appendix A represent the sting-mounted model, if it is assumed that integrals of the form

$$\iint m(x,y)h_i(x,y)dx\,dy$$

are negligibly small. In the free-flight case these integrals are exactly zero, except for the plunge mode where the integral simplifies to the total mass of the airplane, due to the orthogonality of the structural and rigid-body modes.

Subsonic aerodynamics. The subsonic generalized aerodynamic forces

$$\iint \Delta p_i(x,y)h_j(x,y)dx\,dy$$

were formulated through the use of kernel-function aerodynamics. The pressure distribution $\Delta p_i(x,y)$ is obtained by a numerical method similar to that presented in reference 5. The pressure distribution is obtained by numerically solving a linear integral equation which relates the pressure distribution to the downwash.

The solution of the kernel equation for $\Delta p_i(x,y)$ requires that the downwash be specified at known control points. Thirty-six control points were used in these calculations. These points were located at 12.1, 33.6, 56.7, 76.5, 88.5, and 96.8 percent of the panel span (η) and at 5.7, 21.6, 44.0, 67.7, 87.4, and 98.5 percent of the local streamwise chord (x/c). Only the wing, extended to the fuselage center line, is represented aerodynamically.

Substituting the appropriate expressions for the downwash due to rigid loading and that due to flexibility, the generalized aerodynamic forces required to solve the equations of motion (appendix A) are determined.

Supersonic aerodynamics.- Supersonic generalized aerodynamic forces were evaluated through the use of a supersonic Mach-box procedure (ref. 6). As in the kernel program the pressure distribution is obtained by specifying the downwash at known control points. The 56 control points at which the flexible modes were specified (fig. 6) were also used as the downwash control points for this calculation. Only the wing, extended to the fuselage center line, was represented aerodynamically.

Once the pressure distribution due to rigid loading and each flexible mode are known, the generalized aerodynamic forces are calculated. The equations of motion (appendix A) are now solved as before.

Influence-Coefficient Method

A digital computer program developed by The Boeing Company, using the approach discussed in appendix B, was used to predict aeroelastic effects on longitudinal stability and control and lateral control characteristics. Calculations were made for a sting-mounted model using measured flexibility influence coefficients (see table IV).

The free-flight equations presented in appendix B represent the massless, constrained model if the weight matrix $\{W\}$ is assumed to be 0. Equation (B4), therefore, becomes

$$\{F\} = q\left[\diagdown S \diagdown\right]\left[A\right]\{\alpha\}$$

When the panel weights are set equal to zero, the aeroelastic characteristics become a function of planform and structure at a given test condition. Comparisons of aerodynamic characteristics with and without mass effects are presented in table V.

The aerodynamic matrix $[A]$ was formulated through the use of constant-pressure panels that can be used at subsonic and supersonic speeds (ref. 7) and which were coincident with the structural panels (fig. 9). The aerodynamic representation included the forebody, wing, and cylindrical afterbody.

Once the area matrix $\left[\diagdown S \diagdown\right]$, aerodynamic matrix $[A]$, and flexibility influence-coefficient matrix $[\Theta]$ are evaluated, the equations in appendix B are solved for the flexible aerodynamic characteristics as a function of rigid loading and test condition.

RESULTS

This section compares longitudinal aerodynamic characteristics obtained with the rigid model and the flexible model and from theoretical calculations. Also included is a presentation of lateral experimental results obtained for the flexible model and a comparison of lateral-control effectiveness with influence-coefficient calculations. The rigid model is assumed perfectly rigid, and no corrections to the data due to flexibility are included.

Longitudinal Aerodynamic Characteristics

A comparison of analyses and wind-tunnel data in predicting the variation of lift-curve slope C_{L_α} and aerodynamic center X_{ac}, in percent of the reference chord, as a function of Mach number is presented in figure 10. Measured results are given for both the rigid model (assumed independent of dynamic pressure) and the flexible model at a dynamic pressure 23.94 kN/m^2. The effect of dynamic pressure at all Mach numbers is to reduce C_{L_α} significantly and to shift the aerodynamic center in a destabilizing forward direction. Reductions in C_{L_α} of about 37 percent and shifts in the aerodynamic center as large as 18 percent of $\bar{c}$ are evident at $M = 1.2$. These phenomena are associated with structural deflections outboard on the wing which tend to reduce the local angle of attack and, subsequently, to reduce the contribution of the outboard portion of the wing to the total lift. This reduction in lift results in a lower lift-curve slope and a forward shift in the aerodynamic center. In general, correlation between analyses and experiment is reasonable.

The effect of dynamic pressure on lift-curve slope is predicted somewhat better than the effect of dynamic pressure on aerodynamic-center location. Figure 11 compares analyses and wind-tunnel data in predicting the variation of the ratio of flexible C_{L_α} to rigid C_{L_α} and aerodynamic-center movement between rigid and flexible models as a function of dynamic pressure. Data are presented for Mach numbers of 0.6, 0.9, 1.2, 2.3, and 2.7 over a range of dynamic pressure. The shift in aerodynamic center,

$$\Delta X_{ac} = \left(X_{ac,rigid} - X_{ac,flex}\right)$$

is a measure of the movement of the aerodynamic center from its location on the rigid model as indicated in figure 10. In general, the agreement between analyses and wind-tunnel data in predicting the variation in C_{L_α} is good. For most cases, the agreement between modal and influence-coefficient techniques is comparable; however, the aerodynamic-center movement with dynamic pressure is predicted better with the modal technique at $M = 0.6$, 0.9, and 1.2. Both techniques show good agreement with wind-tunnel data at $M = 2.3$ and $M = 2.7$. It should be noted that at these higher Mach numbers the shift in aerodynamic center is predicted quite well even though neither analysis predicted the absolute position of the aerodynamic center (see fig. 10).

Figure 12 presents a comparison of analyses and experiment in predicting lift and pitching-moment coefficients at $\alpha = 0^\circ$ as a function of dynamic pressure. The calculated data are generated by putting into the program the camber and twist distribution of the wing mean-camber line (fig. 2). Only flexible-model results are presented since the slope of the mean-camber line for the rigid model applies only to the design cruise point. It should be noted that calculated data at a dynamic pressure of zero correspond to a rigid configuration with the flexible-model jig-shape camber and twist.

At Mach numbers of 0.6, 0.9, and 1.2, the influence-coefficient analysis appears to predict the pitching-moment coefficients somewhat better than the modal approach. At Mach numbers of 0.6 and 0.9, both methods are directly comparable for lift coefficient. At $M = 1.2$, the influence-coefficient method predicts both lift coefficient and pitching-moment coefficient somewhat better. The results at $M = 2.3$ and 2.7 indicate that both methods predicted the lift coefficient quite well, but for these cases the modal method appears to predict the pitching-moment coefficient somewhat better.

The reason one method appears to give better results at one Mach number than at others is probably the aerodynamic representations utilized in both methods. The modal method uses kernel function subsonically and Mach-box aerodynamics supersonically, whereas the influence-coefficient technique uses constant-pressure panels throughout and includes fuselage effects. In all cases the trend is accurately predicted, and in most cases the increment between measured data is estimated quite well using either technique.

A comparison between wind-tunnel data and analyses in predicting control-surface effectiveness in pitch is presented in figure 13. At $M = 0.6$ and 0.9 only influence-coefficient analysis data are presented since the modal technique could only be applied to the supersonic case. (The kernel-function program used does not provide for inclusion of control-surface aerodynamics.) Data at Mach numbers of 1.2, 2.3, and 2.7 compare both influence-coefficient and modal analyses with experimental results. Wind-tunnel data for the rigid model were not available at these Mach numbers for the control surface under investigation.

Correlation between experiment and analyses is quite poor for predicting the absolute level. The increment in control effectiveness, however, is predicted somewhat better. It is believed that part of this problem is due to the inadequacy of both aerodynamic theories (Mach-box and constant-pressure panels) to properly predict the rigid loading because of the proximity of the control surface to both the vertical tail and the outboard engine. The problem was further aggravated by the flexibility of the control-surface attachment points. Since both analytical methods at $M = 1.2$, 2.3, and 2.7 predict about the same rigid loading, the differences in calculations are attributed to the limited number of modes used in the modal calculation.

Lateral Aerodynamic Characteristics

The variation of measured lateral stability derivatives C_{l_β}, C_{n_β}, and C_{Y_β} for the flexible model as a function of angle of attack at different dynamic pressures is presented in figure 14. These derivatives were estimated around $\beta = 0^{\circ}$ by taking, for example,

$$C_{l_{\beta}} = \frac{(C_l)_{\beta=2^{\circ}} - (C_l)_{\beta=0^{\circ}}}{2}$$

At present the theoretical calculations have not been extended to predict these lateral-stability characteristics. The general analytical approach outlined previously can be applied to the lateral case by using the appropriate antisymmetric structural and aerodynamic representations.

For the Mach number and dynamic-pressure range investigated, the flexible model exhibited positive effective dihedral $\left(-C_{l_{\beta}}\right)$ except at the larger negative angles of attack, a positive value of $C_{n_{\beta}}$ except at the larger negative angles of attack at $M = 2.3$ and 2.7, and a negative side-force derivative $C_{Y_{\beta}}$. For this configuration, dynamic pressure appears to have a less significant effect on the lateral-directional characteristics than on the longitudinal characteristics. The primary effect is a reduction in $C_{l_{\beta}}$, at all Mach numbers, with increasing dynamic pressure.

The effect of dynamic pressure on control-surface effectiveness in roll is presented in figure 15. Calculations using the influence-coefficient technique were made to predict this effect. At all Mach numbers the effect of an increase in dynamic pressure is to reduce appreciably the aileron effectiveness in roll. At $M = 1.2$ and $q = 33$ kN/m^2 the model exhibits zero control effectiveness. Once again, the correlation between analysis and experiment in predicting control-surface effectiveness is quite poor. As stated previously, this can be attributed to poor prediction of the rigid loading. It is interesting to note that zero effectiveness in pitch ($M = 1.2$, fig. 13) and aileron reversal in roll ($M = 1.2$, fig. 15) are analytically predicted reasonably close to the experimental results using the influence-coefficient analysis.

CONCLUDING REMARKS

Both wind-tunnel studies and analytical calculation of 0.015-size rigid and flexibly scaled models of a proposed supersonic transport configuration have been conducted at subsonic and supersonic speeds to measure the effect of flexibility on the aerodynamic characteristics. Analytical calculations using both a modal approach and structural influence-coefficient approach are presented.

Examination of the analytical and experimental data indicates that:

1. The analyses did predict reasonably well the effect of flexibility on the basic longitudinal characteristics; however, the analyses are shown to be poor in predicting control-surface derivatives in both pitch and roll.

2. Both the modal approach and the structural influence-coefficient approach yield generally comparable results.

Even though the primary purpose of this investigation was to evaluate analytical techniques, it has been shown experimentally that:

1. The longitudinal aerodynamic characteristics of the flexible model were affected strongly by flexibility effects which included large reductions in lift-curve slope, destabilizing shifts in the aerodynamic center, and large reductions in control effectiveness.

2. The lateral aerodynamic characteristics of the flexible model were not greatly affected by flexibility except for control effectiveness in roll.

Langley Research Center,
National Aeronautics and Space Administration,
Hampton, Va., February 10, 1972.

APPENDIX A

MODAL METHOD FOR DETERMINING LONGITUDINAL STABILITY AND CONTROL CHARACTERISTICS

A detailed analysis of the procedure for calculating aeroelastic effects on longitudinal stability and control using the modal approach is presented.

The deformation of the airplane as a function of rigid loading is determined by solving Lagrange's equations of motion. From these calculated deformations the effective wing loading is obtained which, in turn, is used to calculate the flexible stability and control characteristics.

A digital computer program, using the approach discussed in reference 8, was developed to predict aeroelastic effects on longitudinal stability and control.

Equations of motion.- Under the following assumptions

(1) The forward speed V of the airplane is constant

(2) Small angle-of-attack variation $\left(C_N \approx C_L\right)$

(3) Small structural deformation

(4) Structural motion is slow enough that structural acceleration and structural velocity are negligibly small

(5) Orthogonal structural modes

the linearized free-flight longitudinal equations of motion appear in a general form (in the body-axis system) as follows:

$$M_i\ddot{q}_i(t) + \omega_i{}^2 M_i q_i(t) = Q_i(t) \tag{A1}$$

where

$$M_i = \iint m(x,y)h_i{}^2(x,y)dx\,dy \tag{A1a}$$

$$Q_i(t) = \iint Z(x,y,t)h_i(x,y)dx\,dy \tag{A1b}$$

$$Z(x,y,t) = \Delta p(x,y,t) - ngm(x,y) \tag{A1c}$$

$$\Delta p(x,y,t) = \sum_{j=1}^{m} \Delta p_j(x,y,t)q_j(t) \tag{A1d}$$

Generalized forces and moments.- In order to determine the generalized forces and moments $Q_i(t)$, it is necessary to relate the downwash $w(x,y,t)$ to the displacement $H(x,y,t)$ of the system. It is assumed that the displacement $H(x,y,t)$ can be represented by a superposition of the normal modes of vibration so that

$$H(x,y,t) = h_1(x,y)q_1(t) + h_2(x,y)q_2(t) + \ldots + h_m(x,y)q_m(t)$$

where q_i specifies the magnitude of the displacement in the ith mode, and $h_i(x,y)$ gives the shape of the mode. Letting $h_1(x,y)$ be rigid-body plunge and $h_2(x,y)$ be rigid-body pitch, then

$$h_1(x,y) = 1 \qquad h_2(x,y) = x$$

$$q_1(t) = z \qquad q_2(t) = \theta$$

The displacement can now be written as

$$H(x,y,t) = z + x\theta + \sum_{i=3}^{m} h_i(x,y)q_i(t)$$

The downwash $w(x,y,t)$ associated with the displacement $H(x,y,t)$ is given by

$$w(x,y,t) = \left(V \frac{\partial}{\partial x} + \frac{\partial}{\partial t}\right) H(x,y,t)$$

Downwash due to angle of attack.- Assuming the downwash associated with $\dot{\theta}$ is small and using assumption (4), $\dot{q}_i = 0$ where $i \geqq 3$, the downwash due to angle of attack may be expressed as

$$w(x,y) = V\left[\sum_{i=3}^{m} \frac{\partial h_i(x,y)}{\partial x} q_i + \alpha\right] \tag{A2}$$

where

$$\alpha = \theta + \frac{\dot{z}}{V} \tag{A2a}$$

The downwash is composed of two parts; namely,

Downwash due to flexibility: $V \sum_{i=3}^{m} \frac{\partial h_i(x,y)}{\partial x} q_i$

Downwash due to rigid loading: $V\alpha$

Once the downwash distribution is known over the wing (eq. (A2)), the pressure distribution Δp_i for each flexible and rigid mode can be obtained from available aerodynamic theories. In the modal framework, pressure distributions are determined in the following manner:

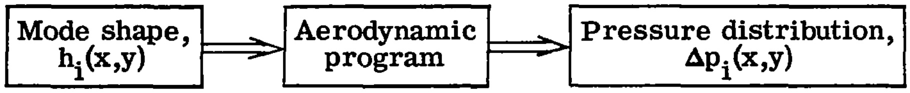

Determination of structural deformation.- Using free-free normal modes (both rigid-body and structural) and downwash due to angle of attack, the longitudinal equations of motion (A1) can be written as

$$
\begin{aligned}
M\ddot{Z} &= q_3 \iint \Delta p_3(x,y)dx\,dy + \ldots + q_m \iint \Delta p_m(x,y)dx\,dy \\
&\quad + \alpha \iint \Delta p_\alpha(x,y)dx\,dy - Mgn
\end{aligned}
\tag{A3}
$$

$$
\begin{aligned}
I\ddot{\theta} &= q_3 \iint x\,\Delta p_3(x,y)dx\,dy + \ldots + q_m \iint x\,\Delta p_m(x,y)dx\,dy \\
&\quad + \alpha \iint x\,\Delta p_\alpha(x,y)dx\,dy
\end{aligned}
\tag{A4}
$$

$$
\left.
\begin{aligned}
\omega_3^2 M_3 q_3 &= q_3 \iint h_3(x,y)\,\Delta p_3(x,y)dx\,dy + \ldots + q_m \iint h_3(x,y)\,\Delta p_m(x,y)dx\,dy + \alpha \iint h_3(x,y)\,\Delta p_\alpha(x,y)dx\,dy \\
&\;\;\vdots \\
\omega_m^2 M_m q_m &= q_3 \iint h_m(x,y)\,\Delta p_3(x,y)dx\,dy + \ldots + q_m \iint h_m(x,y)\,\Delta p_m(x,y)dx\,dy + \alpha \iint h_m(x,y)\,\Delta p_\alpha(x,y)dx\,dy
\end{aligned}
\right\}
\tag{A5}
$$

where

$$\omega_1 = \omega_2 = 0$$

$$M = \iint m(x,y)h_1^2(x,y)dx\,dy = \iint m(x,y)dx\,dy$$

$$I = \iint m(x,y)h_2^2(x,y)dx\,dy = \iint x^2 m(x,y)dx\,dy$$

and integrals of the form

$$ng \iint m(x,y)h_i(x,y)dx\,dy \equiv 0 \qquad (i = 2, 3, \ldots, m)$$

due to orthogonality of the free-free modes.

Once the generalized masses M_i, the natural structural frequencies ω_i, and the aerodynamic forces per unit generalized displacement $\iint h_i(x,y)\ \Delta p_j(x,y)dx\ dy$ are evaluated, equations (A5) are solved simultaneously for $\bar{q}_i$, the generalized displacement q_i per unit angle of attack α.

Final form of flexible characteristics.- Defining normal force and pitching moment per unit generalized displacement as

$$N_i = \iint \Delta p_i(x,y)dx\ dy \qquad \overline{M}_i = \iint x\ \Delta p_i(x,y)dx\ dy$$

the plunge equation (A3) can be expressed in terms of $\bar{q}_i$ as

$$M\ddot{Z} = \alpha\left(\bar{q}_3N_3 + \bar{q}_4N_4 + \ldots + \bar{q}_mN_m + N_\alpha\right) - Mgn \tag{A6}$$

The aerodynamic terms in equation (A6) can be equated to the normal-force coefficient as

$$\frac{1}{2}\rho V^2 SC_N = \alpha\left(\bar{q}_3N_3 + \bar{q}_4N_4 + \ldots + \bar{q}_mN_m + N_\alpha\right)$$

Differentiating with respect to α, the flexible lift-curve slope is obtained as a function of the modal properties $\bar{q}_i$ and N_i as

$$C_{L_{\alpha,flex}} \approx C_{N_{\alpha,flex}} = \frac{1}{\frac{1}{2}\rho V^2 S}\left(\bar{q}_3N_3 + \bar{q}_4N_4 + \ldots + \bar{q}_mN_m\right) + C_{N_{\alpha,rigid}} \tag{A7}$$

Using the pitching-moment equation (A4), the static stability derivative $C_{m_{\alpha,flex}}$ can be expressed in terms of $\bar{q}_i$ and $\overline{M}_i$ as

$$C_{m_{\alpha,flex}} = \frac{1}{\frac{1}{2}\rho V^2 S\bar{c}}\left(\bar{q}_3\overline{M}_3 + \bar{q}_4\overline{M}_4 + \ldots + \bar{q}_m\overline{M}_m\right) + C_{m_{\alpha,rigid}} \tag{A8}$$

In a similar manner, the aerodynamic coefficients, such as $C_{L,o}$, $C_{m,o}$, $C_{L_{\delta_e}}$, $C_{m_{\delta_e}}$, C_{L_q}, and C_{m_q} can be evaluated by using the appropriate loading conditions, that is, by specifying the proper downwash distribution associated with each rigid loading. In order to evaluate $C_{L,o_{flex}}$ and $C_{m,o_{flex}}$, for example, replace integrals of the form

$$\alpha \iint h_i(x,y)\ \Delta p_\alpha(x,y)dx\ dy$$

in equations (A3) to (A5) with integrals of the form

$$\iint h_i(x,y)\ \Delta p(x,y)_{\text{camber and twist}}\ dx\ dy$$

and solve as before.

APPENDIX B

INFLUENCE-COEFFICIENT METHOD FOR DETERMINING LONGITUDINAL STABILITY AND CONTROL CHARACTERISTICS

A detailed analysis of the procedure developed by The Boeing Company for calculating the aeroelastic effects on longitudinal stability and control characteristics using the influence-coefficient approach is presented.

The airplane is first divided into a number of panels (see fig. 9). For each panel an aerodynamic matrix element A_{ij} is developed which relates the pressure at panel i due to a unit rotation at panel j. A structural flexibility matrix element Θ_{ji} is obtained which relates a change in angle of attack at panel j due to a unit load at panel i. With these matrices, which define the aerodynamics and flexibility of the airplane, the following set of matrix equations can be written:

$$\{L\} = q\lceil S \rfloor [A] \{\alpha\} \tag{B1}$$

$$\{\alpha\} = \alpha_r\{1\} + \{\alpha_o\} + \{\Delta\alpha_{flex}\} \tag{B2}$$

$$\{\Delta\alpha_{flex}\} = [\Theta]\{F\} \tag{B3}$$

$$\{F\} = q\lceil S \rfloor [A] \{\alpha\} - n\{W\} \tag{B4}$$

In order to solve for lift-curve slope, the preceding equations can be solved in the following manner:

$$\{\alpha\} = \alpha_r\{1\} + \{\alpha_o\} + [\Theta]\{F\}$$

Substitute for $\{F\}$, equation (B4); then

$$\{\alpha\} = \alpha_r\{1\} + \{\alpha_o\} + [\Theta]\Big(q\lceil S \rfloor [A]\{\alpha\} - n\{W\}\Big)$$

Solving for $\{\alpha\}$ and substituting this result into equation (B1) results in the total lift

$$L = \lfloor 1 \rfloor \{L\} = q\lfloor 1 \rfloor \lceil S \rfloor [A] \left\{\Big(\lceil 1 \rfloor - q[\Theta]\lceil S \rfloor [A]\Big)^{-1}\Big(\alpha_r\{1\} + \{\alpha_o\} - n[\Theta]\{W\}\Big)\right\}$$

Since the load factor n is defined as $\frac{\text{Lift}}{\text{Weight}}$ and $C_L = \frac{\text{Lift}}{qS}$, the previous equation can be expressed as

$$C_L = \frac{\lfloor 1 \rfloor \lceil S \rfloor [A]}{S} \left\{\Big(\lceil 1 \rfloor - q[\Theta]\lceil S \rfloor [A]\Big)^{-1}\Big(\alpha_r\{1\} + \{\alpha_o\} - \frac{qSC_L}{W}[\Theta]\{W\}\Big)\right\}$$

Differentiating this expression with respect to α_r and simplifying results in the final form of the lift-curve slope; that is,

$$C_{L_{\alpha,flex}} = \frac{\lfloor 1 \rfloor \lceil S \rfloor \left[A\right] \left(\lceil 1 \rfloor - q\left[\Theta\right] \lceil S \rfloor \left[A\right] \right)^{-1} \{1\}}{S\left(1 + \frac{q}{W} \lfloor 1 \rfloor \lceil S \rfloor \left[A\right] \left(\lceil 1 \rfloor - q\left[\Theta\right] \lceil S \rfloor \left[A\right] \right)^{-1} \left[\Theta\right] \{W\}\right)} \tag{B5}$$

Since the lift L_i on each panel is known, the pitching-moment derivatives can be readily calculated from panel geometry; that is,

$$\{\overline{M}\} = \lceil X \rfloor \{L\}$$

In a similar manner, expressions can be derived for other aerodynamic characteristics such as $C_{L,o}$, $C_{m,o}$, $C_{L_{\delta_e}}$, $C_{m_{\delta_e}}$, C_{L_q}, and C_{m_q}.

The principal advantage of the direct influence-coefficient approach is the capability for separation of inertia loading effects from aerodynamic loading effects. A comparison of these characteristics is presented in table V. The aerodynamic characteristics presented are separated into three categories: aeroelastic effects due to both flexibility and inertia, aeroelastic effects due only to flexibility (referred to as massless derivatives in ref. 1), and rigid-airplane characteristics.

REFERENCES

1. Roskam, J.; Holgate, T.; and Shimizu, G.: Elastic Wind-Tunnel Models for Predicting Longitudinal Stability Derivatives of Elastic Airplanes. J. Aircraft, vol. 5, no. 6, Nov.-Dec. 1968, pp. 543-550.

2. Chevalier, Howard L.; Dornfeld, Gerald M.; and Schwanz, Robert C.: An Analytical Method for Predicting the Stability and Control Characteristics of Large Elastic Airplanes at Subsonic and Supersonic Speeds. Pt. II – Application. Aeroelastic Effects From a Flight Mechanics Standpoint, AGARD CP No. 46, Mar. 1970, pp. 12-15 – 12-28.

3. Abel, Irving: Evaluation of Techniques for Predicting Static Aeroelastic Effects on Flexible Aircraft. J. Aircraft, vol. 9, no. 1, Jan. 1972, pp. 43-47.

4. Gauzy, H.: Measurement of Inertia and Structural Damping. AGARD Manual on Aeroelasticity, Part IV, Chapter 3, Oct. 1968.

5. Watkins, Charles E.; Woolston, Donald S.; and Cunningham, Herbert J.: A Systematic Kernel Function Procedure for Determining Aerodynamic Forces on Oscillating or Steady Finite Wings at Subsonic Speeds. NASA TR R-48, 1959.

6. Donato, Vincent W.; and Huhn, Charles R., Jr.: Supersonic Unsteady Aerodynamics for Wings With Trailing Edge Control Surfaces and Folded Tips. AFFDL-TR-68-30, U.S. Air Force, Aug. 1968. (Available from DDC as AD 840 598.)

7. Woodward, F. A.; Tinoco, E. N.; and Larsen, J. W.: Analysis and Design of Supersonic Wing-Body Combinations, Including Flow Properties in the Near Field. Part I – Theory and Application. NASA CR-73106, 1967.

8. Wykes, John H.; and Lawrence, Robert E.: Aerothermoelasticity: Its Impact on Stability and Control of Winged Aerospace Vehicles. J. Aircraft, vol. 2, no. 6, Nov.-Dec. 1965, pp. 517-526.

TABLE I

GEOMETRIC PROPERTIES OF MODELS

Wing	
Aspect ratio	1.630
Span, meters	0.580
Area, $meters^2$	0.207
Root chord at fuselage center line, meters	0.815
Tip chord, meters	0.034
Reference chord, meters	0.487
Fuselage	
Length, meters	1.167
Diameter at base, meters	0.045
Vertical tails	
Area, $meters^2$	0.005
Thickness-chord ratio	0.029

TABLE II

MODEL SCALE FACTORS

Quantity	Symbol	Formula	Factor
Length	L_m/L_A	Selected	0.015
Dynamic pressure	q_m/q_A	$\left(\frac{\rho_m}{\rho_A}\right)\left(\frac{V_m}{V_A}\right)^2$ selected	1.2
Mach number	M_m/M_A	$\left(\frac{V_m}{V_A}\right)\left(\frac{a_A}{a_m}\right)$	1.0
Air loads	F_m/F_A	$\left(\frac{q_m}{q_A}\right)\left(\frac{L_m}{L_A}\right)^2$	2.7×10^{-4}
Deflection per unit load	δ_m/δ_A	$\left(\frac{q_A}{q_m}\right)\left(\frac{L_A}{L_m}\right)$	55.6

Scaling rule: $\left(\frac{q_m}{q_A}\right)\left(\frac{\delta_m}{\delta_A}\right)\left(\frac{S_m}{S_A}\right)^{1/2} = 1.0$

TABLE III

NONDIMENSIONAL MODE-SHAPE DATA

$\eta = 0.00$, c = 0.8110 m		$\eta = 0.121$, c = 0.6139 m		$\eta = 0.336$, c = 0.4813 m		$\eta = 0.567$, c = 0.2933 m		$\eta = 0.765$, c = 0.1430 m		$\eta = 0.885$, c = 0.0889 m		$\eta = 0.968$, c = 0.0498 m	
x/c	h_i	x/c	h_i	x/c	h_i	x/c	h_i	x/c	h_i	x/c	h_i	x/c	h_i
Mode 1: ω = 27.19 hertz, i = 1													
0.031	-0.038	0.018	-0.010	0.026	0.041	0.038	0.132	0.055	0.401	0.054	0.580	0.061	0.854
.170	-.009	.154	.000	.161	.055	.171	.155	.183	.447	.180	.622	.193	.873
.308	-.001	.290	.012	.297	.070	.304	.201	.312	.484	.303	.654	.315	.896
.445	.018	.426	.035	.432	.093	.437	.242	.441	.519	.429	.682	.447	.916
.584	.046	.562	.061	.566	.132	.569	.300	.571	.562	.554	.718	.563	.922
.733	.079	.698	.095	.701	.178	.702	.360	.700	.606	.680	.735	.695	.927
.860	.130	.837	.141	.836	.253	.825	.436	.830	.651	.811	.777	.822	.939
.998	.180	.982	.214	.973	.336	.967	.518	.965	.722	.940	.802	.954	1.000
Mode 2: ω = 42.87 hertz, i = 2													
0.031	0.033	0.018	0.010	0.026	-0.009	0.038	-0.035	0.055	0.216	0.054	0.548	0.061	0.780
.170	.008	.154	.000	.161	-.019	.171	-.018	.183	.272	.180	.563	.193	.799
.308	.000	.290	-.004	.297	-.031	.304	.001	.312	.329	.303	.603	.315	.840
.445	-.009	.426	-.017	.432	-.035	.437	.029	.441	.393	.429	.653	.447	.860
.584	-.028	.562	-.032	.566	-.023	.569	.097	.571	.467	.554	.691	.563	.884
.733	-.033	.698	-.030	.701	-.001	.702	.185	.700	.530	.680	.741	.695	.917
.860	-.011	.837	-.008	.836	.051	.825	.286	.830	.603	.811	.805	.822	.958
.998	-.001	.982	-.001	.973	.153	.967	.417	.965	.689	.940	.855	.954	1.000
Mode 3: ω = 68.21 hertz, i = 3													
0.031	-0.002	0.018	-0.005	0.026	-0.006	0.038	-0.001	0.055	0.090	0.054	0.394	0.061	0.693
.170	-.001	.154	-.002	.161	-.004	.171	-.002	.183	.134	.180	.441	.193	.732
.308	-.001	.290	-.001	.297	-.004	.304	-.003	.312	.177	.303	.486	.315	.783
.445	-.001	.426	-.004	.432	-.002	.437	-.002	.441	.226	.429	.531	.447	.803
.584	-.001	.562	-.002	.566	-.010	.569	-.001	.571	.285	.554	.582	.563	.846
.733	-.005	.698	-.009	.701	-.026	.702	.005	.700	.336	.680	.642	.695	.891
.860	-.044	.837	-.046	.836	-.066	.825	.044	.830	.401	.811	.702	.822	.933
.998	-.099	.982	-.106	.973	-.108	.967	.116	.965	.462	.940	.745	.954	1.000
Mode 4: ω = 103.09 hertz, i = 4													
0.031	-0.001	0.018	-0.001	0.026	0.011	0.038	0.044	0.055	0.046	0.054	0.280	0.061	0.671
.170	-.001	.154	.002	.161	.016	.171	.041	.183	.056	.180	.317	.193	.683
.308	.001	.290	.004	.297	.019	.304	.034	.312	.071	.303	.351	.315	.722
.445	.004	.426	.008	.432	.022	.437	.016	.441	.086	.429	.394	.447	.753
.584	.007	.562	.010	.566	.020	.569	-.001	.571	.109	.554	.443	.563	.809
.733	.005	.698	.009	.701	.006	.702	-.033	.700	.130	.680	.483	.695	.854
.860	.001	.837	.003	.836	-.033	.825	-.072	.830	.158	.811	.551	.822	.932
.998	-.001	.982	.003	.973	-.163	.967	-.087	.965	.188	.940	.618	.954	1.000
Mode 5: ω = 148.65 hertz, i = 5													
0.031	-0.004	0.018	-0.004	0.026	0.033	0.038	-0.160	0.055	-0.809	0.054	-0.372	0.061	0.164
.170	-.003	.154	.008	.161	.040	.171	-.308	.183	-.646	.180	-.263	.193	.280
.308	.014	.290	.023	.297	.018	.304	-.477	.312	-.480	.303	-.126	.315	.389
.445	.027	.426	.028	.432	-.008	.437	-.540	.441	-.298	.429	-.001	.447	.483
.584	.021	.562	.015	.566	-.120	.569	-.492	.571	-.112	.554	.077	.563	.610
.733	-.003	.698	-.023	.701	-.244	.702	-.284	.700	-.005	.680	.257	.695	.725
.860	-.181	.837	-.171	.836	-.121	.825	-.032	.830	.148	.811	.461	.833	.868
.998	-.402	.982	-.351	.973	.052	.967	.201	.965	.345	.940	.644	.954	1.000

TABLE IV

STRUCTURAL INFLUENCE-COEFFICIENT MEASUREMENTS

(a) Matrix [A]

Load point	Panel deflection per unit load, meters/newton, measured at position:																
	11	12	13	14	15	16	17	18	19	20	21	22	23	24	25	26	27
11	$.037 \times 10^{-4}$	$.046 \times 10^{-4}$	$.057 \times 10^{-4}$	$.009 \times 10^{-4}$	$.012 \times 10^{-4}$	$.017 \times 10^{-4}$	$.022 \times 10^{-4}$	$.029 \times 10^{-4}$	$.039 \times 10^{-4}$	$.050 \times 10^{-4}$	$.058 \times 10^{-4}$	$.061 \times 10^{-4}$	$.015 \times 10^{-4}$	$.018 \times 10^{-4}$	$.023 \times 10^{-4}$	$.030 \times 10^{-4}$	$.038 \times 10^{-4}$
12	.051	.069	.107	.008	.010	.020	.027	.037	.058	.084	.103	.116	.018	.021	.027	.038	.054
13	.071	.118	.205	.010	.015	.022	.030	.048	.078	.126	.171	.198	.019	.023	.029	.047	.071
14	.006	.006	.006	.014	.006	.006	.007	.007	.007	.007	.007	.007	.008	.008	.009	.009	.014
15	.013	.013	.013	.009	.016	.012	.013	.014	.014	.012	.015	.015	.018	.016	.017	.017	.017
16	.018	.019	.021	.010	.013	.025	.021	.023	.024	.026	.026	.026	.023	.029	.026	.027	.027
17	.029	.029	.031	.011	.015	.021	.036	.029	.031	.034	.035	.035	.022	.027	.034	.034	.034
18	.037	.040	.045	.012	.016	.023	.029	.038	.041	.046	.049	.050	.023	.027	.036	.044	.047
19	.045	.055	.068	.012	.015	.022	.026	.035	.054	.065	.074	.079	.021	.024	.031	.043	.057
20	.059	.067	.119	.011	.016	.025	.031	.044	.070	.083	.130	.146	.023	.026	.034	.049	.072
21	.071	.114	.166	.013	.017	.026	.034	.049	.083	.135	.246	.335	.025	.028	.037	.056	.085
22	.063	.111	.173	.011	.014	.021	.027	.041	.076	.135	.312	.678	.020	.022	.029	.045	.075
23	.018	.018	.019	.014	.019	.023	.022	.023	.024	.025	.026	.025	.083	.039	.032	.031	.031
24	.023	.023	.025	.017	.018	.028	.026	.027	.028	.030	.031	.030	.040	.066	.042	.037	.035
25	.033	.033	.034	.017	.020	.027	.035	.038	.039	.041	.041	.040	.032	.043	.065	.054	.050
26	.039	.042	.049	.020	.018	.025	.033	.042	.048	.053	.054	.054	.027	.029	.048	.063	.062
27	.049	.058	.069	.016	.019	.026	.032	.045	.062	.074	.082	.082	.028	.033	.044	.061	.083
28	.059	.061	.102	.015	.019	.027	.035	.038	.076	.104	.123	.133	.029	.034	.046	.066	.092
29	.068	.103	.138	.015	.019	.029	.037	.053	.086	.133	.180	.215	.029	.033	.045	.067	.100
30	.070	.114	.160	.014	.018	.027	.035	.051	.090	.148	.230	.309	.027	.031	.041	.063	.100
31	.065	.113	.167	.010	.015	.021	.029	.043	.085	.152	.256	.348	.022	.025	.032	.054	.092
32	.027	.027	.027	.017	.020	.029	.034	.038	.038	.038	.037	.034	.037	.056	.073	.059	.053
33	.035	.035	.035	.019	.021	.029	.037	.044	.046	.048	.047	.045	.036	.046	.070	.073	.066
34	.046	.050	.053	.018	.022	.030	.038	.051	.062	.068	.070	.069	.036	.043	.062	.082	.090
35	.057	.069	.079	.019	.023	.032	.041	.055	.078	.095	.096	.107	.037	.043	.059	.083	.110
36	.067	.085	.109	.020	.025	.034	.042	.059	.091	.122	.144	.157	.039	.043	.059	.085	.119
37	.074	.107	.139	.020	.025	.035	.044	.063	.100	.146	.188	.219	.039	.043	.059	.087	.127
38	.079	.123	.164	.019	.025	.034	.043	.063	.106	.165	.234	.290	.039	.042	.057	.086	.130
39	.082	.131	.182	.018	.023	.033	.042	.062	.110	.179	.269	.344	.036	.039	.053	.083	.131
40	.069	.120	.174	.011	.016	.024	.030	.047	.095	.170	.273	.360	.025	.023	.037	.065	.113
41	.059	.069	.077	.024	.028	.036	.044	.061	.085	.103	.110	.110	.046	.050	.071	.100	.131
42	.063	.078	.089	.023	.028	.037	.046	.064	.093	.115	.127	.131	.047	.051	.071	.102	.138
43	.065	.087	.104	.022	.025	.034	.042	.060	.095	.128	.149	.160	.041	.045	.063	.096	.137
44	.067	.097	.120	.021	.025	.033	.040	.059	.099	.138	.176	.200	.038	.042	.060	.093	.139
45	.070	.106	.138	.022	.023	.031	.039	.059	.102	.154	.204	.242	.026	.038	.055	.089	.138
46	.074	.115	.154	.017	.038	.030	.038	.058	.106	.167	.235	.288	.034	.037	.053	.087	.140
47	.076	.126	.172	.018	.022	.030	.037	.058	.111	.182	.266	.337	.032	.034	.051	.086	.142
48	.071	.128	.181	.016	.018	.023	.030	.051	.105	.185	.286	.371	.025	.026	.040	.074	.132
49	.073	.134	.192	.015	.018	.025	.030	.050	.108	.194	.308	.404	.025	.025	.040	.074	.135
50	.069	.112	.140	.017	.019	.025	.032	.054	.104	.167	.227	.271	.026	.026	.048	.089	.150
51	.070	.115	.151	.016	.019	.024	.033	.054	.108	.175	.246	.297	.027	.028	.046	.089	.151
52	.074	.122	.162	.014	.017	.025	.033	.057	.114	.184	.265	.328	.025	.027	.048	.090	.156
53	.077	.128	.174	.015	.018	.025	.034	.056	.116	.192	.283	.354	.027	.027	.047	.087	.155
54	.078	.132	.179	.014	.017	.024	.033	.057	.116	.195	.291	.371	.026	.026	.047	.086	.158
55	.079	.140	.190	.014	.018	.026	.035	.059	.121	.209	.317	.404	.026	.027	.048	.091	.163
56	.079	.144	.202	.018	.021	.026	.032	.056	.123	.214	.334	.431	.027	.028	.043	.087	.157
57	.085	.150	.208	.015	.018	.025	.034	.059	.130	.224	.348	.452	.027	.025	.047	.090	.165
58	.082	.142	.191	.013	.018	.026	.035	.062	.130	.218	.321	.405	.023	.026	.050	.099	.180
59	.084	.148	.204	.016	.019	.025	.034	.061	.132	.227	.340	.437	.025	.024	.049	.096	.179
60	.086	.155	.213	.013	.018	.026	.033	.059	.138	.234	.358	.459	.023	.026	.047	.097	.180
61	.086	.159	.223	.014	.017	.025	.033	.061	.137	.242	.376	.489	.023	.024	.047	.097	.182

TABLE IV

STRUCTURAL INFLUENCE-COEFFICIENT MEASUREMENTS – Continued

(a) Matrix [A] – Continued

Load point	Panel deflection per unit load, meters/newton, measured at position:																
	28	29	30	31	32	33	34	35	36	37	38	39	40	41	42	43	44
11	$.047\times10^{-4}$	$.055\times10^{-4}$	$.058\times10^{-4}$	$.064\times10^{-4}$	$.021\times10^{-4}$	$.028\times10^{-4}$	$.037\times10^{-4}$	$.038\times10^{-4}$	$.034\times10^{-4}$	$.047\times10^{-4}$	$.059\times10^{-4}$	$.065\times10^{-4}$	$.053\times10^{-4}$	$.033\times10^{-4}$	$.037\times10^{-4}$	$.050\times10^{-4}$	$.034\times10^{-4}$
12	.074	.095	.105	.121	.025	.033	.044	.054	.064	.102	.134	.119	.134	.042	.087	.084	.093
13	.108	.149	.174	.201	.026	.032	.054	.069	.069	.127	.174	.195	.212	.078	.086	.099	.120
14	.009	.009	.009	.008	.009	.009	.017	.012	.002	.008	.013	.010	.007	.015	.012	.016	.022
15	.018	.018	.017	.018	.019	.020	.017	.020	.018	.022	.025	.014	.017	.023	.024	.022	.025
16	.028	.029	.027	.029	.030	.031	.030	.031	.030	.035	.039	.055	.033	.029	.034	.033	.042
17	.037	.038	.037	.038	.034	.039	.039	.041	.034	.043	.047	.058	.045	.043	.043	.041	.039
18	.050	.054	.053	.057	.038	.047	.049	.055	.056	.070	.070	.078	.064	.059	.065	.070	.065
19	.069	.080	.083	.092	.032	.039	.054	.072	.065	.080	.092	.105	.097	.067	.070	.075	.099
20	.103	.133	.147	.170	.032	.048	.068	.091	.103	.148	.176	.186	.194	.100	.116	.132	.146
21	.128	.189	.240	.291	.034	.049	.070	.105	.124	.188	.236	.292	.286	.093	.114	.142	.169
22	.125	.208	.290	.367	.026	.032	.062	.103	.140	.204	.264	.352	.353	.085	.090	.149	.184
23	.032	.033	.031	.032	.039	.037	.033	.038	.035	.046	.042	.063	.045	.045	.048	.046	.039
24	.037	.038	.035	.037	.058	.049	.043	.042	.040	.048	.045	.071	.046	.047	.056	.051	.054
25	.051	.051	.048	.049	.076	.077	.061	.066	.059	.067	.067	.050	.061	.057	.073	.074	.076
26	.065	.066	.063	.066	.055	.065	.069	.082	.058	.084	.080	.079	.078	.083	.087	.087	.091
27	.091	.100	.099	.107	.049	.059	.081	.107	.094	.124	.132	.131	.128	.117	.123	.128	.135
28	.127	.147	.156	.175	.049	.067	.093	.129	.139	.176	.194	.212	.202	.130	.150	.176	.191
29	.146	.216	.250	.297	.045	.059	.087	.136	.166	.244	.295	.344	.343	.143	.174	.214	.244
30	.158	.253	.421	.596	.041	.059	.083	.132	.187	.284	.439	.496	.510	.133	.169	.215	.268
31	.158	.278	.562	1.212	.031	.054	.049	.126	.183	.323	.480	.625	.684	.145	.182	.234	.276
32	.051	.049	.043	.043	.150	.097	.081	.068	.049	.070	.069	.049	.062	.082	.081	.078	.078
33	.065	.064	.058	.057	.099	.130	.097	.087	.062	.080	.083	.075	.073	.101	.101	.104	.091
34	.093	.095	.089	.091	.074	.099	.122	.125	.104	.123	.121	.123	.112	.142	.147	.143	.150
35	.127	.139	.137	.145	.068	.090	.121	.166	.155	.182	.191	.197	.186	.189	.197	.209	.213
36	.160	.190	.202	.223	.065	.088	.123	.176	.205	.248	.274	.294	.279	.207	.235	.267	.291
37	.180	.242	.287	.331	.066	.084	.127	.182	.229	.351	.400	.462	.457	.230	.273	.327	.383
38	.195	.290	.385	.483	.062	.080	.127	.190	.266	.406	.534	.666	.694	.231	.279	.351	.315
39	.207	.330	.471	.617	.057	.079	.118	.184	.271	.452	.645	.920	1.028	.225	.276	.369	.435
40	.194	.336	.505	.681	.039	.050	.094	.168	.250	.458	.714	1.081	1.518	.208	.263	.358	.443
41	.152	.165	.155	.159	.087	.116	.163	.206	.214	.258	.258	.252	.231	.313	.327	.316	.323
42	.169	.189	.184	.193	.086	.114	.160	.216	.239	.297	.304	.314	.288	.315	.371	.367	.363
43	.182	.219	.224	.244	.077	.106	.164	.218	.263	.345	.371	.392	.367	.295	.351	.416	.448
44	.196	.256	.280	.319	.071	.100	.144	.218	.270	.401	.457	.516	.494	.300	.361	.447	.526
45	.204	.284	.337	.403	.065	.090	.146	.223	.295	.451	.532	.642	.638	.290	.348	.447	.539
46	.215	.318	.407	.505	.061	.076	.162	.216	.287	.486	.634	.792	.823	.285	.356	.465	.578
47	.226	.354	.480	.613	.057	.076	.141	.224	.296	.536	.730	.941	1.054	.280	.351	.467	.596
48	.224	.376	.533	.702	.043	.065	.128	.213	.268	.555	.808	1.136	1.257	.239	.343	.475	.618
49	.235	.403	.588	.703	.042	.051	.112	.210	.325	.588	.874	1.267	1.421	.263	.345	.487	.641
50	.233	.338	.405	.494	.054	.112	.165	.255	.351	.552	.704	.831	.845	.338	.434	.592	.734
51	.305	.358	.443	.550	.055	.123	.166	.248	.364	.546	.743	.936	.962	.340	.432	.587	.671
52	.248	.381	.487	.613	.055	.111	.167	.253	.388	.606	.815	1.043	1.103	.331	.451	.616	.778
53	.256	.401	.525	.667	.054	.071	.141	.243	.337	.630	.866	1.119	1.203	.342	.448	.613	.725
54	.257	.411	.550	.702	.053	.078	.144	.252	.388	.639	.898	1.192	1.284	.328	.446	.570	.765
55	.272	.441	.603	.782	.053	.093	.142	.256	.333	.694	.963	1.341	1.428	.354	.455	.613	.795
56	.274	.457	.641	.842	.049	.085	.125	.246	.368	.702	1.036	1.433	1.557	.331	.435	.628	.802
57	.286	.479	.674	.890	.050	.075	.150	.260	.358	.735	1.064	1.507	1.657	.325	.452	.645	.850
58	.294	.469	.616	.789	.057	.108	.180	.296	.393	.777	1.062	1.370	1.426	.417	.516	.711	.915
59	.303	.490	.657	.854	.054	.103	.159	.296	.444	.792	1.113	1.460	1.627	.404	.537	.737	.970
60	.309	.510	.698	.909	.053	.097	.156	.309	.424	.807	1.148	1.627	1.700	.382	.519	.734	.990
61	.315	.530	.738	.971	.051	.087	.159	.292	.476	.835	1.211	1.691	1.859	.413	.536	.770	.928

TABLE IV

STRUCTURAL INFLUENCE-COEFFICIENT MEASUREMENTS – Continued

(a) Matrix [A] – Concluded

Load point	Panel deflection per unit load, meters/newton, measured at position:																
	45	46	47	48	49	50	51	52	53	54	55	56	57	58	59	60	61
11	$.062 \times 10^{-4}$	$.048 \times 10^{-4}$	$.055 \times 10^{-4}$	$.057 \times 10^{-4}$	$.050 \times 10^{-4}$	$.046 \times 10^{-4}$	$.057 \times 10^{-4}$	$.054 \times 10^{-4}$	$.066 \times 10^{-4}$	$.058 \times 10^{-4}$	$.056 \times 10^{-4}$	$.063 \times 10^{-4}$	$.063 \times 10^{-4}$	$.061 \times 10^{-4}$	$.063 \times 10^{-4}$	$.065 \times 10^{-4}$	$.070 \times 10^{-4}$
12	.105	.126	.129	.163	.160	.134	.140	.151	.144	.168	.160	.167	.190	.175	.181	.191	.199
13	.146	.158	.182	.206	.215	.163	.195	.200	.210	.160	.234	.254	.258	.234	.251	.255	.274
14	.013	.005	.010	.014	.010	.014	.003	.010	.017	.010	.007	.010	.005	.007	.006	.010	.011
15	.024	.026	.023	.024	.022	.029	.029	.027	.024	.026	.027	.024	.026	.027	.024	.036	.022
16	.037	.034	.035	.037	.033	.040	.047	.043	.040	.042	.043	.042	.040	.042	.043	.046	.043
17	.046	.040	.045	.045	.048	.050	.060	.055	.061	.056	.057	.057	.057	.058	.055	.063	.060
18	.072	.070	.070	.076	.074	.080	.088	.083	.087	.088	.086	.091	.092	.093	.093	.093	.095
19	.091	.099	.103	.103	.113	.104	.123	.123	.115	.123	.129	.135	.157	.141	.143	.144	.153
20	.163	.179	.194	.219	.227	.198	.220	.231	.213	.243	.258	.263	.277	.274	.281	.297	.308
21	.208	.237	.276	.298	.327	.242	.293	.311	.323	.346	.368	.329	.407	.371	.384	.414	.435
22	.231	.280	.329	.364	.405	.268	.338	.359	.403	.423	.443	.473	.513	.439	.446	.499	.531
23	.047	.049	.050	.049	.047	.055	.059	.057	.065	.058	.063	.059	.058	.065	.067	.065	.066
24	.058	.053	.051	.051	.053	.062	.065	.069	.070	.065	.067	.066	.056	.069	.070	.076	.069
25	.074	.073	.070	.069	.068	.082	.091	.087	.079	.087	.085	.083	.083	.093	.093	.095	.093
26	.090	.089	.089	.093	.094	.105	.112	.116	.122	.114	.116	.116	.114	.124	.126	.124	.130
27	.139	.145	.147	.155	.157	.170	.188	.192	.200	.194	.198	.199	.200	.220	.223	.226	.223
28	.206	.212	.231	.239	.252	.192	.284	.289	.303	.309	.318	.329	.329	.428	.353	.360	.375
29	.266	.319	.357	.393	.423	.354	.420	.438	.460	.480	.501	.522	.546	.536	.556	1.096	.605
30	.214	.407	.488	.505	.598	.423	.516	.560	.577	.649	.697	.722	.757	.697	.732	.796	.826
31	.394	.498	.608	.707	.780	.512	.611	.679	.710	.787	.841	.928	.973	.859	.920	1.005	1.063
32	.077	.077	.071	.079	.071	.091	.098	.094	.088	.089	.088	.088	.093	.106	.102	.103	.101
33	.093	.092	.091	.087	.087	.108	.120	.116	.122	.113	.115	.102	.106	.131	.131	.125	.125
34	.146	.144	.139	.147	.147	.095	.192	.108	.134	.123	.186	.166	.112	.212	.214	.212	.216
35	.223	.226	.228	.234	.238	.278	.305	.311	.276	.315	.319	.317	.322	.361	.372	.371	.369
36	.313	.326	.346	.355	.369	.400	.453	.457	.451	.480	.491	.504	.505	.558	.563	.574	.587
37	.427	.473	.521	.558	.597	.566	.653	.679	.698	.731	.761	.769	.803	.839	.860	.902	.932
38	.521	.617	.721	.808	.878	.699	.932	.898	.936	1.006	1.064	1.122	1.172	1.148	1.193	1.270	1.337
39	.577	.743	.928	1.080	1.209	.817	.990	1.096	1.179	1.294	1.371	1.457	1.585	1.456	1.551	1.670	1.770
40	.617	.817	1.080	1.294	1.454	.871	1.084	1.234	1.099	1.507	1.633	1.756	1.882	1.663	1.803	1.960	2.098
41	.320	.319	.319	.317	.316	.405	.455	.451	.447	.449	.456	.453	.444	.533	.531	.528	.526
42	.361	.381	.388	.393	.397	.493	.552	.553	.543	.556	.569	.563	.554	.654	.656	.664	.666
43	.462	.468	.489	.498	.511	.613	.690	.707	.683	.717	.714	.728	.741	.838	.844	.853	.871
44	.548	.587	.630	.658	.688	.764	.876	.898	.871	.931	.952	.973	.986	1.102	1.119	1.147	1.177
45	.630	.694	.776	.838	.891	.895	1.027	1.075	1.109	1.159	1.200	1.252	1.282	1.381	1.408	1.469	1.521
46	.695	.836	.972	1.088	1.187	1.029	1.216	1.316	1.347	1.473	1.550	1.642	1.703	1.724	1.816	1.921	2.009
47	.759	.960	1.208	1.410	1.592	1.155	1.430	1.569	1.657	1.858	1.978	1.953	2.244	2.181	2.325	2.482	2.623
48	.808	1.064	1.404	1.788	2.128	1.262	1.586	1.810	1.983	2.239	2.414	2.656	2.852	2.613	2.831	3.074	3.299
49	.867	1.173	1.594	2.132	2.803	1.363	1.753	2.018	2.514	2.579	2.829	3.109	3.359	3.027	3.288	3.612	3.902
50	.874	1.008	1.143	1.245	1.347	1.440	1.618	1.739	1.759	1.832	1.950	2.025	2.090	2.330	2.360	2.483	2.724
51	.899	1.093	1.302	1.424	1.570	1.528	1.774	1.908	1.931	2.133	2.253	2.356	2.428	2.643	2.765	2.912	3.026
52	.954	1.159	1.414	1.636	1.851	1.577	1.928	2.136	2.225	2.451	2.600	2.757	2.905	3.040	3.216	3.415	3.617
53	.982	1.236	1.557	1.844	2.092	1.637	2.011	2.271	2.471	2.722	2.914	3.150	3.332	3.450	3.649	3.894	4.096
54	.994	1.292	1.602	1.964	2.262	1.679	2.067	2.351	2.590	2.901	3.135	3.435	3.633	3.713	3.961	4.279	4.528
55	1.058	1.393	1.824	2.230	2.624	1.806	2.253	2.608	2.914	3.241	3.612	3.935	4.236	4.201	4.534	4.872	5.293
56	1.109	1.460	1.941	2.412	2.846	1.881	2.392	2.766	3.100	3.543	3.905	4.369	4.677	4.566	5.007	5.485	5.908
57	1.139	.955	2.060	2.588	3.059	1.930	2.496	2.903	3.258	3.798	4.172	4.702	5.211	4.882	5.427	6.029	6.578
58	1.215	1.597	1.978	2.379	2.751	2.161	2.719	3.081	3.381	3.849	4.133	4.607	4.927	5.716	6.142	6.526	6.891
59	1.265	1.676	2.150	2.621	3.042	2.260	2.870	3.282	3.575	4.186	4.582	5.113	5.498	6.165	7.019	7.615	8.319
60	1.288	1.729	2.275	2.800	3.287	2.357	2.941	3.446	3.851	4.470	4.871	5.462	6.072	6.528	7.566	8.750	9.833
61	1.346	1.806	2.407	3.012	3.532	2.391	3.070	3.615	4.121	4.769	5.270	5.983	6.623	6.932	8.200	9.797	11.652

TABLE IV

STRUCTURAL INFLUENCE-COEFFICIENT MEASUREMENTS – Continued

(b) Matrix [B]

Load point	Panel deflection per unit load, meters/newton, measured at position:																
	11	12	13	14	15	16	17	18	19	20	21	22	23	24	25	26	27
11	$.046 \times 10^{-4}$	$.057 \times 10^{-4}$	$.071 \times 10^{-4}$	$.010 \times 10^{-4}$	$.015 \times 10^{-4}$	$.022 \times 10^{-4}$	$.028 \times 10^{-4}$	$.035 \times 10^{-4}$	$.047 \times 10^{-4}$	$.059 \times 10^{-4}$	$.067 \times 10^{-4}$	$.071 \times 10^{-4}$	$.019 \times 10^{-4}$	$.022 \times 10^{-4}$	$.027 \times 10^{-4}$	$.035 \times 10^{-4}$	$.042 \times 10^{-4}$
12	.064	.069	.126	.010	.017	.026	.032	.044	.066	.094	.114	.126	.022	.025	.031	.043	.056
13	.087	.138	.224	.012	.018	.029	.037	.059	.091	.143	.188	.214	.023	.027	.035	.054	.079
14	.006	.006	.006	0.000	.001	.003	.003	.003	.003	.005	.005	.005	0.000	.001	.001	.001	.002
15	.011	.011	.011	0.000	.002	.006	.009	.009	.010	.010	.010	.010	.002	.004	.006	.007	.007
16	.016	.017	.018	.005	.006	.009	.011	.013	.014	.015	.016	.017	.005	.006	.009	.010	.010
17	.026	.027	.029	.005	.009	.013	.019	.022	.024	.026	.028	.028	.010	.014	.017	.019	.021
18	.035	.039	.050	.007	.011	.018	.023	.027	.033	.037	.041	.042	.013	.017	.021	.023	.026
19	.046	.058	.075	.009	.014	.021	.026	.033	.043	.055	.065	.075	.016	.019	.022	.027	.033
20	.059	.083	.120	.009	.014	.023	.030	.039	.057	.078	.099	.108	.017	.021	.026	.034	.043
21	.070	.104	.159	.009	.015	.024	.031	.043	.067	.100	.126	.141	.018	.021	.026	.037	.050
22	.062	.097	.158	.006	.010	.018	.024	.034	.112	.093	.120	.135	.013	.015	.019	.027	.040
23	.012	.013	.013	.001	.002	.004	.006	.007	.009	.009	.010	.010	-.003	-.001	.001	.002	.003
24	.016	.017	.017	.001	.003	.006	.009	.010	.012	.013	.014	.014	-.001	.001	.004	.006	.006
25	.020	.021	.022	.002	.005	.009	.013	.014	.015	.017	.018	.018	.002	.005	.007	.008	.009
26	.027	.032	.037	.004	.007	.013	.017	.019	.021	.026	.029	.030	.006	.008	.010	.010	.011
27	.037	.046	.060	.005	.009	.015	.019	.023	.029	.038	.045	.048	.007	.010	.012	.013	.014
28	.045	.061	.086	.003	.009	.016	.021	.027	.036	.051	.062	.067	.008	.011	.013	.015	.018
29	.051	.077	.118	.005	.009	.017	.022	.029	.044	.066	.082	.092	.009	.011	.014	.017	.024
30	.055	.085	.138	.003	.008	.016	.022	.030	.046	.073	.095	.106	.008	.011	.013	.017	.025
31	.054	.087	.145	.001	.007	.015	.021	.028	.046	.074	.097	.110	.007	.010	.013	.016	.024
32	-.016	-.017	-.017	.001	.002	-.005	-.008	-.009	-.008	-.009	-.010	-.010	.005	.003	.002	.001	.001
33	-.020	-.022	-.022	.001	-.003	-.007	-.010	-.011	-.011	-.013	-.013	-.013	.002	0.000	-.001	0.000	0.000
34	-.026	-.032	-.039	-.001	-.004	-.009	-.011	-.013	-.014	-.019	-.022	-.024	.001	-.001	0.000	.002	.002
35	-.034	-.046	-.065	-.002	-.006	-.010	-.013	-.009	-.021	-.030	-.038	-.042	-.001	-.001	0.000	.001	.001
36	-.040	-.058	-.089	-.002	-.006	-.011	-.014	-.018	-.027	-.042	-.053	-.050	-.002	-.002	-.001	-.002	-.008
37	-.050	-.075	-.119	-.002	-.007	-.010	-.013	-.023	-.036	-.057	-.073	-.081	-.003	-.004	-.003	-.005	-.008
38	-.056	-.087	-.143	-.002	-.007	-.013	-.018	-.025	-.042	-.067	-.087	-.098	-.003	-.005	-.003	-.006	-.011
39	-.055	-.091	-.156	-.005	-.007	-.013	-.015	-.023	-.041	-.070	-.094	-.106	-.004	-.004	-.002	-.003	-.009
40	-.048	-.083	-.159	-.008	-.009	-.011	-.014	-.018	-.035	-.063	-.085	-.099	-.005	-.005	0.000	-.001	-.003
41	-.027	-.037	-.052	.004	-.001	-.006	-.009	-.009	-.009	-.013	-.019	-.021	.007	.005	.008	.013	.018
42	-.030	-.043	-.065	.002	-.001	-.006	-.008	-.009	-.011	-.020	-.026	-.029	.007	.006	.010	.014	.018
43	-.034	-.049	-.079	.001	-.002	-.007	-.009	-.010	-.014	-.026	-.033	-.038	.005	.005	.009	.014	.017
44	-.039	-.059	-.098	.001	-.007	-.007	-.010	-.012	-.019	-.033	-.045	-.050	.005	.005	.009	.013	.014
45	-.045	-.070	-.119	.001	-.003	-.008	-.009	-.013	-.023	-.042	-.057	-.065	.005	.006	.010	.014	.015
46	-.047	-.075	-.130	.003	-.002	-.010	-.013	-.017	-.027	-.048	-.065	-.074	.003	.002	.005	.009	.009
47	-.049	-.083	-.149	-.004	-.005	-.009	-.010	-.014	-.028	-.054	-.075	-.087	.002	.003	.009	.013	.013
48	-.050	-.083	-.152	-.001	-.005	-.011	-.015	-.019	-.031	-.058	-.078	-.089	-.002	-.003	0.000	.004	.004
49	-.054	-.090	-.163	.002	-.005	-.013	-.018	-.022	-.035	-.063	-.086	-.097	-.003	-.005	-.002	.002	.001
50	-.038	-.061	-.109	.003	-.005	-.009	-.012	-.012	-.016	-.030	-.041	-.047	.003	.001	.005	.014	.021
51	-.039	-.066	-.118	.001	-.003	-.008	-.012	-.013	-.018	-.035	-.048	-.054	.003	.001	.006	.014	.019
52	-.041	-.070	-.125	-.002	-.004	-.012	-.012	-.011	-.018	-.035	-.050	-.060	.002	.001	.007	.016	.022
53	-.042	-.074	-.136	.001	-.003	-.010	-.011	-.014	-.022	-.042	-.058	-.067	.002	-.001	.005	.013	.019
54	-.016	-.078	-.144	.002	-.003	-.010	-.013	-.014	-.024	-.045	-.063	-.071	.002	-.001	.005	.014	.018
55	-.047	-.084	-.154	.001	-.003	-.010	-.013	-.014	-.025	-.048	-.069	-.090	.001	-.001	.005	.014	.017
56	-.047	-.088	-.164	-.002	-.005	-.010	-.011	-.013	-.024	-.051	-.074	-.086	.001	0.000	.008	.015	.019
57	-.055	-.095	-.175	.001	-.003	-.010	-.014	-.018	-.031	-.062	-.081	-.092	-.002	-.001	.004	.011	.014
58	-.045	-.080	-.151	.002	-.001	-.009	-.010	-.010	-.018	-.039	-.058	-.067	.003	.002	.011	.023	.030
59	-.046	-.083	-.160	-.001	-.003	-.009	-.010	-.009	-.017	-.041	-.062	-.072	.002	.002	.013	.023	.028
60	-.050	-.088	-.169	.005	-.001	-.009	-.013	-.013	-.022	-.047	-.068	-.078	.004	.002	.011	.021	.026
61	-.052	-.096	-.184	.001	-.004	-.010	-.014	-.014	-.025	-.053	-.076	-.087	.003	.001	.010	.021	.033

TABLE IV

STRUCTURAL INFLUENCE-COEFFICIENT MEASUREMENTS – Continued

(b) Matrix [B] – Continued

Load point	Panel deflection per unit load, meters/newton, measured at position:																
	28	29	30	31	32	33	34	35	36	37	38	39	40	41	42	43	44
11	$.058\times10^{-4}$	$.061\times10^{-4}$	$.064\times10^{-4}$	$.071\times10^{-4}$	$.026\times10^{-4}$	$.030\times10^{-4}$	$.035\times10^{-4}$	$.042\times10^{-4}$	$.051\times10^{-4}$	$.064\times10^{-4}$	$.070\times10^{-4}$	$.077\times10^{-4}$	$.075\times10^{-4}$	$.039\times10^{-4}$	$.051\times10^{-4}$	$.049\times10^{-4}$	$.066\times10^{-4}$
12	.078	.099	.109	.126	.028	.034	.034	.063	.074	.100	.119	.122	.128	.053	.064	.073	.087
13	.116	.158	.181	.212	.029	.048	.067	.083	.106	.161	.195	.216	.225	.076	.094	.111	.136
14	.002	.002	.003	.004	-.001	.002	.003	.005	-.003	.002	.001	-.010	.005	-.003	-.005	-.007	-.006
15	.009	.008	.007	.007	.003	.003	.006	.003	.003	.009	.006	.010	.004	.003	.005	.007	.006
16	.012	.013	.013	.014	.006	.005	.011	.009	.002	.011	.014	-.014	.013	.005	.010	.008	.002
17	.023	.025	.023	.026	.013	.019	.015	.017	.015	.026	.026	.017	.018	.016	.017	.018	.009
18	.030	.034	.034	.038	.017	.016	.021	.024	.019	.033	.036	.029	.035	.018	.015	.023	.019
19	.042	.052	.056	.061	.018	.021	.021	.027	.029	.042	.053	.047	.057	.019	.021	.026	.035
20	.059	.077	.085	.097	.019	.024	.032	.038	.047	.069	.085	.078	.094	.029	.031	.043	.044
21	.072	.095	.107	.124	.024	.033	.043	.043	.047	.085	.107	.117	.125	.031	.038	.050	.059
22	.062	.086	.098	.115	.011	.019	.017	.038	.038	.076	.096	.099	.112	.017	.023	.033	.046
23	.005	.005	.006	.007	-.004	-.003	.003	-.002	.008	.003	.005	-.007	.008	-.002	-.004	-.005	-.003
24	.007	.009	.010	.010	-.002	-.001	-.003	.003	.009	.003	.010	.009	.009	-.003	-.003	-.002	.012
25	.010	.011	.011	.012	.001	.003	-.015	.005	.001	.005	.005	.006	.005	-.003	-.005	-.002	-.002
26	.014	.017	.018	.020	.003	.002	.002	.004	0.000	.011	.010	.013	.015	-.008	-.005	-.006	-.005
27	.019	.026	.029	.033	.004	.008	-.001	.003	.003	.010	.019	.024	.022	-.010	-.011	-.006	-.007
28	.026	.035	.041	.047	.004	.006	.003	.005	.011	.019	.027	.032	.031	-.011	-.011	-.006	-.018
29	.035	.049	.057	.067	.004	.006	.009	.006	.021	.025	.037	.052	-.049	-.011	-.013	-.003	-.008
30	.038	.055	.065	.077	.003	-.001	.008	.014	.010	.034	.050	.056	.054	-.022	-.018	-.003	.009
31	.038	.056	.066	.078	.002	-.003	.007	.009	.013	.035	.047	.053	.057	-.021	-.007	-.006	-.002
32	.001	.001	0.000	0.000	.010	.010	.010	.008	.015	.014	.009	.012	.009	.019	.022	.022	.016
33	.001	.001	0.000	0.000	.008	.012	.012	.015	.018	.015	.013	.015	.011	.026	.029	.027	.027
34	.001	-.001	-.003	-.005	.011	.012	.018	.018	.021	.019	.017	.003	.011	.034	.039	.038	.040
35	-.004	-.008	-.012	-.015	.012	.016	.025	.021	.025	.016	.010	.015	.004	.045	.042	.047	.039
36	-.017	-.022	-.026	.025	.014	.017	.019	.021	-.001	.013	.009	.002	-.006	.045	.045	.045	.045
37	-.017	-.029	-.037	-.044	.011	-.012	.018	.016	.018	.003	-.013	-.025	-.023	.042	.050	.040	.038
38	-.023	-.038	-.047	-.057	.013	.012	.008	.014	.019	-.003	-.020	-.033	-.029	.046	.042	.043	.040
39	-.022	-.039	-.051	-.062	.012	.014	.009	.017	.015	-.007	-.026	-.037	-.029	.045	.047	.040	.032
40	-.017	-.034	-.045	-.057	.011	.029	.039	.018	.013	-.001	-.003	.047	-.020	.057	.048	.049	.032
41	.018	.017	.015	.015	.024	.030	.051	.045	.056	.054	.052	.049	.045	.073	.083	.074	.089
42	.018	.015	.011	.011	.026	.032	.042	.050	.054	.037	.055	.030	.046	.078	.087	.086	.087
43	.016	.012	.007	.006	.024	.033	.047	.054	.054	.051	.049	.063	.041	.079	.083	.087	.084
44	.011	.005	0.000	-.003	.026	.037	.040	.044	.050	.050	.045	.066	.038	.078	.088	.084	.079
45	.009	-.001	-.008	-.013	.028	.039	.039	.055	.051	.049	.044	.034	.029	.087	.094	.088	.095
46	.003	-.007	-.014	-.020	.035	.035	.035	.046	.053	.041	.036	.035	.017	.085	.082	.089	.070
47	.003	-.011	-.021	-.030	.027	.034	.030	.043	.054	.040	.037	-.001	.007	.081	.089	.097	.086
48	-.005	-.018	-.027	-.034	.015	.022	.023	.037	.044	.045	.013	.036	.003	.069	.078	.071	.061
49	-.007	-.022	-.033	-.041	.013	.015	.029	.043	.029	.029	.018	-.017	.017	.074	.073	.070	.085
50	.022	.017	.013	.010	.021	.035	.035	.061	.057	.078	.062	.095	.069	.091	.092	.124	.087
51	.019	.013	.008	.005	.022	.023	.042	.067	.057	.058	.070	.037	.050	.085	.112	.132	.099
52	.021	.015	.007	.006	.024	.041	.041	.075	.082	.076	.056	.083	.039	.100	.110	.108	.089
53	-.016	.008	.001	-.003	.021	.039	.034	.053	.035	.069	.042	.085	.047	.096	.120	.122	.171
54	.015	.006	-.002	-.006	.022	.018	.047	.059	.071	.078	.037	.052	.038	.092	.096	.102	.074
55	.013	.002	-.006	-.013	.023	.015	.022	.044	.076	.077	.057	.008	.029	.104	.113	.110	.114
56	.012	-.001	-.010	-.017	.025	.030	.044	.072	.069	.053	.042	.043	.053	.100	.113	.116	.119
57	.008	-.005	-.014	-.021	.023	.033	.042	.057	.073	.065	.056	.027	.018	.089	.099	.093	.125
58	.028	.020	.013	.009	.026	.071	.058	.082	.089	.060	.081	.082	.063	.104	.130	.135	.105
59	.026	.020	.009	.005	.031	.054	.058	.097	.102	.095	.086	.034	.048	.122	.045	.137	.068
60	.025	.015	.006	.002	.030	.043	.058	.077	.087	.069	.076	.070	.065	.137	.145	.131	.067
61	.024	.013	.002	-.002	.031	.042	.040	.106	.092	.095	.086	.087	.047	.147	.131	.137	.118

TABLE IV

STRUCTURAL INFLUENCE-COEFFICIENT MEASUREMENTS – Concluded

(b) Matrix [B] – Concluded

Load point	Panel deflection per unit load, meters/newton, measured at position:															
	45	46	47	48	49	50	51	52	53	54	55	56	57	58	59	60	61
11	.066×10^{-4}	.066×10^{-4}	.073×10^{-4}	.073×10^{-4}	.079×10^{-4}	.066×10^{-4}	.070×10^{-4}	.081×10^{-4}	.073×10^{-4}	.083×10^{-4}	.089×10^{-4}	.083×10^{-4}	.088×10^{-4}	.079×10^{-4}	.082×10^{-4}	.081×10^{-4}	.082×10^{-4}
12	.101	.110	.122	.131	.140	.106	.122	.127	.135	.142	.138	.155	.163	.147	.149	.163	.163
13	.159	.184	.208	.229	.244	.240	.212	.223	.231	.251	.260	.277	.282	.254	.270	.284	.295
14	0.000	-.003	.002	.001	.002	-.002	.002	.002	-.005	.002	.004	.002	.002	-.001	.001	.002	.002
15	.003	.003	.006	.005	.003	-.002	-.002	.002	.008	.002	.005	.005	.002	0.000	.001	-.001	-.003
16	.010	.006	.009	.009	.009	.005	.009	.005	.002	.005	0.000	.006	.011	.002	.002	-.001	.001
17	.022	.020	.023	.024	.021	.017	.017	.019	.025	.018	.018	.018	.015	.017	.016	.007	.014
18	.030	.029	.029	.031	.031	.023	.020	.025	.024	.029	.025	.027	.031	.022	.022	.021	.023
19	.028	.037	.043	.051	.052	.045	.034	.038	.036	.036	.054	.049	.042	.036	.039	.045	.031
20	.060	.065	.074	.083	.083	.055	.065	.069	.078	.079	.079	.087	.089	.070	.073	.084	.086
21	.067	.089	.097	.107	.114	.063	.082	.082	.095	.097	.107	.112	.108	.086	.097	.103	.108
22	.053	.075	.079	.094	.096	.046	.054	.069	.081	.081	.079	.090	.104	.067	.074	.073	.087
23	-.001	0.000	.002	.005	.005	-.002	-.003	-.001	-.005	-.001	.001	.004	.006	-.002	-.001	.001	.004
24	.002	.002	.002	.003	.002	-.004	-.003	-.005	-.002	.001	-.003	.002	.004	-.003	-.001	-.007	.001
25	.003	-.001	.001	0.000	.002	-.007	-.004	-.007	-.003	-.005	-.007	-.005	-.004	-.009	-.013	-.006	-.007
26	-.005	0.000	.001	.002	.002	-.010	-.013	-.013	-.003	-.011	-.007	-.007	-.005	-.016	-.013	-.012	-.008
27	0.000	-.003	.003	.008	.011	-.015	-.011	-.011	-.006	-.013	-.006	-.002	-.006	-.019	-.018	-.014	-.017
28	0.000	-.004	.013	.014	.020	-.018	-.013	-.011	-.016	-.007	-.003	-.002	.003	-.024	-.019	-.015	-.010
29	.006	.015	.020	.032	.034	-.010	-.007	-.005	.011	.006	.002	.020	.023	-.018	-.003	-.002	-.005
30	.014	.017	.030	.038	.049	-.011	-.006	0.000	0.000	.013	.020	.023	.019	-.008	0.000	.009	.021
31	.011	.010	.024	.038	.044	-.010	-.021	0.000	-.013	.013	.017	.023	.031	-.005	.003	.007	.021
32	.015	.020	.019	.020	.015	.030	.034	.034	.030	.034	.033	.031	.028	.038	.040	.037	.042
33	.031	.025	.026	.022	.024	.043	.047	.050	.048	.043	.043	.043	.039	.054	.053	.051	.053
34	.037	.035	.034	.033	.032	.054	.064	.062	.051	.057	.053	.057	.054	.074	.074	.070	.077
35	.040	.035	.035	.030	.031	.004	.072	.073	.062	.065	.065	.058	.057	.086	.086	.078	.084
36	.043	.029	.028	.024	.067	.067	.067	.062	.062	.063	.061	.037	.057	.097	.089	.083	.083
37	.031	.025	.017	.018	.014	.062	.066	.059	.069	.055	.053	.050	.039	.086	.078	.067	.074
38	.033	.018	.012	.007	.001	.060	.059	.058	.057	.047	.045	.035	.034	.079	.074	.070	.066
39	.027	.019	.011	.009	-.005	.061	.060	.054	.053	.052	.038	.035	.030	.079	.068	.057	.056
40	.027	.022	.013	.005	-.002	.056	.068	.065	.079	.041	.039	.046	.060	.079	.073	.019	.059
41	.081	.085	.083	.083	.078	.122	.134	.134	.139	.134	.143	.127	.123	.162	.157	.160	.162
42	.088	.083	.086	.081	.083	.126	.141	.136	.144	.137	.121	.134	.142	.167	.172	.166	.167
43	.090	.087	.082	.080	.075	.127	.140	.140	.132	.132	.130	.133	.129	.173	.163	.163	.168
44	.087	.089	.083	.078	.081	.131	.136	.148	.140	.141	.137	.140	.136	.176	.179	.182	.171
45	.090	.081	.081	.070	.072	.135	.146	.141	.136	.136	.133	.130	.132	.176	.171	.176	.172
46	.081	.070	.074	.062	.054	.131	.143	.142	.126	.126	.123	.118	.117	.165	.167	.151	.151
47	.079	.076	.070	.059	.056	.130	.127	.125	.125	.124	.113	.107	.105	.165	.164	.144	.151
48	.062	.063	.057	.049	.043	.111	.124	.122	.085	.113	.113	.107	.093	.130	.132	.141	.127
49	.071	.068	.049	.037	.041	.111	.119	.121	.102	.099	.083	.086	.108	.136	.132	.142	.113
50	.099	.102	.103	.103	.106	.152	.179	.195	.176	.174	.160	.165	.167	.203	.197	.199	.203
51	.107	.111	.099	.108	.079	.155	.174	.156	.180	.162	.120	.148	.168	.213	.195	.172	.160
52	.130	.108	.106	.098	.087	.155	.134	.195	.152	.155	.164	.157	.119	.200	.206	.210	.194
53	.109	.103	.094	.095	.097	.163	.166	.180	.142	.163	.167	.156	.172	.204	.203	.189	.190
54	.099	.091	.099	.095	.082	.150	.178	.178	.173	.173	.185	.146	.137	.199	.178	.174	.199
55	.106	.107	.095	.089	.085	.162	.175	.180	.151	.157	.141	.139	.109	.191	.181	.204	.193
56	.100	.094	.102	.087	.094	.154	.175	.163	.171	.158	.152	.127	.110	.208	.191	.182	.197
57	.116	.112	.094	.085	.080	.162	.195	.170	.170	.170	.180	.138	.179	.193	.208	.195	.197
58	.151	.142	.123	.130	.142	.204	.221	.211	.213	.205	.181	.201	.194	.256	.246	.264	.228
59	.149	.119	.121	.124	.101	.138	.232	.210	.209	.222	.204	.172	.176	.251	.225	.238	.226
60	.126	.134	.140	.123	.118	.201	.234	.213	.211	.202	.208	.163	.204	.274	.248	.239	.260
61	.165	.138	.140	.128	.104	.218	.267	.211	.208	.229	.224	.211	.143	.264	.258	.286	.290

TABLE V

LONGITUDINAL AERODYNAMIC CHARACTERISTICS – INFLUENCE-COEFFICIENT METHOD

Characteristic	Flexible with mass	Flexible – massless	Rigid
C_{L_α}	$\frac{\lfloor 1 \rfloor [G] \{1\}}{S\left(1 + \frac{q}{W} \lfloor 1 \rfloor [G] [\Theta] \{W\}\right)}$	$\frac{\lfloor 1 \rfloor [G] \{1\}}{S}$	$\frac{\lfloor 1 \rfloor \lceil S \rfloor [A] \{1\}}{S}$
C_{m_α}	$\frac{1}{S\bar{c}}\left(\lfloor 1 \rfloor \lceil X \rfloor [G] \{1\} - \frac{q \lfloor 1 \rfloor \lceil X \rfloor [G] [\Theta] \{W\} \lfloor 1 \rfloor [G] \{1\}}{\left(W + q \lfloor 1 \rfloor [G] [\Theta] \{W\}\right)}\right)$	$\frac{\lfloor 1 \rfloor \lceil X \rfloor [G] \{1\}}{S\bar{c}}$	$\frac{\lfloor 1 \rfloor \lceil X \rfloor \lceil S \rfloor [A] \{1\}}{S\bar{c}}$
$C_{L,o}$	$\frac{\lfloor 1 \rfloor [G] \{\alpha_o\}}{S\left(1 + \frac{q}{W} \lfloor 1 \rfloor [G] [\Theta] \{W\}\right)}$	$\frac{\lfloor 1 \rfloor [G] \{\alpha_o\}}{S}$	$\frac{\lfloor 1 \rfloor \lceil S \rfloor [A] \{\alpha_o\}}{S}$
$C_{m,o}$	$\frac{1}{S\bar{c}}\left(\lfloor 1 \rfloor \lceil X \rfloor [G] \{\alpha_o\} - \frac{q \lfloor 1 \rfloor \lceil X \rfloor [G] [\Theta] \{W\} \lfloor 1 \rfloor [G] \{\alpha_o\}}{\left(W + q \lfloor 1 \rfloor [G] [\Theta] \{W\}\right)}\right)$	$\frac{\lfloor 1 \rfloor \lceil X \rfloor [G] \{\alpha_o\}}{S\bar{c}}$	$\frac{\lfloor 1 \rfloor \lceil X \rfloor \lceil S \rfloor [A] \{\alpha_o\}}{S\bar{c}}$
C_{L_q}	$\frac{\lfloor 1 \rfloor [G] \{X\}}{SV\left(1 + \frac{q}{W} \lfloor 1 \rfloor [G] [\Theta] \{W\}\right)}$	$\frac{\lfloor 1 \rfloor [G] \{X\}}{SV}$	$\frac{\lfloor 1 \rfloor \lceil S \rfloor [A] \{X\}}{SV}$
C_{m_q}	$\frac{1}{S\bar{c}V}\left(\lfloor 1 \rfloor \lceil X \rfloor [G] \{X\} - \frac{q \lfloor 1 \rfloor \lceil X \rfloor [G] [\Theta] \{W\} \lfloor 1 \rfloor [G] \{X\}}{\left(W + q \lfloor 1 \rfloor [G] [\Theta] \{W\}\right)}\right)$	$\frac{\lfloor 1 \rfloor \lceil X \rfloor [G] \{X\}}{S\bar{c}V}$	$\frac{\lfloor 1 \rfloor \lceil X \rfloor \lceil S \rfloor [A] \{X\}}{S\bar{c}V}$
	where $[G] = \lceil S \rfloor [A] \left(\lceil 1 \rfloor - q [\Theta] \lceil S \rfloor [A]\right)^{-1}$		

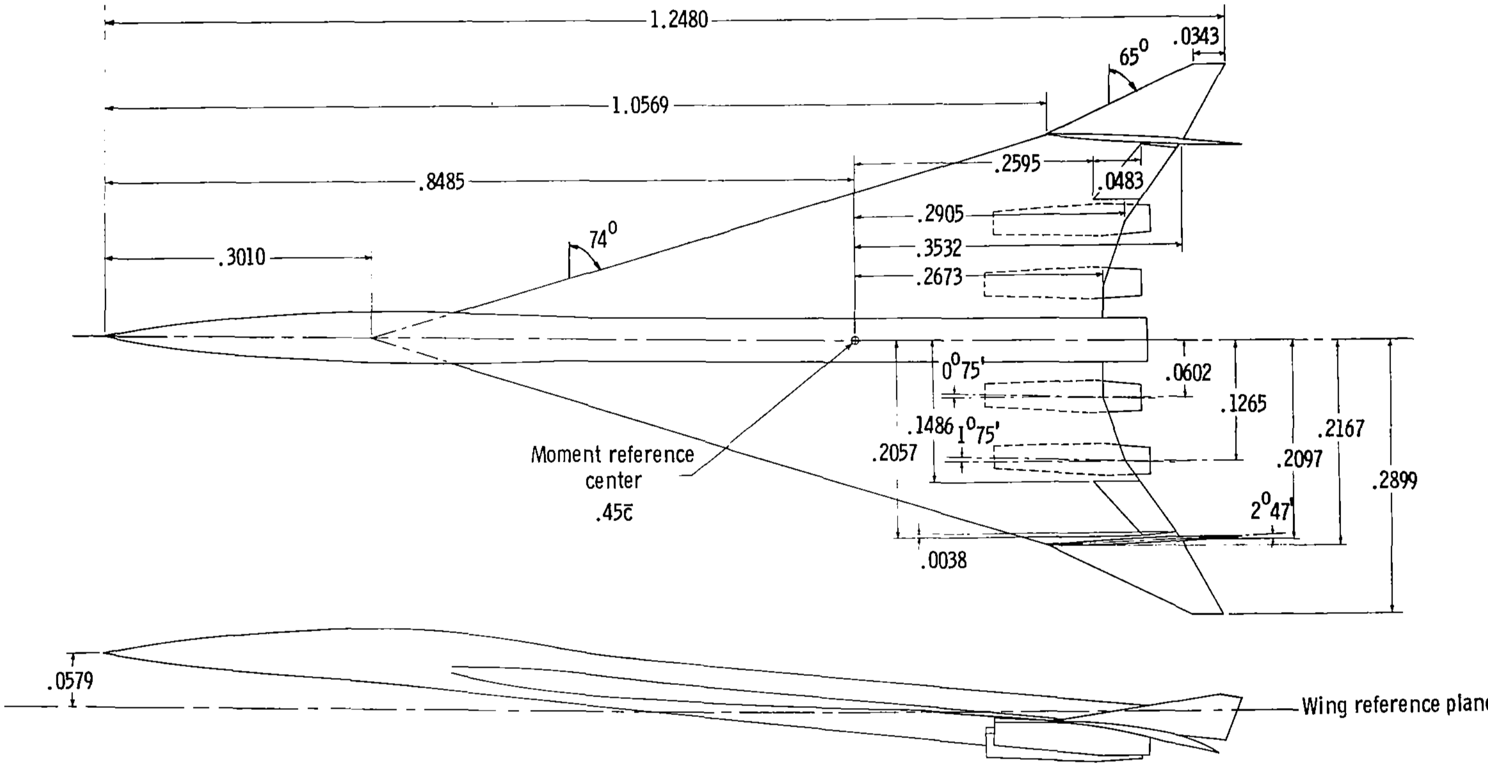

Figure 1.- Details of models. (All linear dimensions are in meters unless otherwise noted.)

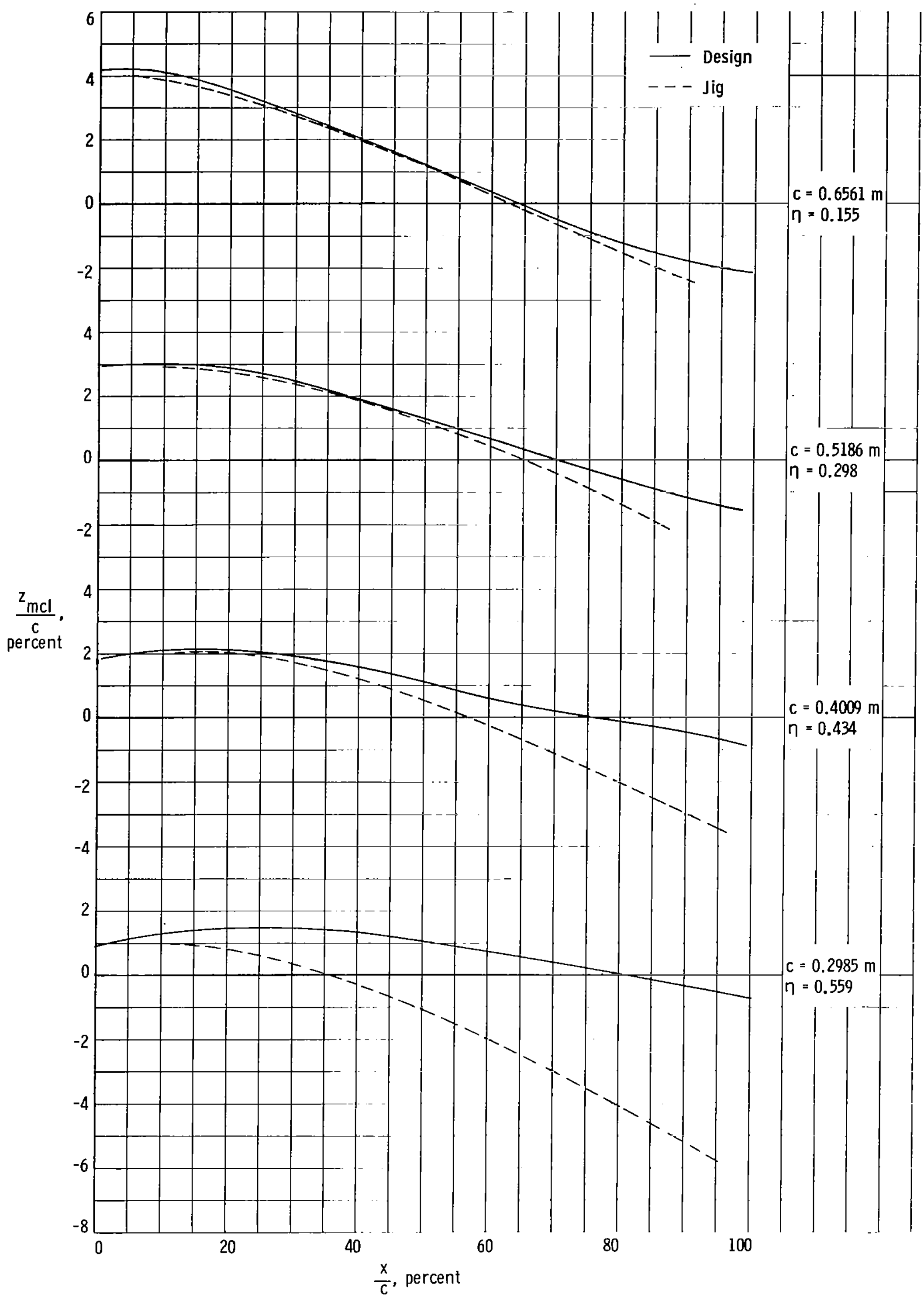

Figure 2.- Variation of mean-camber line for rigid and jig shapes.

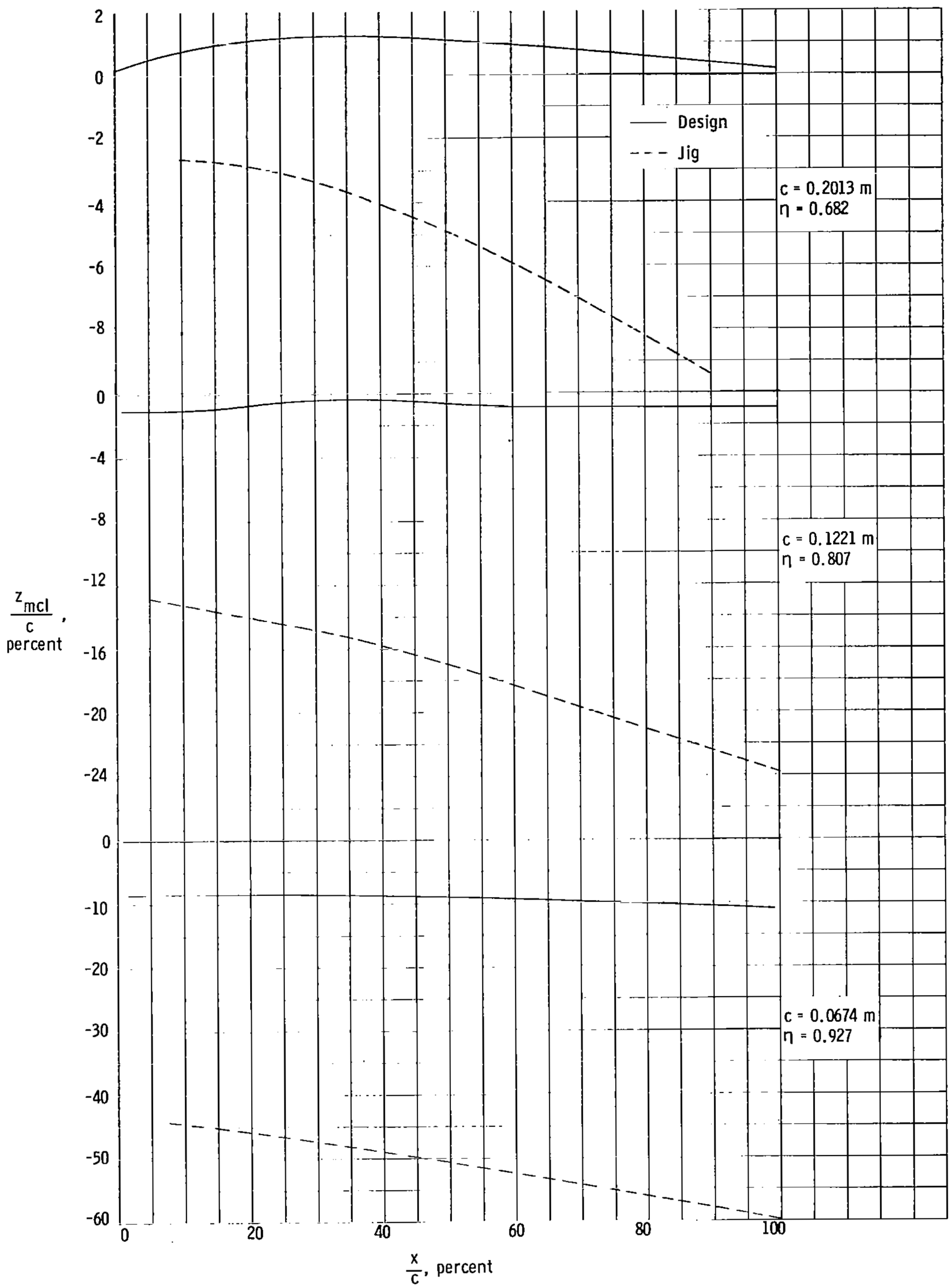

Figure 2.- Concluded.

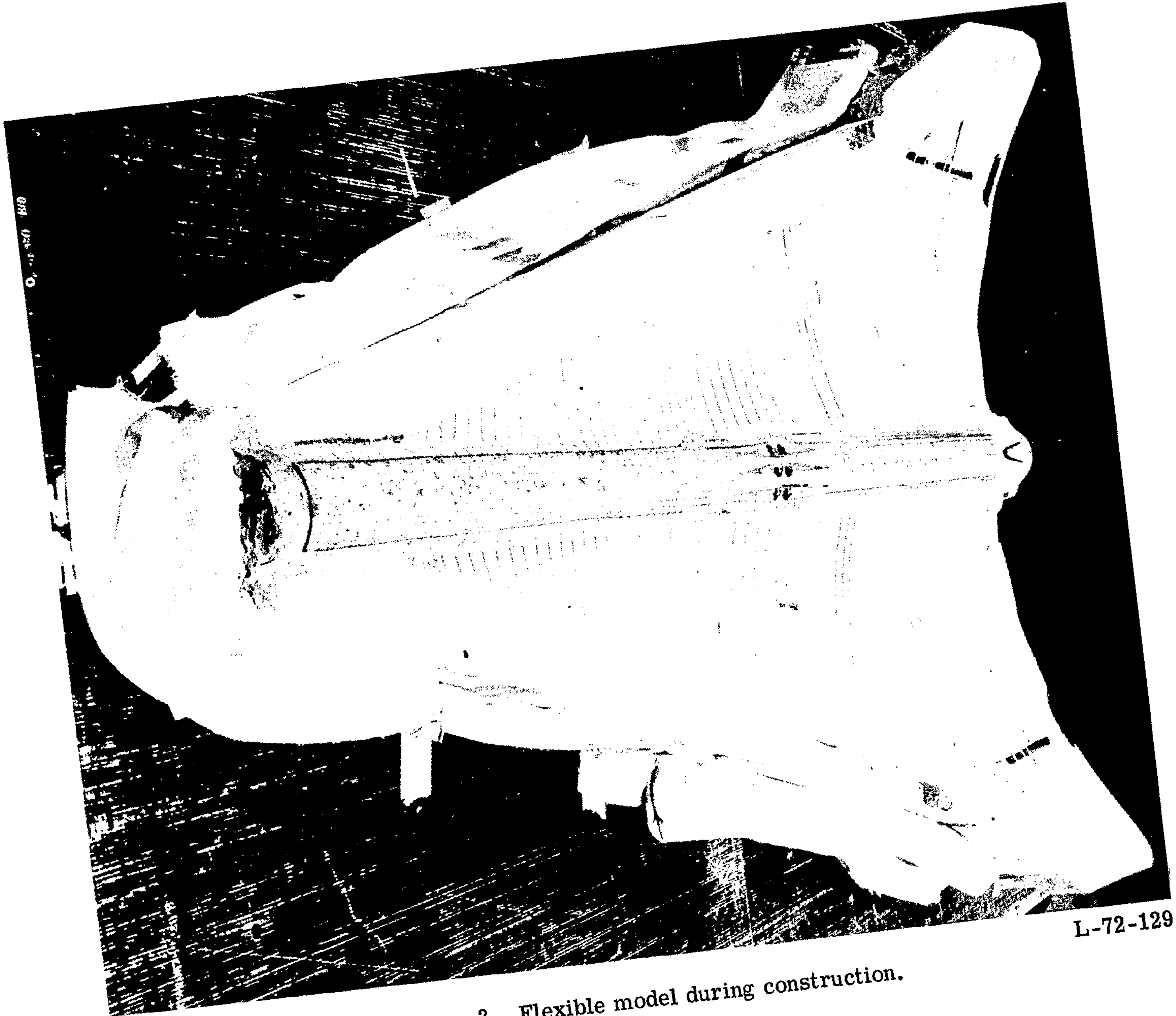

L-72-129

Figure 3.- Flexible model during construction.

L-70-619

Figure 4.- Flexible model prior to wind-tunnel test.

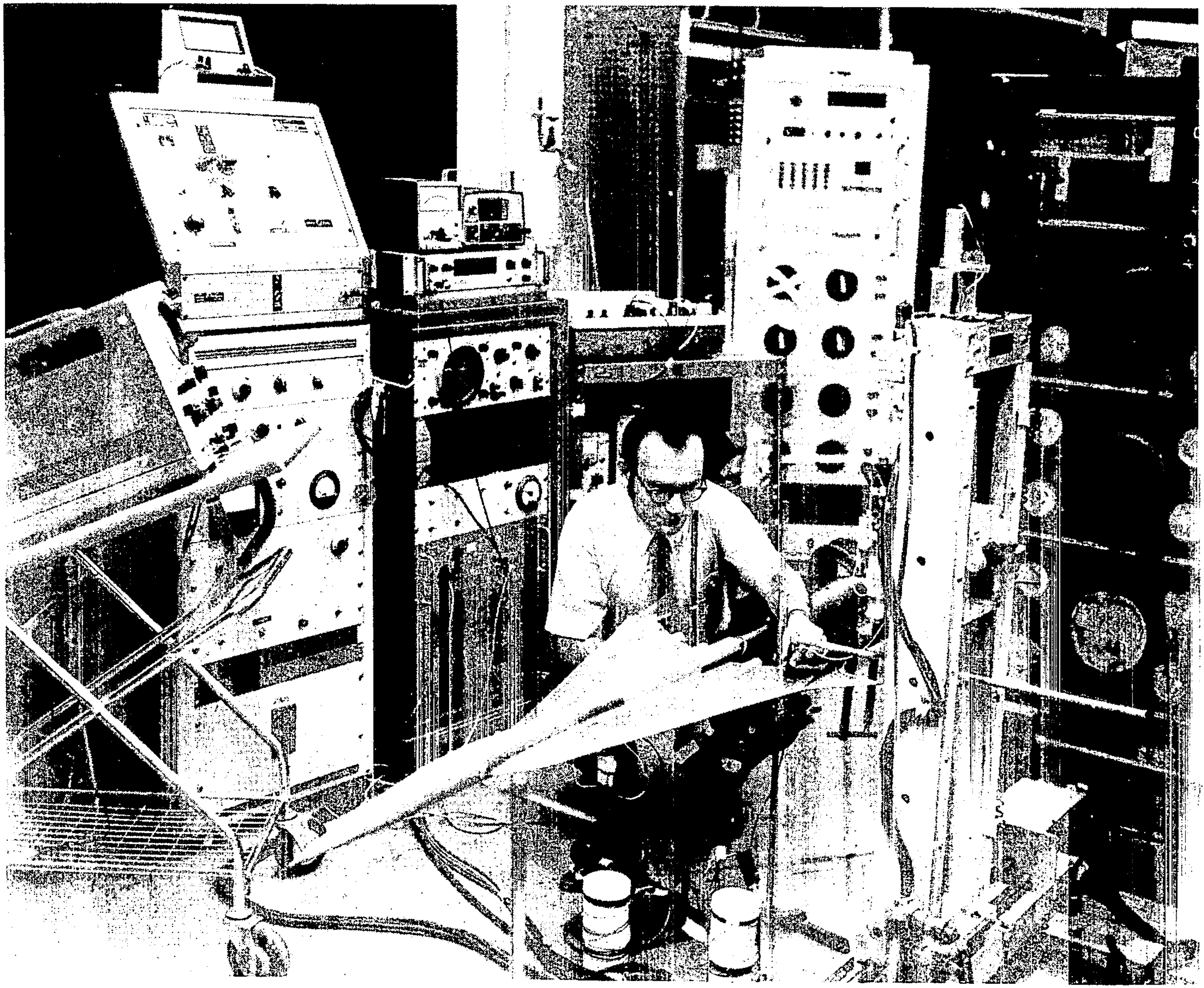

L-69-7866

Figure 5.- Mode-shape measuring apparatus.

Pt.	$\frac{x}{c}$	η	Pt.	$\frac{x}{c}$	η	Pt.	$\frac{x}{c}$	η	Pt.	$\frac{x}{c}$	η	Pt.	$\frac{x}{c}$	η	Pt.	$\frac{x}{c}$	η	Pt.	$\frac{x}{c}$	η
1	.031	.00	9	.018	.121	17	.026	.336	25	.038	.567	33	.055	.765	41	.054	.885	49	.061	.968
2	.170	.00	10	.154	.121	18	.161	.336	26	.171	.567	34	.183	.765	42	.180	.885	50	.193	.968
3	.308	.00	11	.290	.121	19	.297	.336	27	.304	.567	35	.312	.765	43	.303	.885	51	.315	.968
4	.445	.00	12	.426	.121	20	.432	.336	28	.437	.567	36	.441	.765	44	.429	.885	52	.447	.968
5	.584	.00	13	.562	.121	21	.566	.336	29	.569	.567	37	.571	.765	45	.554	.885	53	.563	.968
6	.733	.00	14	.698	.121	22	.701	.336	30	.702	.567	38	.700	.765	46	.680	.885	54	.695	.968
7	.860	.00	15	.837	.121	23	.836	.336	31	.825	.567	39	.830	.765	47	.811	.885	55	.822	.968
8	.998	.00	16	.982	.121	24	.973	.336	32	.967	.567	40	.965	.765	48	.940	.885	56	.954	.968

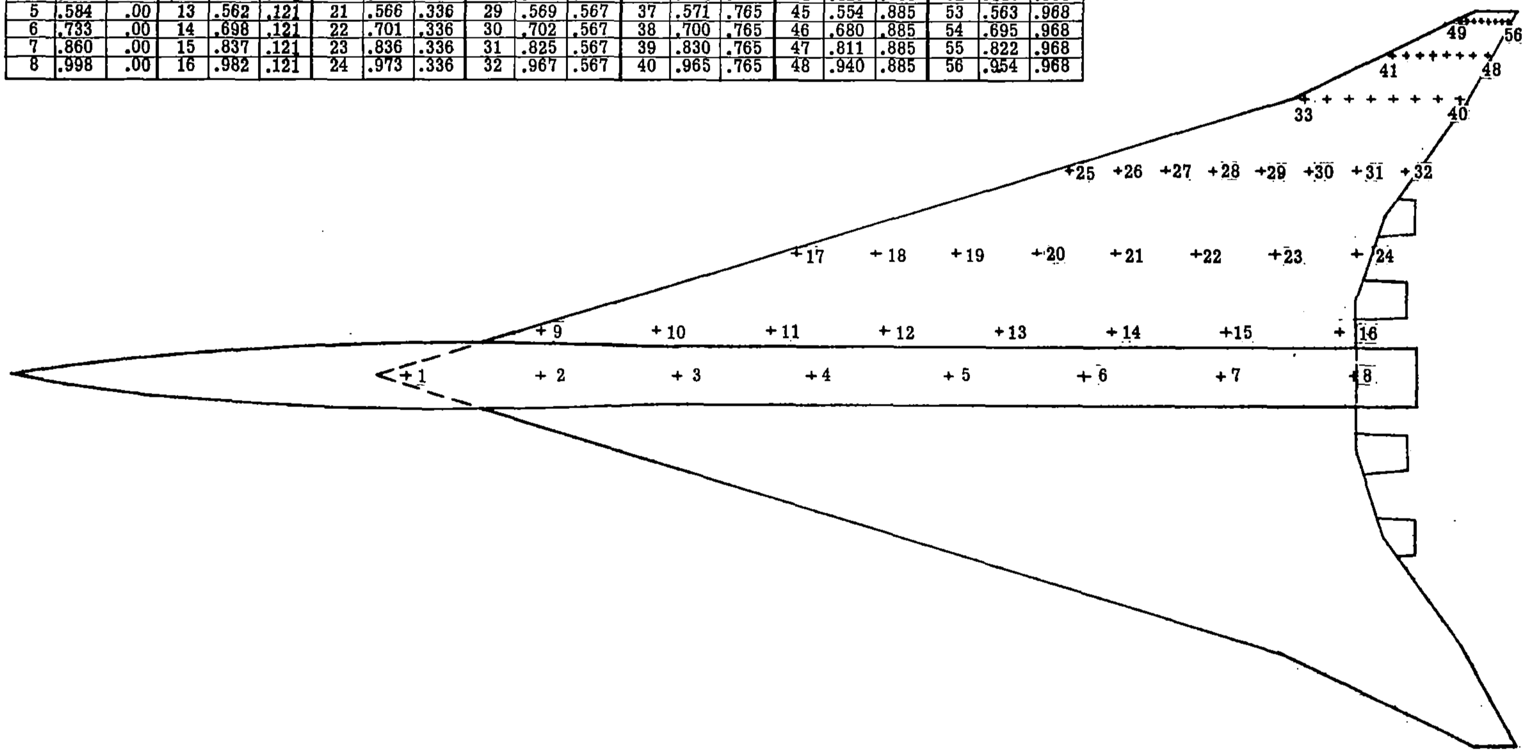

Figure 6.- Model control points for vibration test.

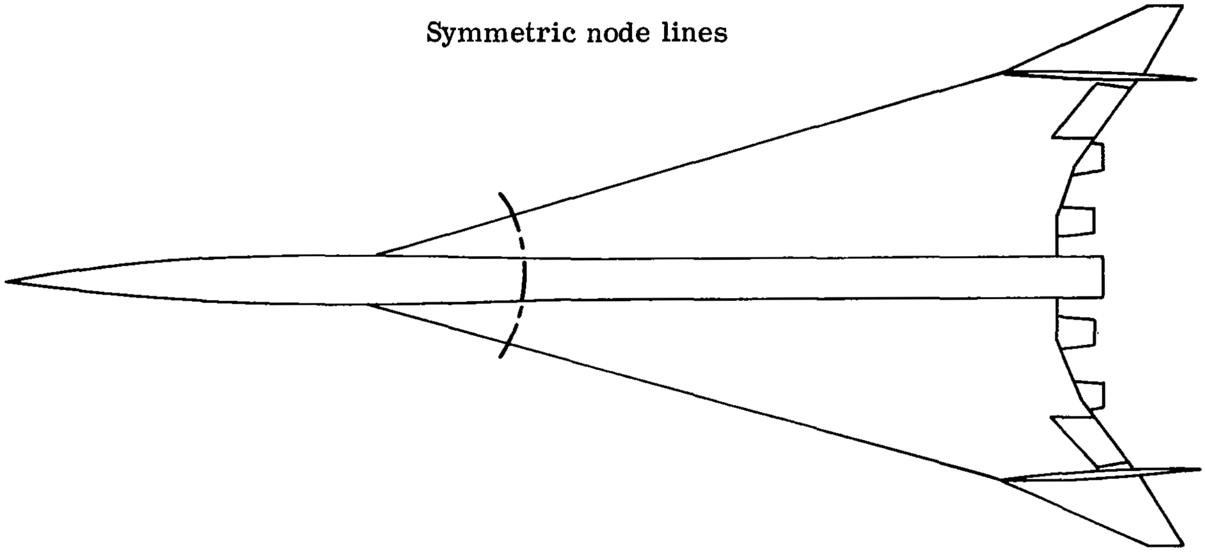

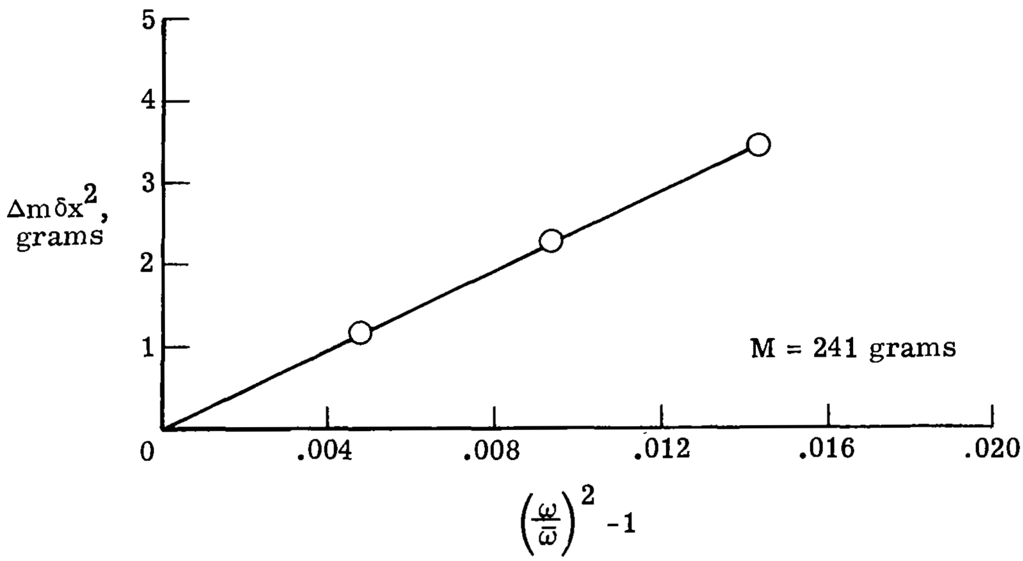

(a) ω = 27.19 hertz.

Figure 7.- Determination of generalized mass and node lines of flexible model.

Symmetric node lines

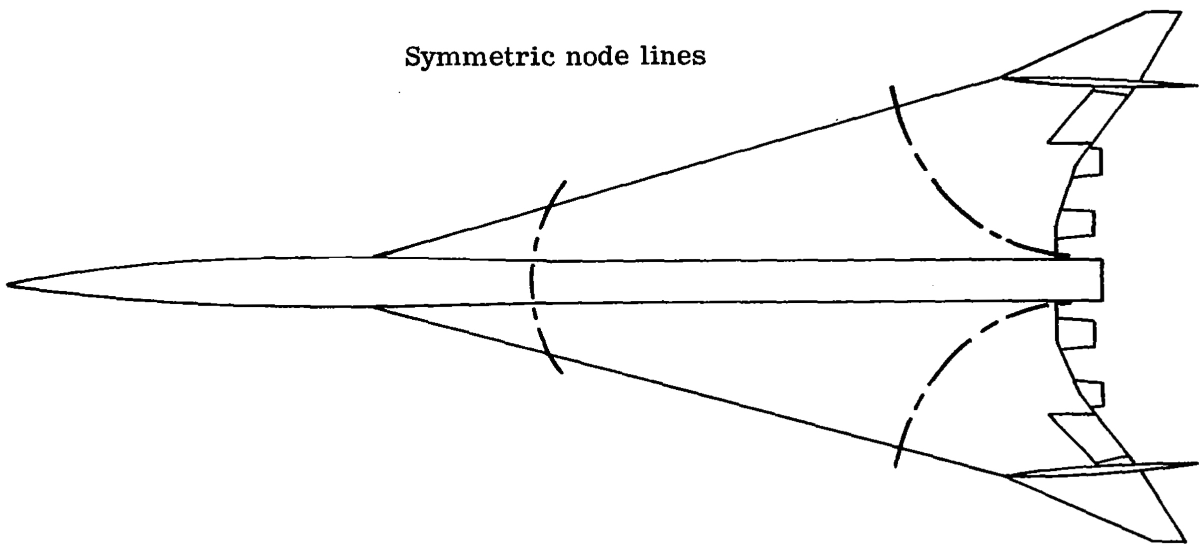

Generalized mass

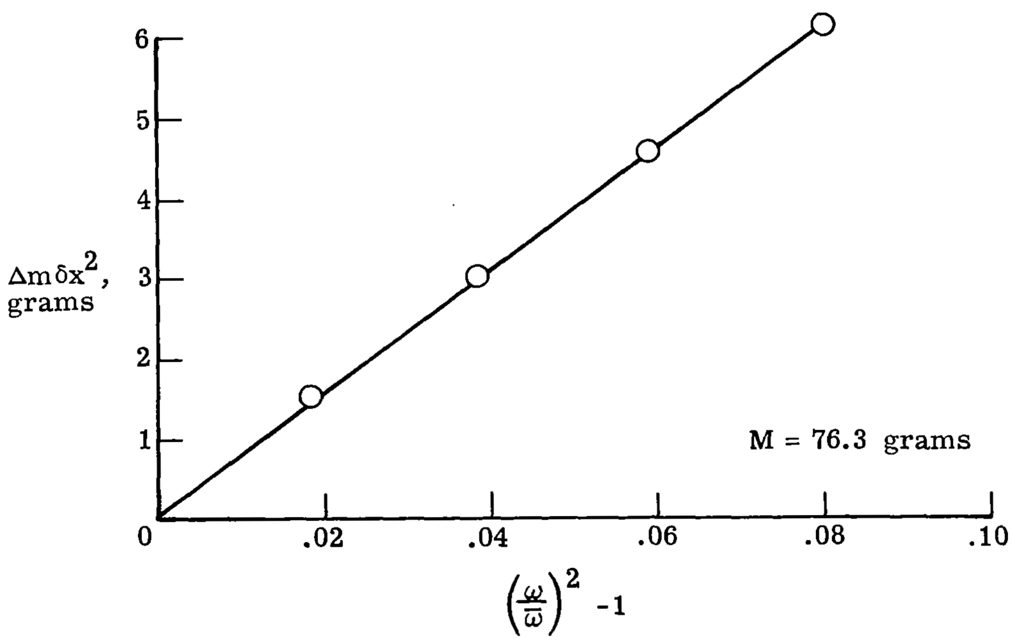

(b) ω = 42.87 hertz.

Figure 7.- Continued.

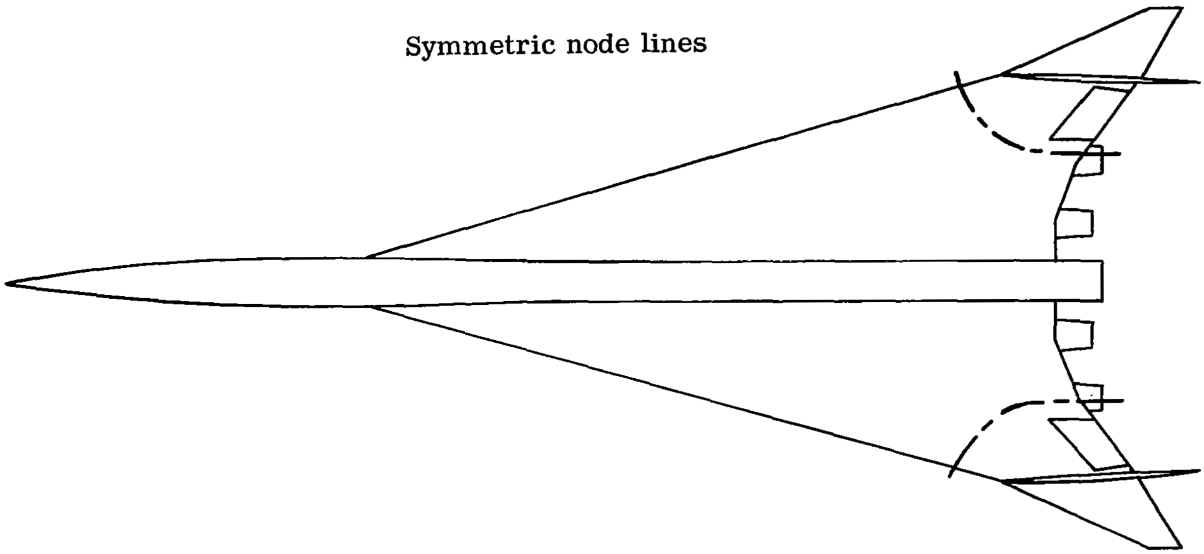

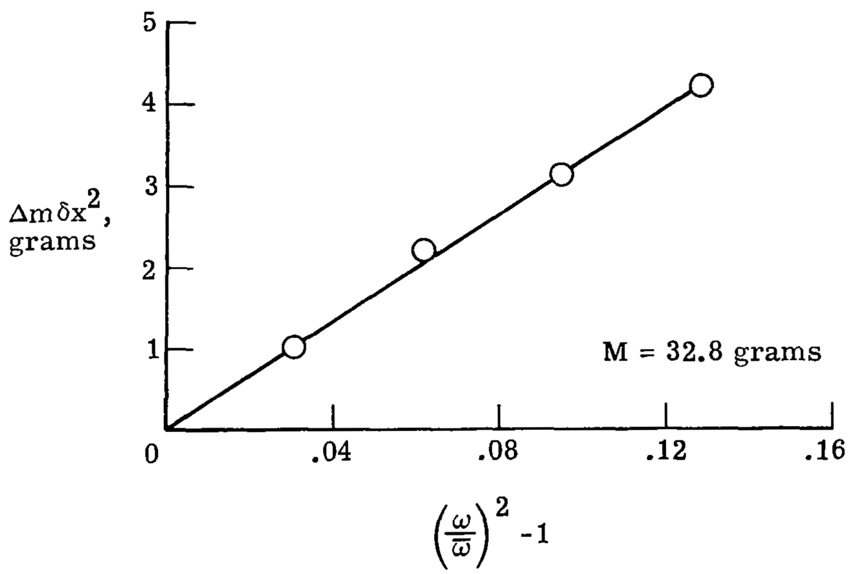

(c) ω = 68.21 hertz.

Figure 7.- Continued.

Symmetric node lines

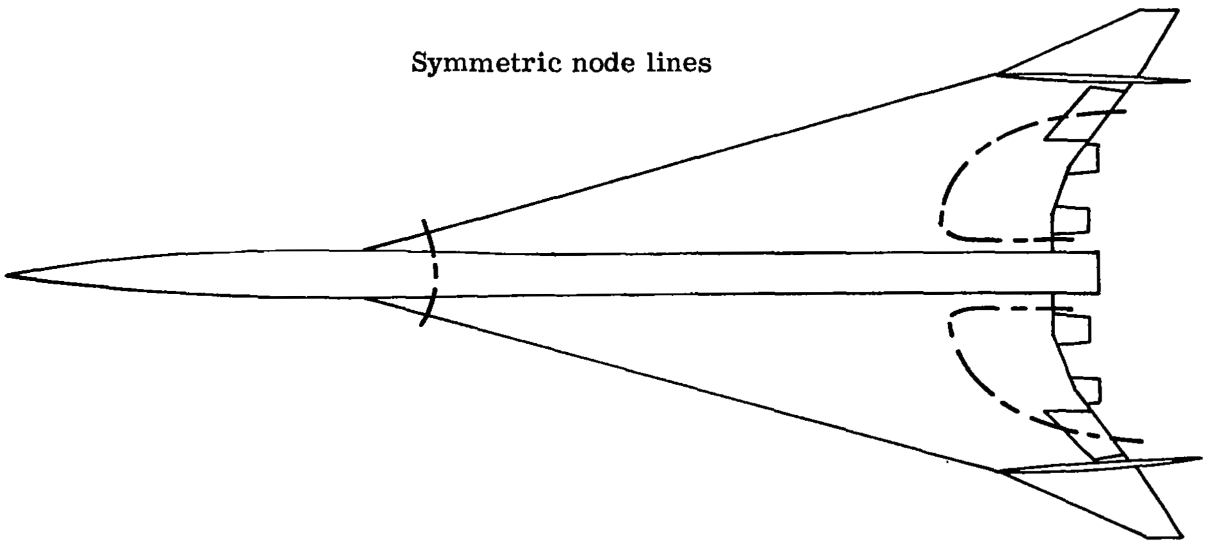

Generalized mass

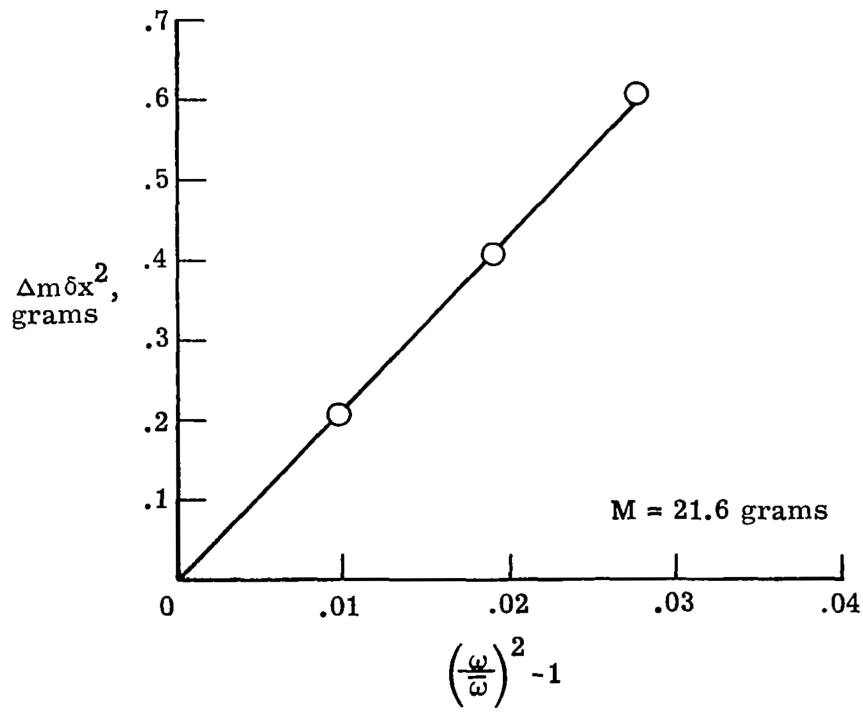

(d) ω = 103.09 hertz.

Figure 7.- Continued.

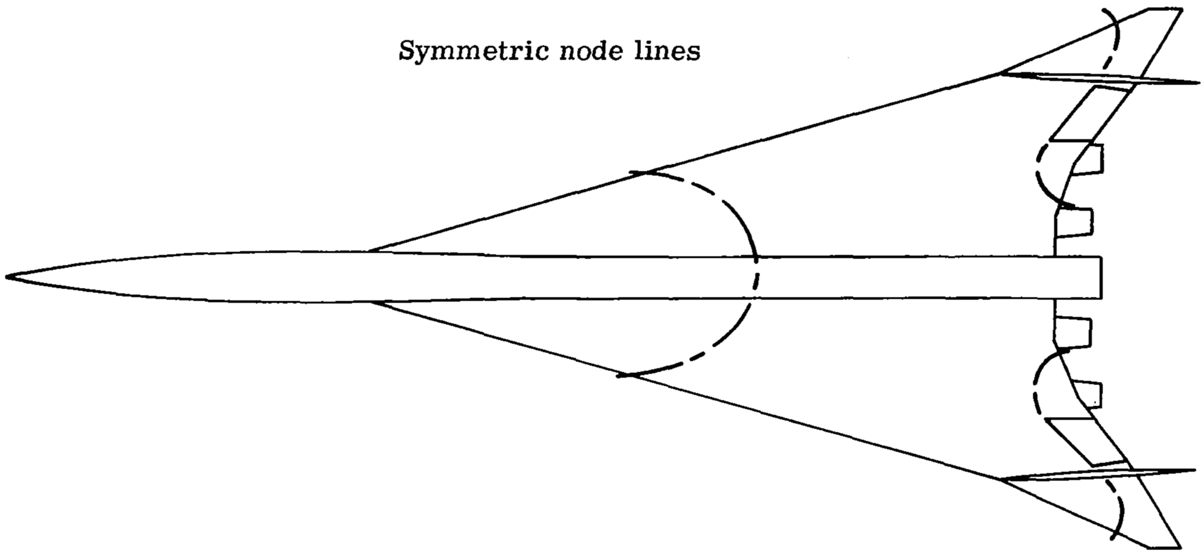

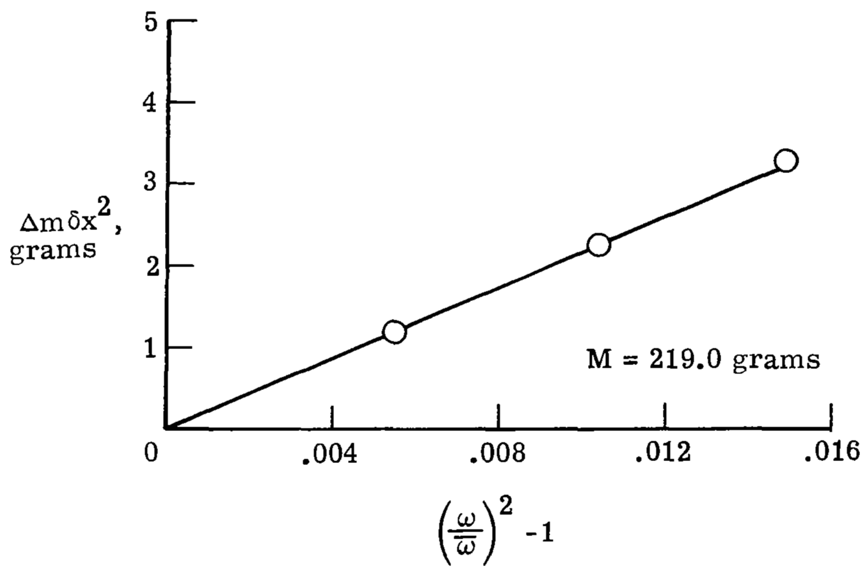

(e) ω = 148.65 hertz.

Figure 7.- Concluded.

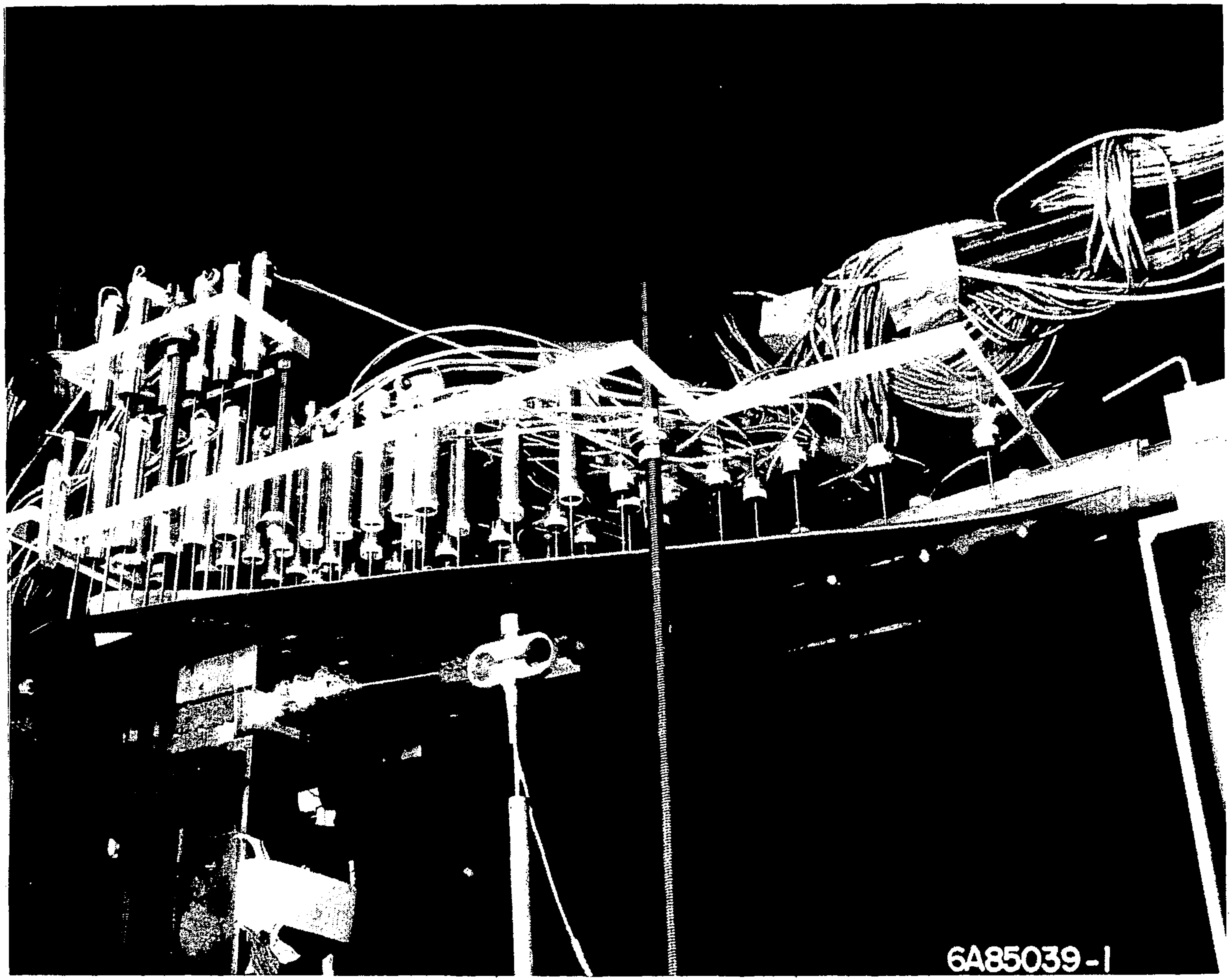

L-72-130

Figure 8.- Test setup for measuring structural influence coefficients.

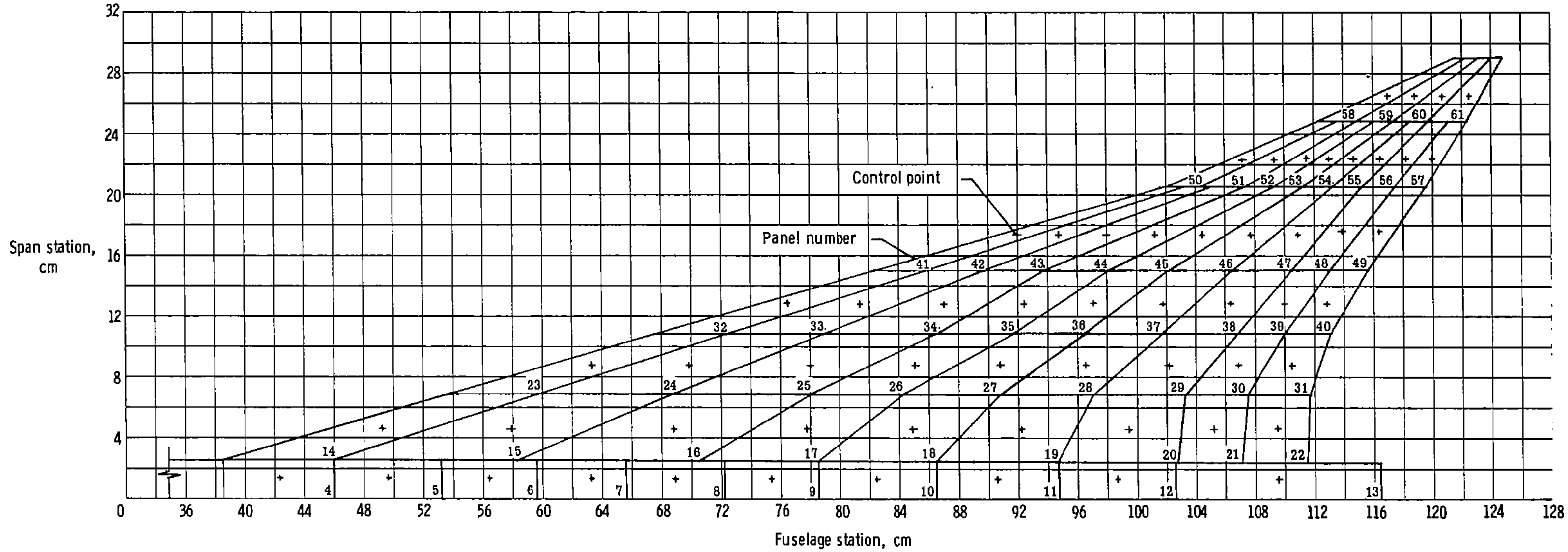

Figure 9.- Control-point location and paneling scheme for influence-coefficient analysis.

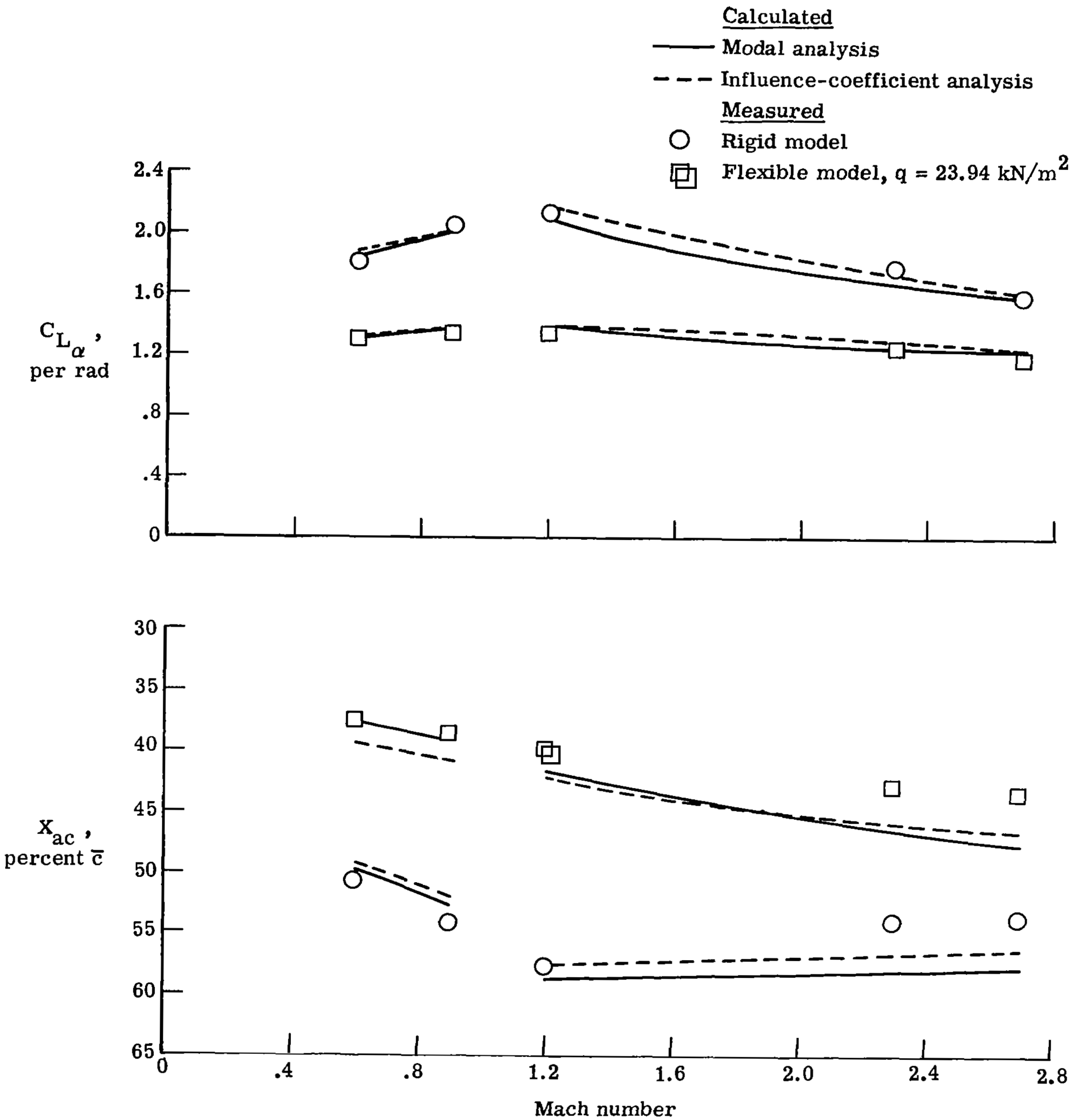

Figure 10.- Variation of lift-curve slope and aerodynamic center with Mach number.

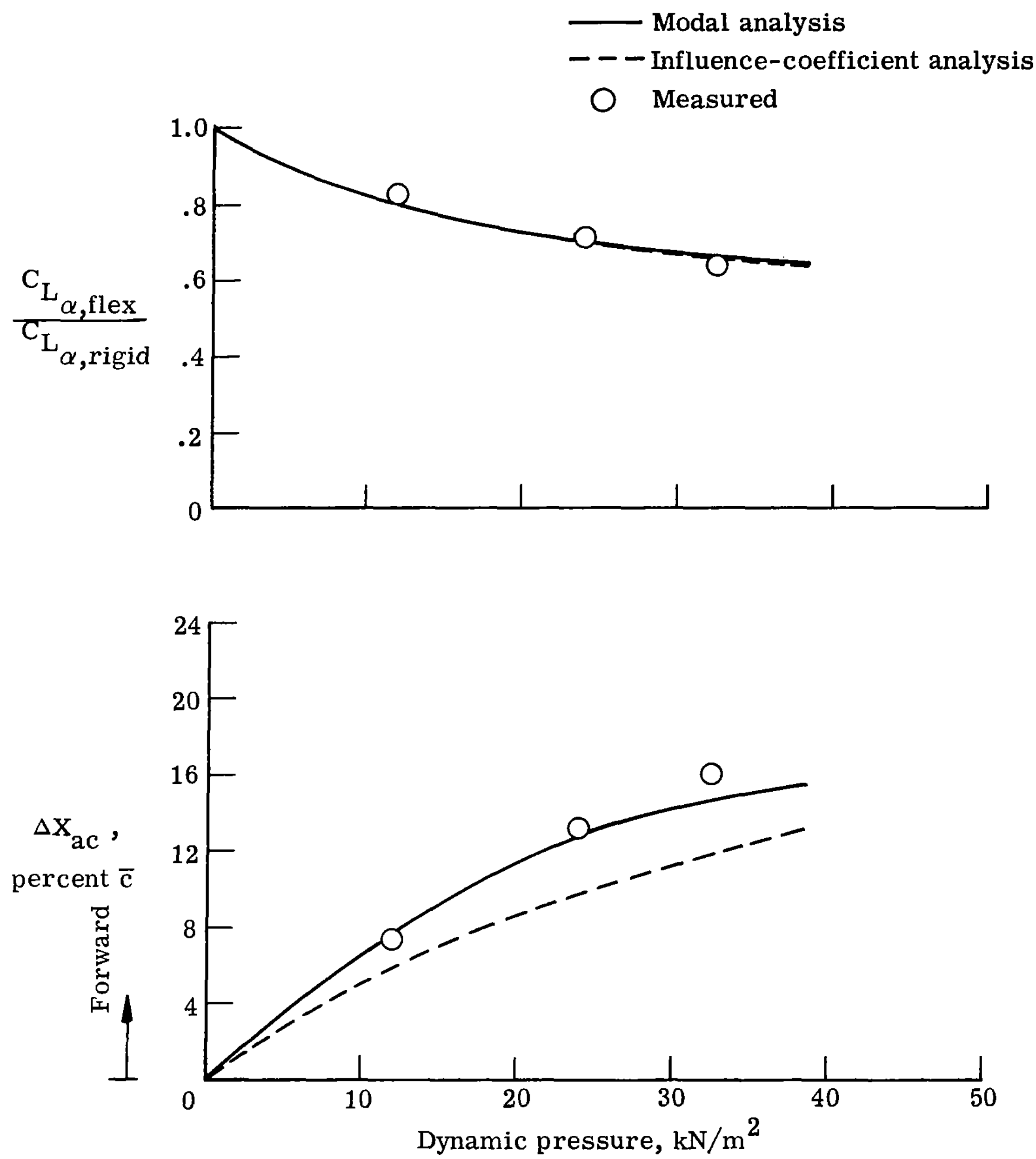

(a) M = 0.6.

Figure 11.- Effect of dynamic pressure on measured and calculated flexible-to-rigid C_{L_α} and aerodynamic-center movement.

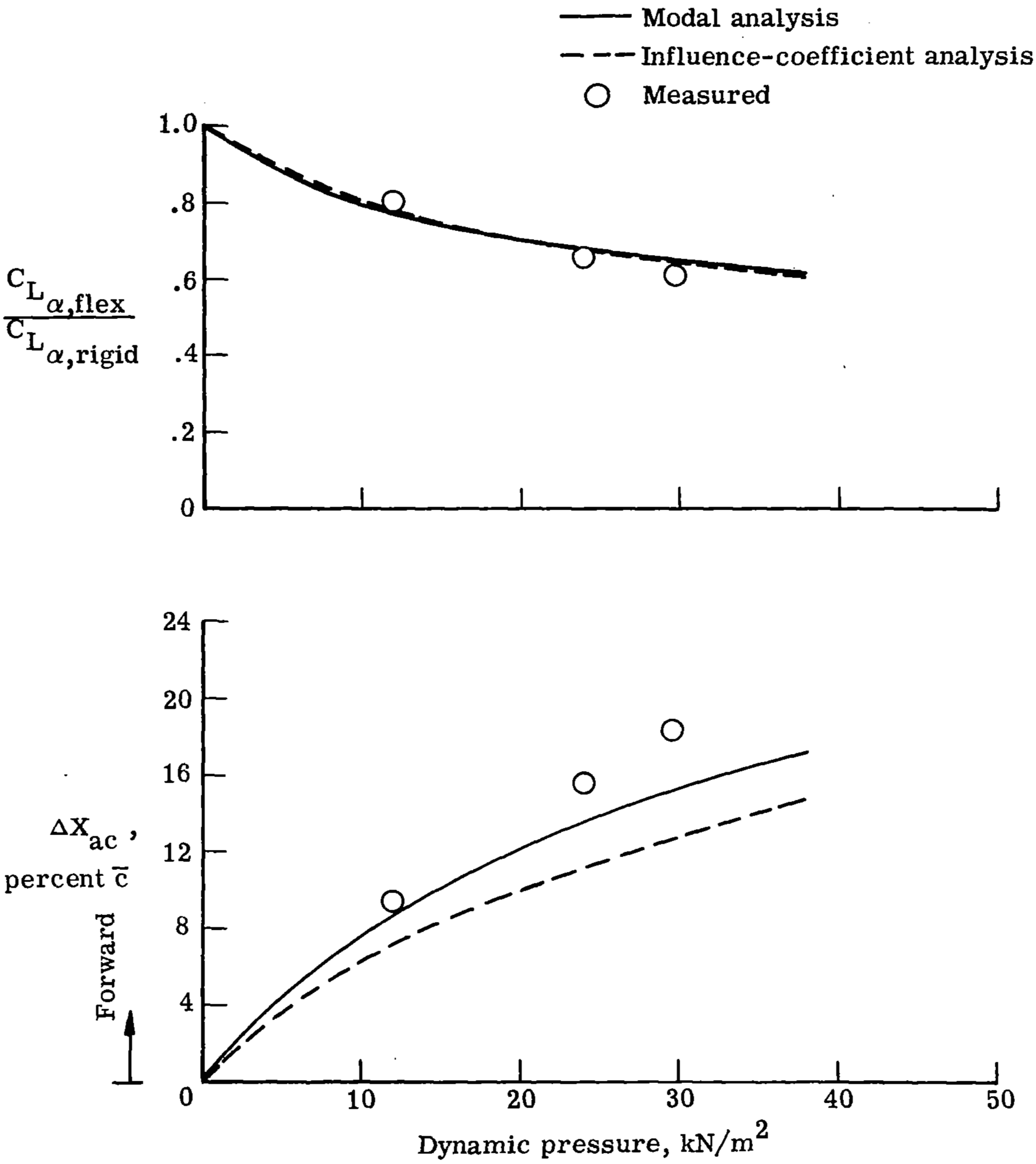

(b) M = 0.9.

Figure 11.- Continued.

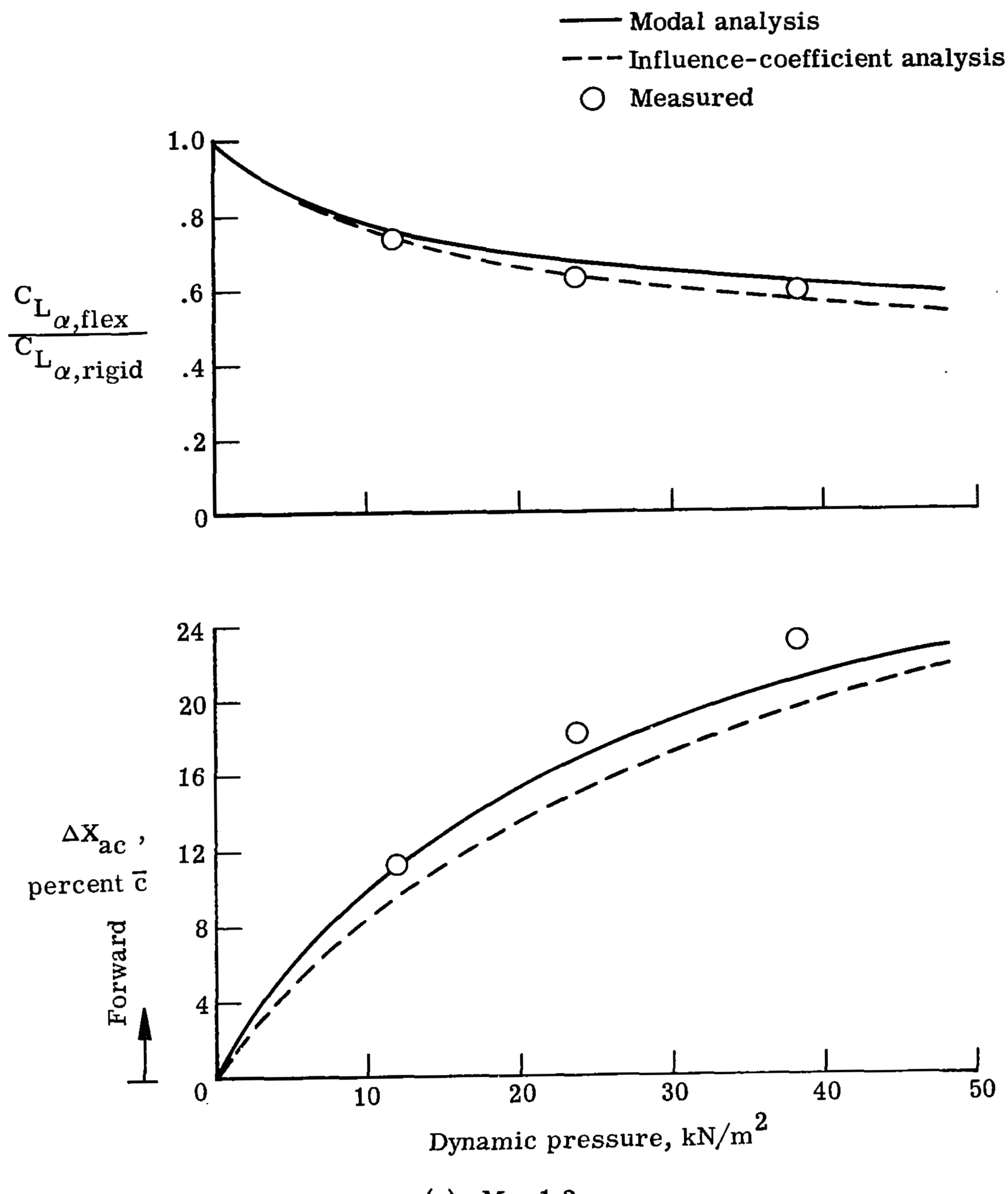

(c) M = 1.2.

Figure 11.- Continued.

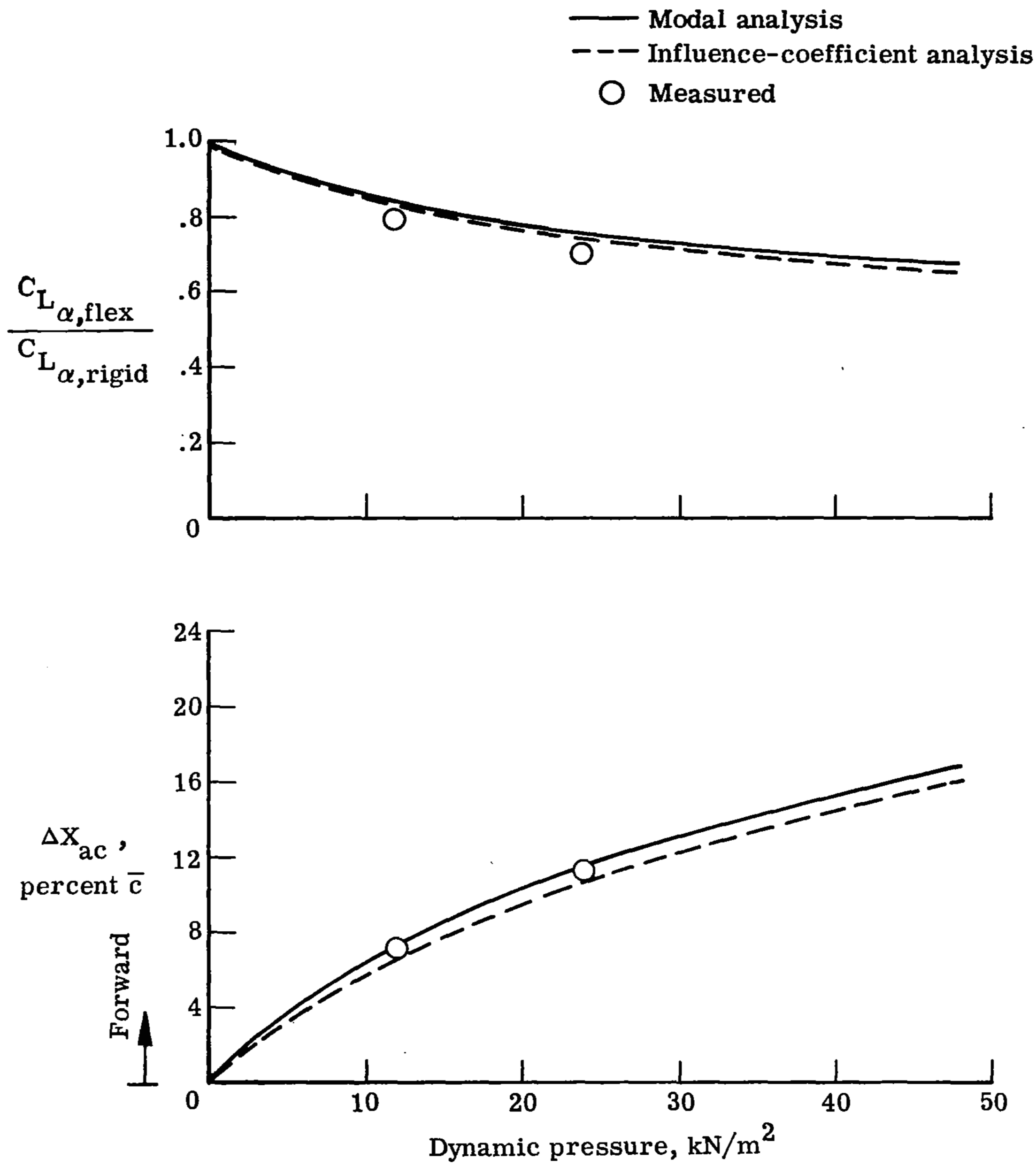

(d) M = 2.3.

Figure 11.- Continued.

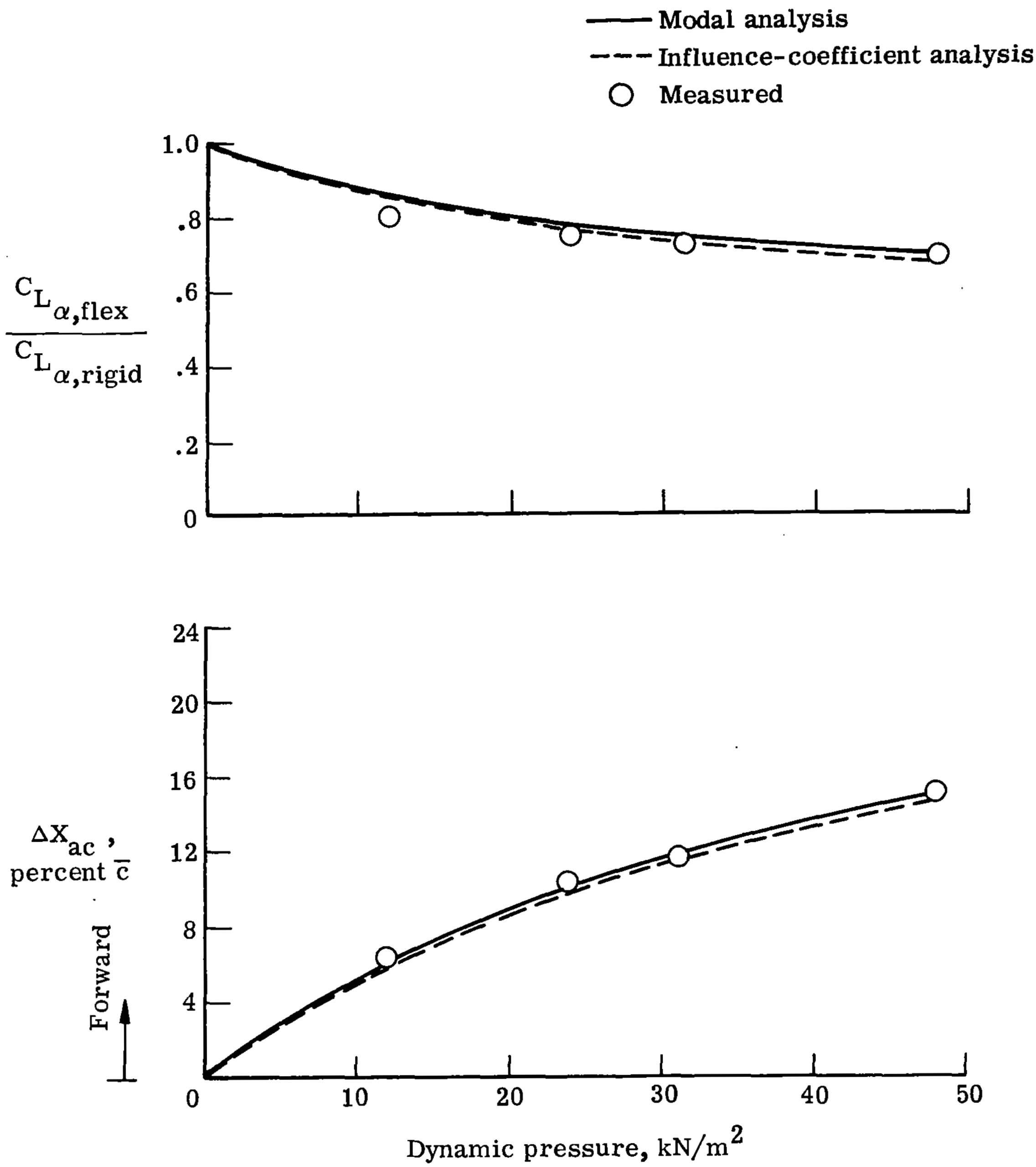

(e) M = 2.7.

Figure 11.- Concluded.

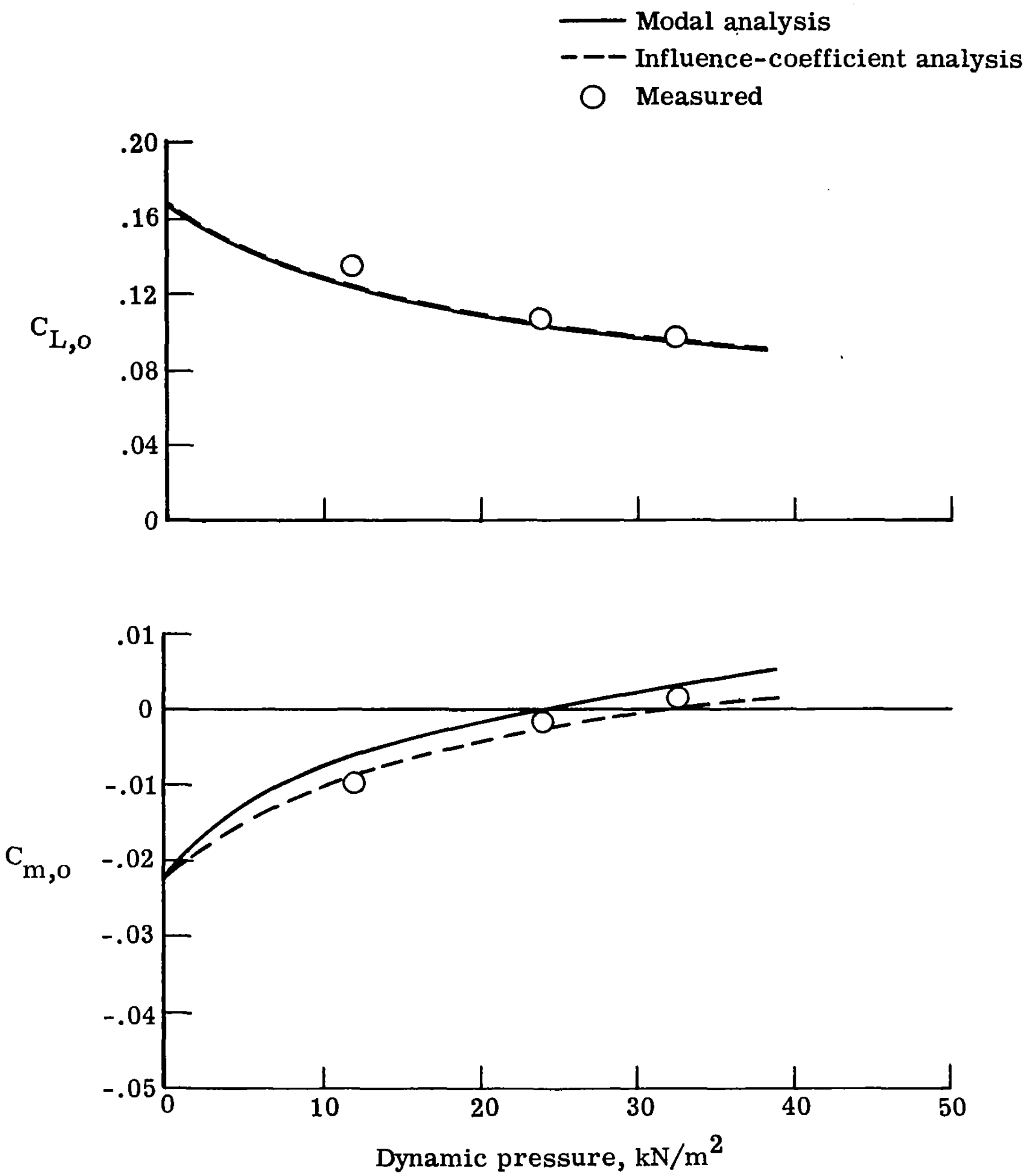

(a) M = 0.6.

Figure 12.- Effect of dynamic pressure on measured and calculated $C_{L,o}$ and $C_{m,o}$.

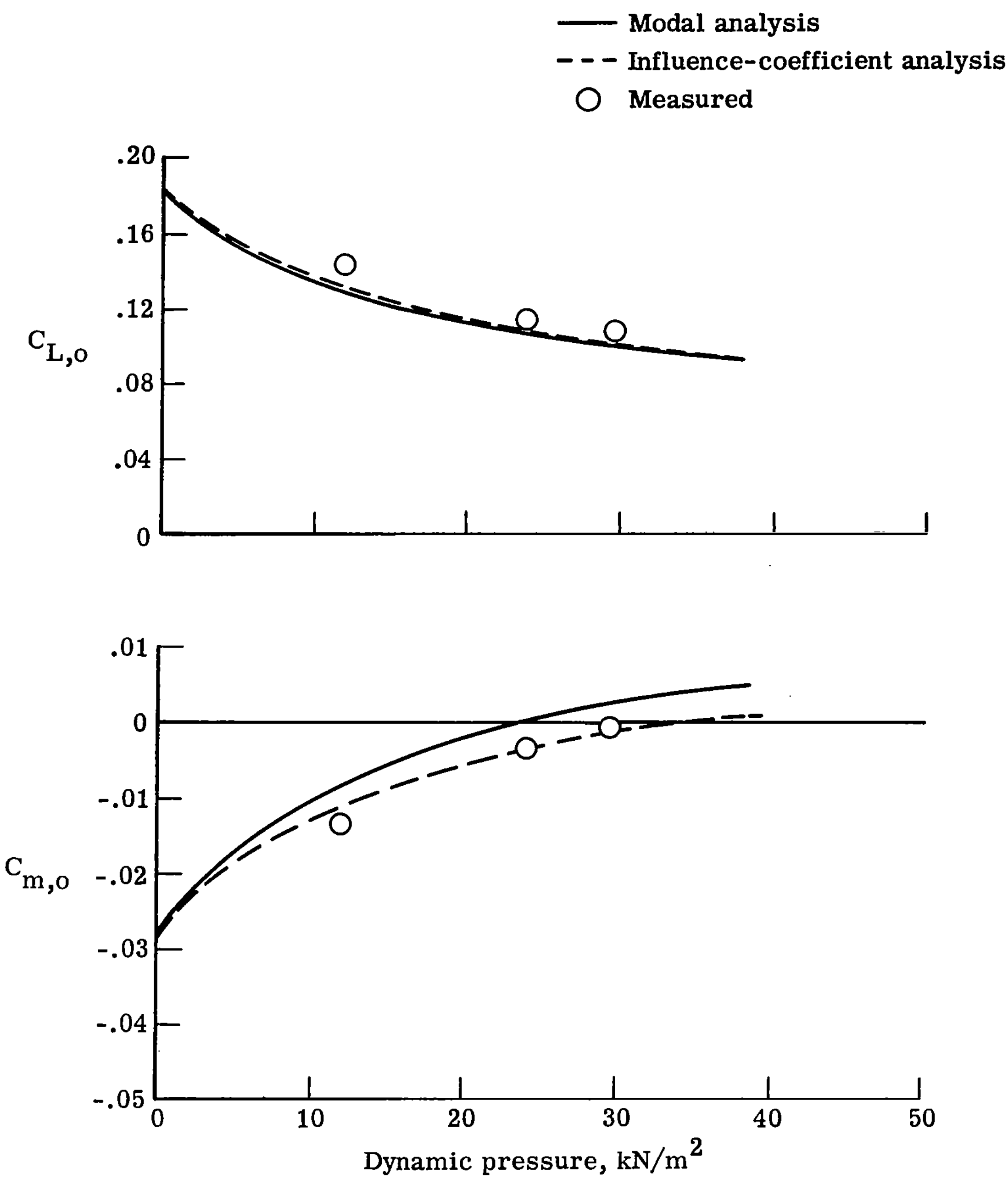

(b) M = 0.9.

Figure 12.- Continued.

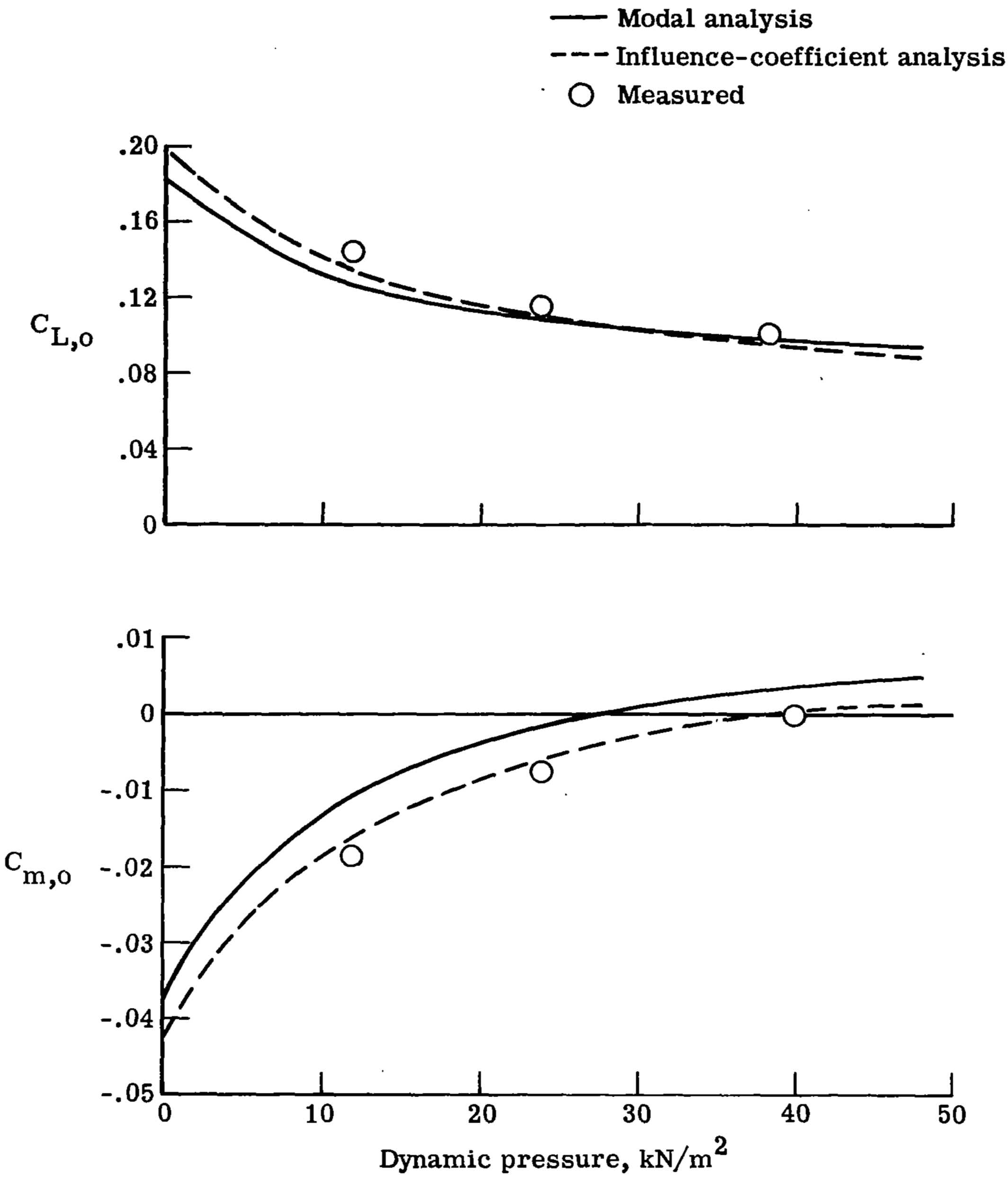

(c) M = 1.2.

Figure 12.- Continued.

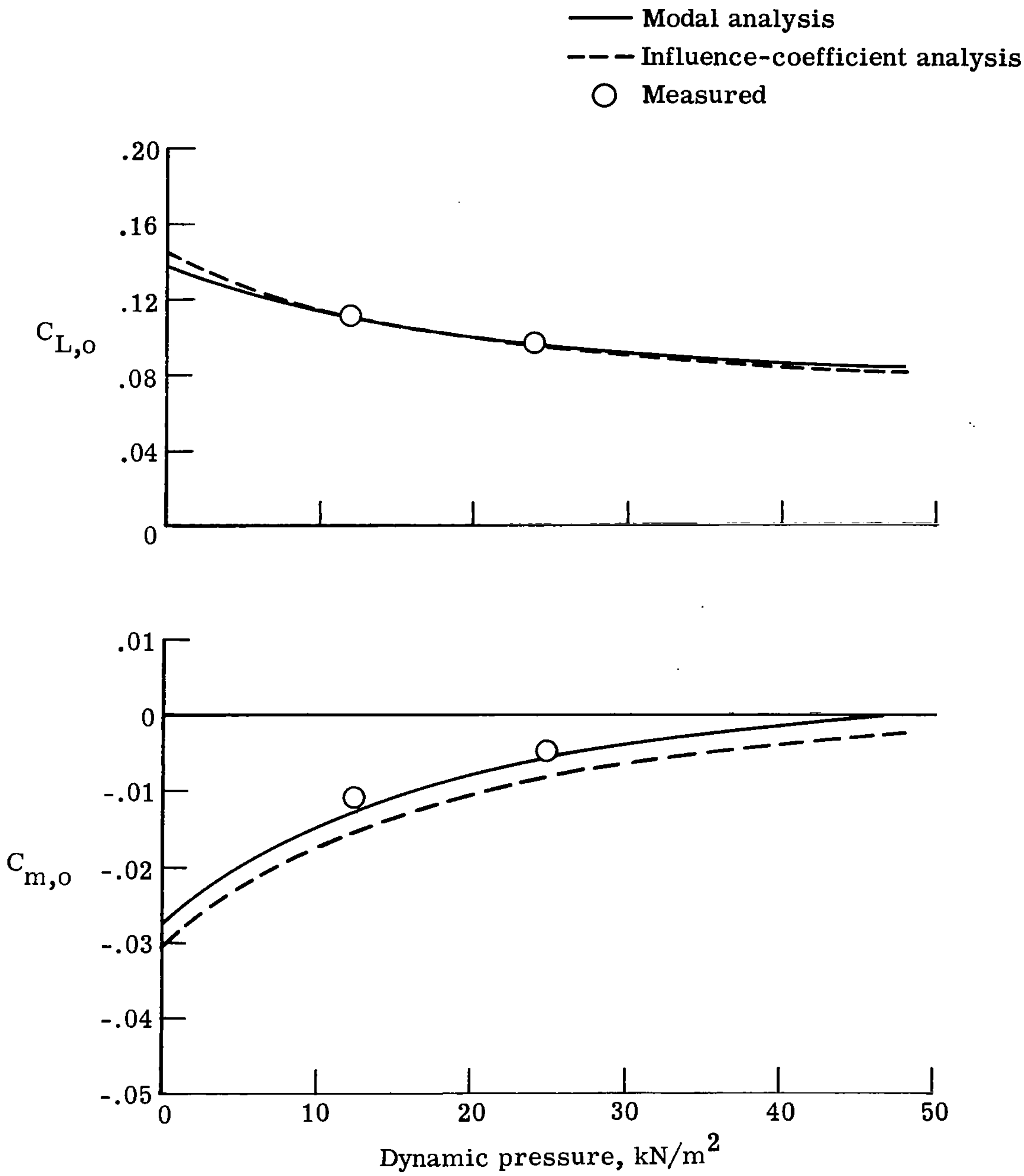

(d) M = 2.3.

Figure 12.- Continued.

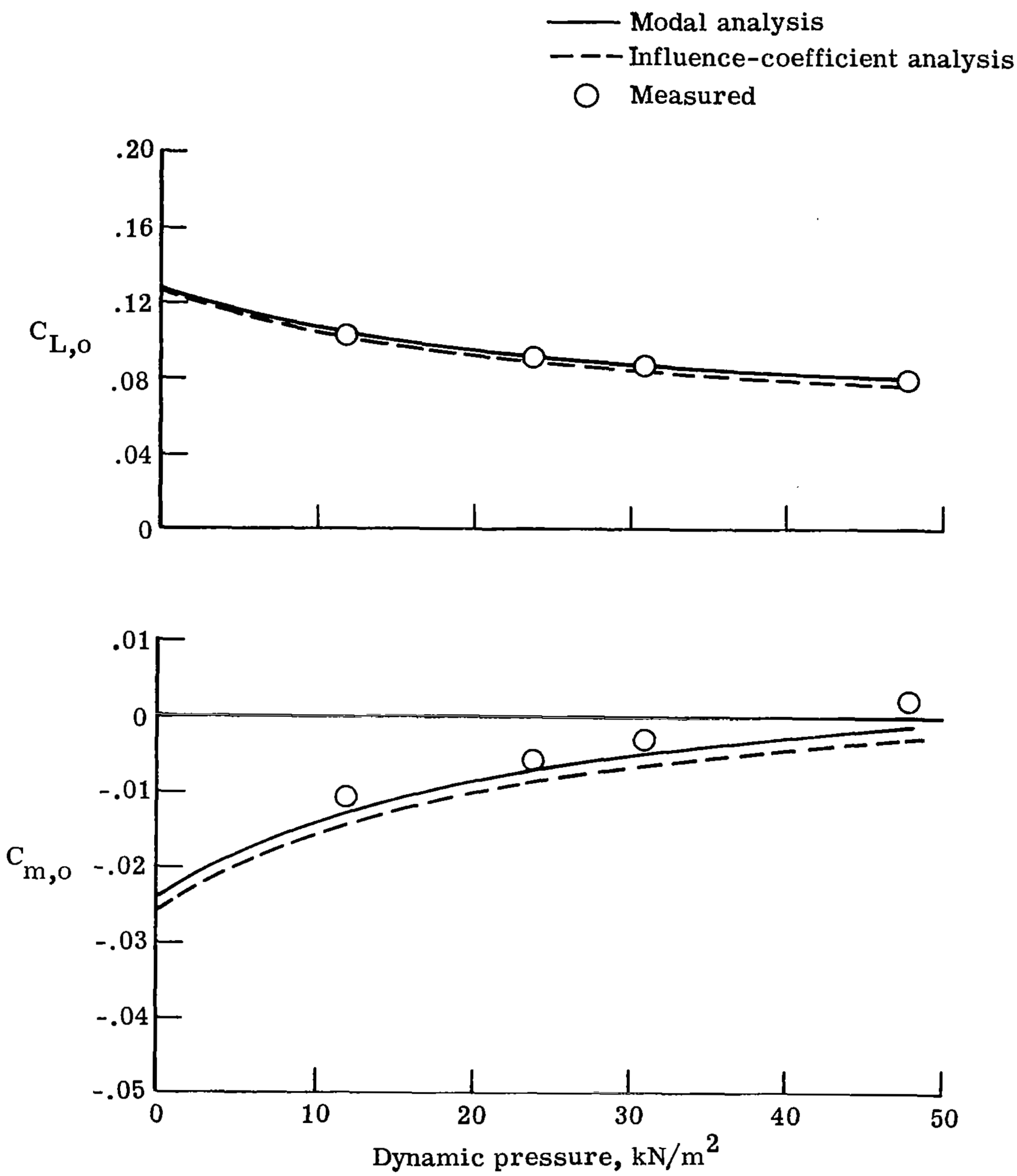

(e) M = 2.7.

Figure 12.- Concluded.

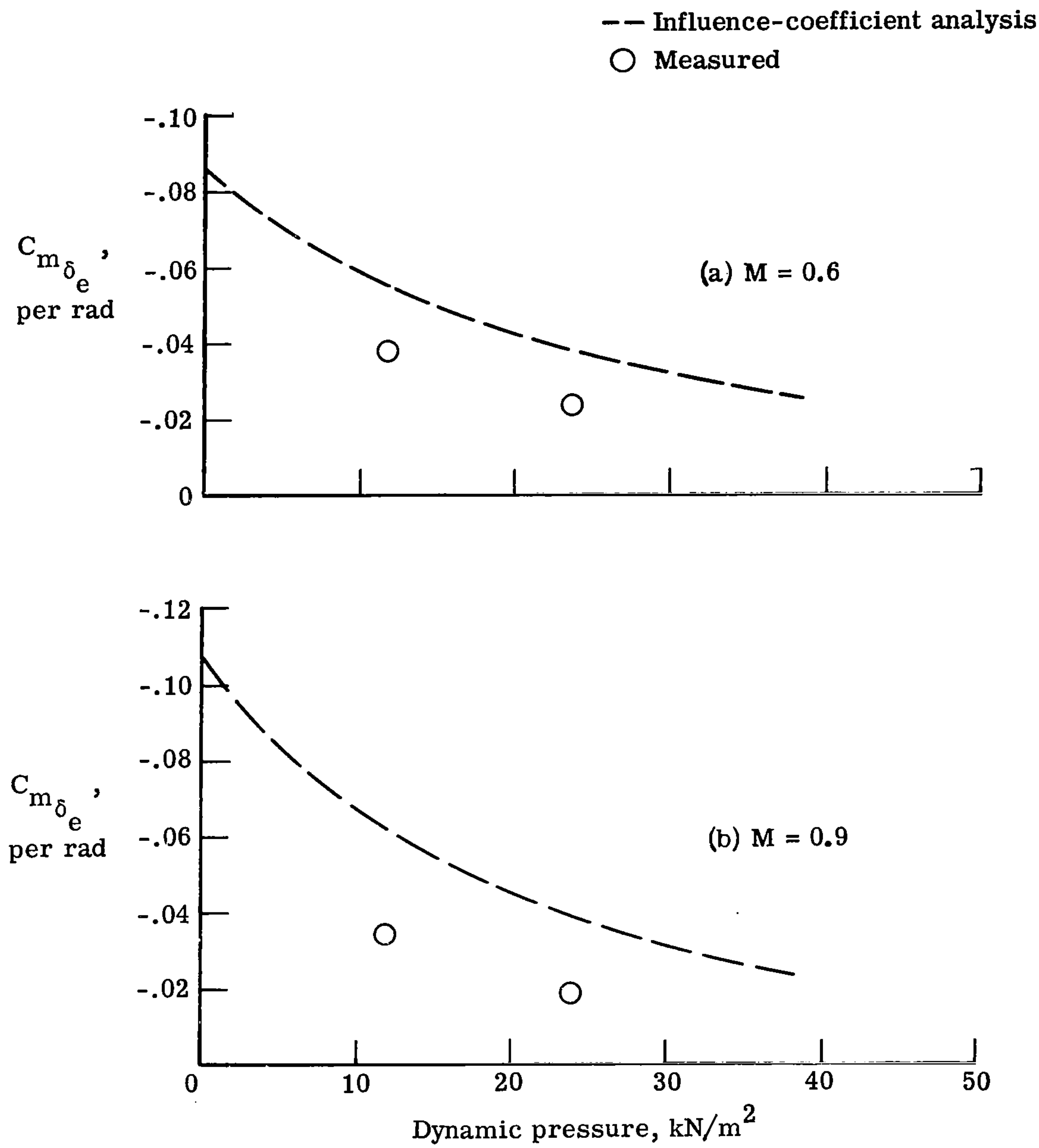

Figure 13.- Effect of dynamic pressure on pitch-control effectiveness.

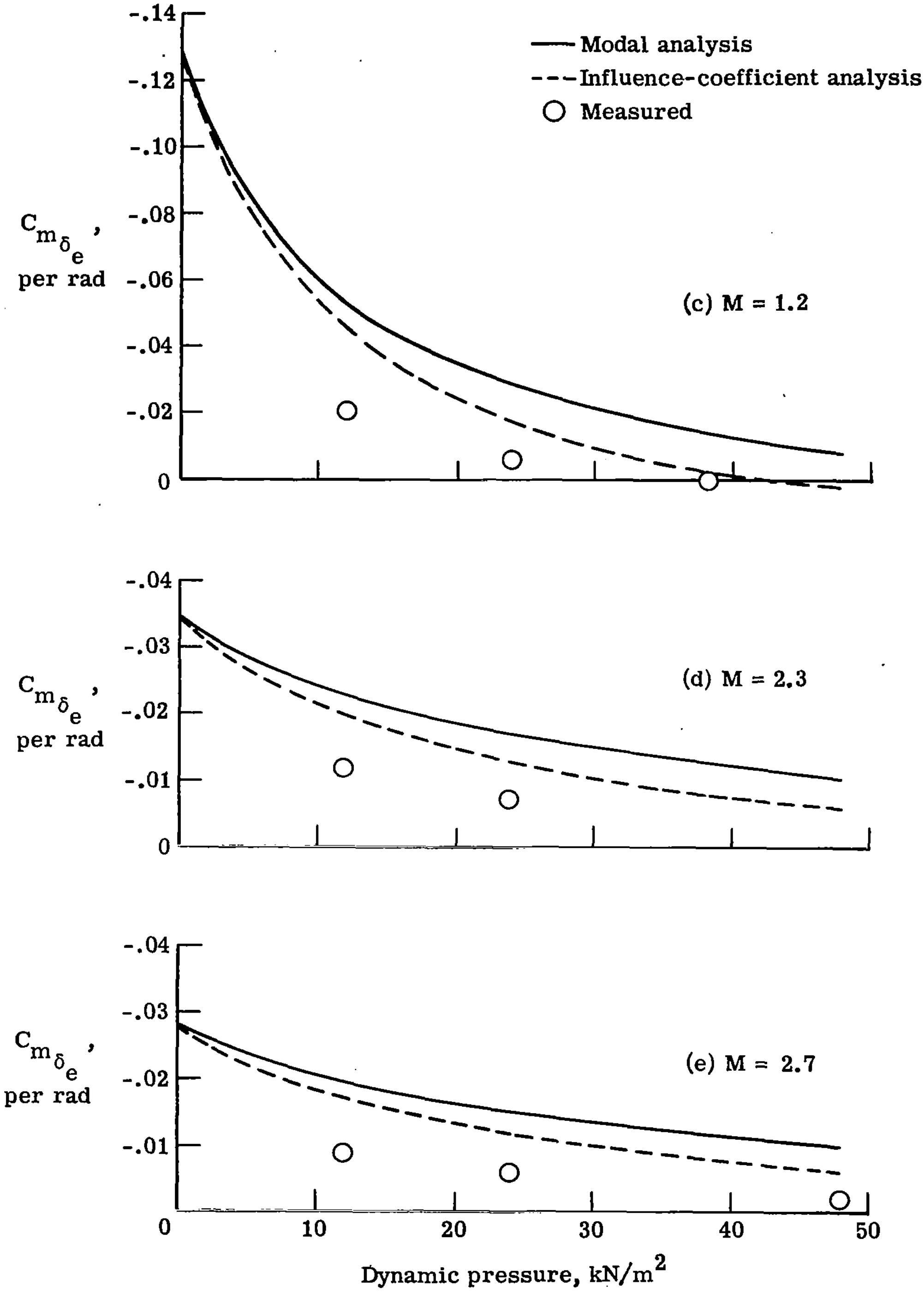

Figure 13.- Concluded.

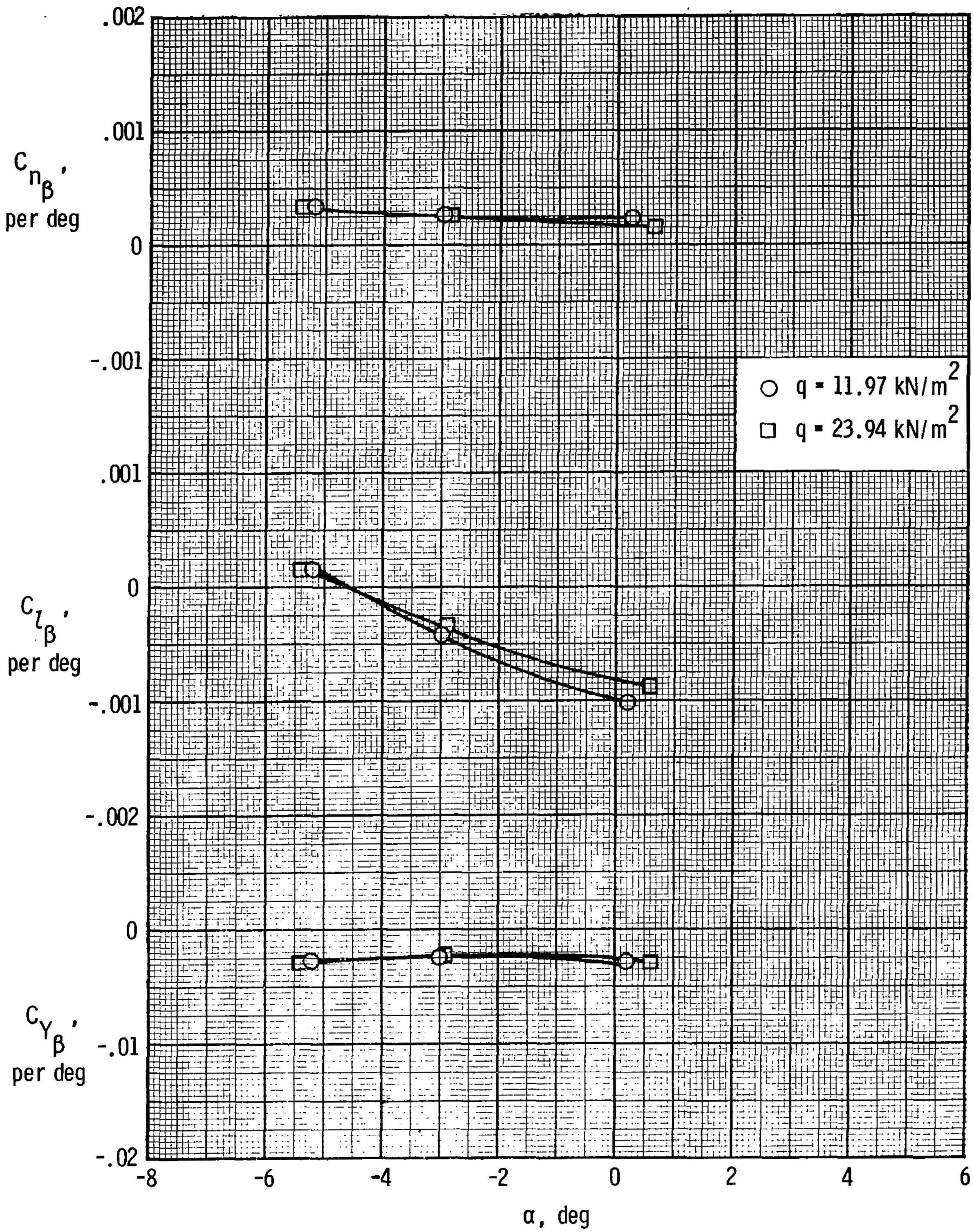

(a) M = 0.6.

Figure 14.- Effect of dynamic pressure on lateral-directional stability derivatives.

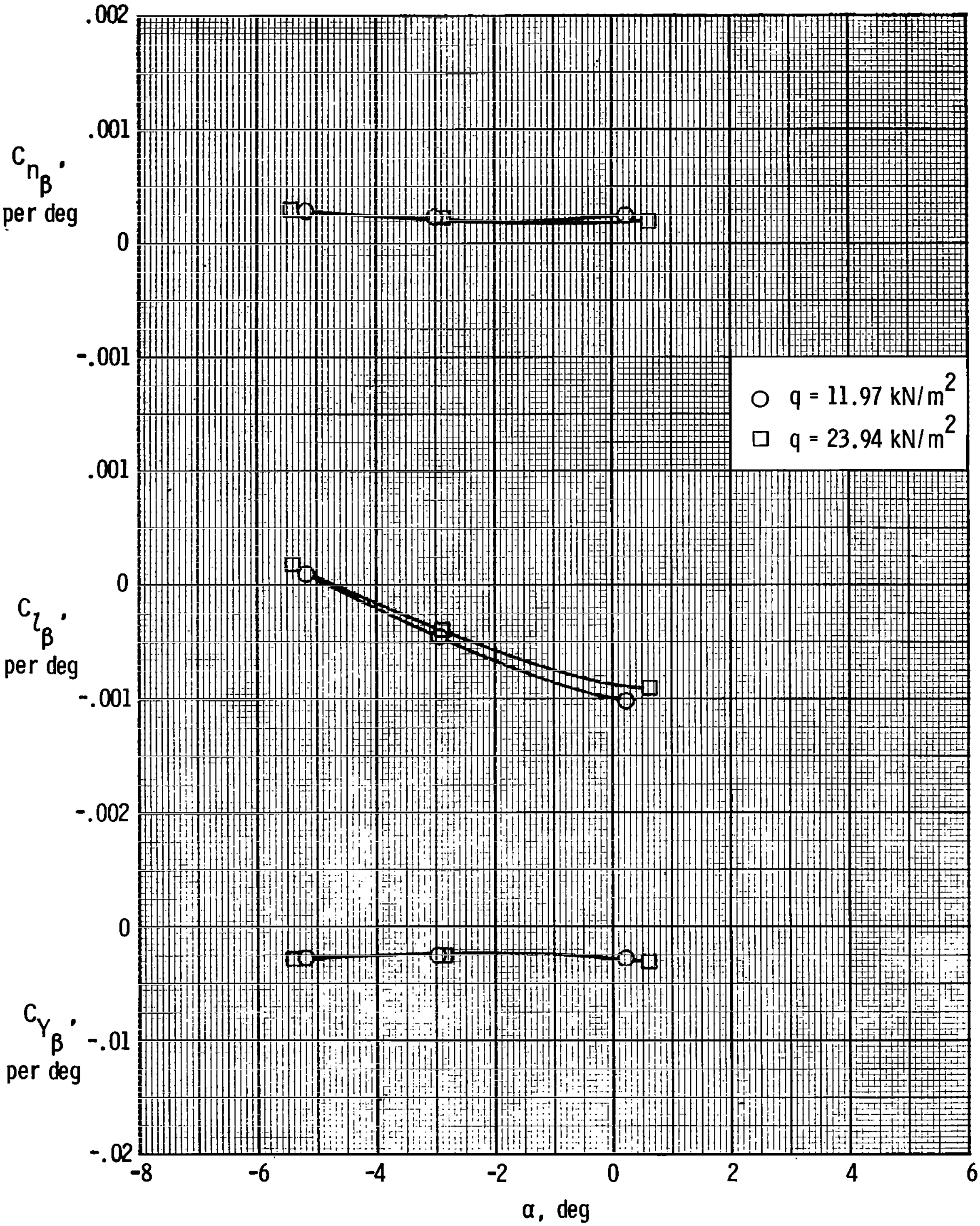

(b) M = 0.9.

Figure 14.- Continued.

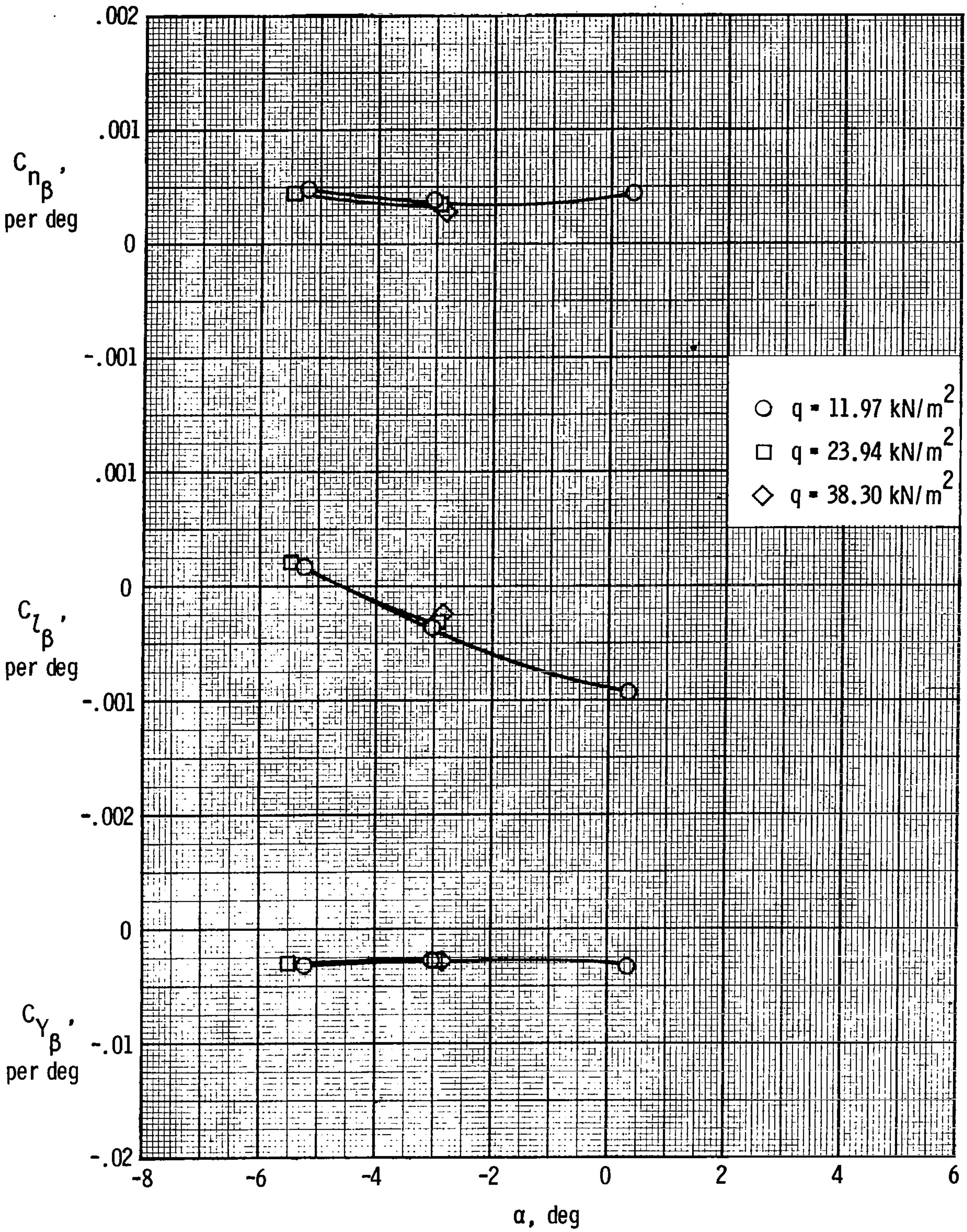

(c) M = 1.2.

Figure 14.- Continued.

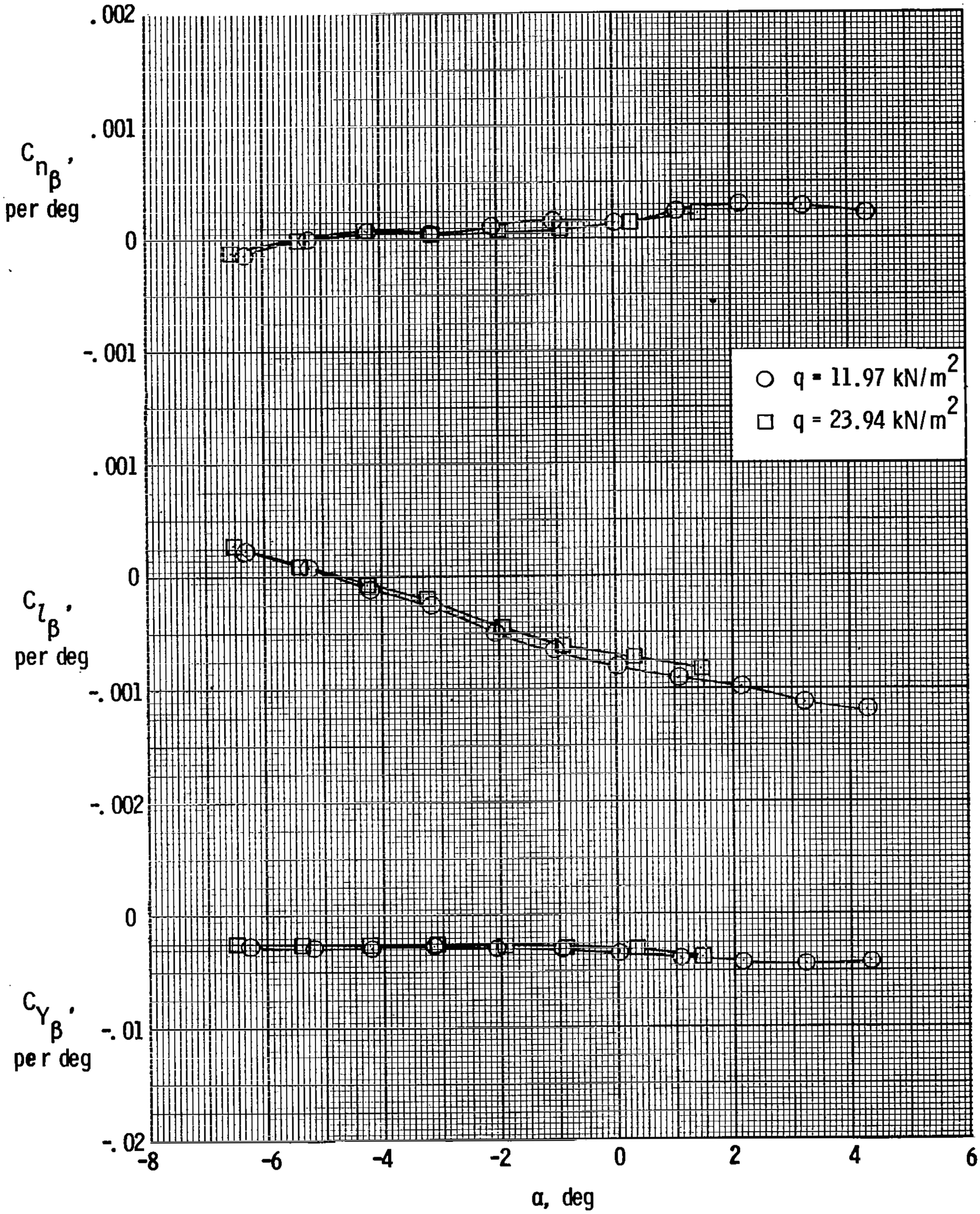

(d) M = 2.3.

Figure 14.- Continued.

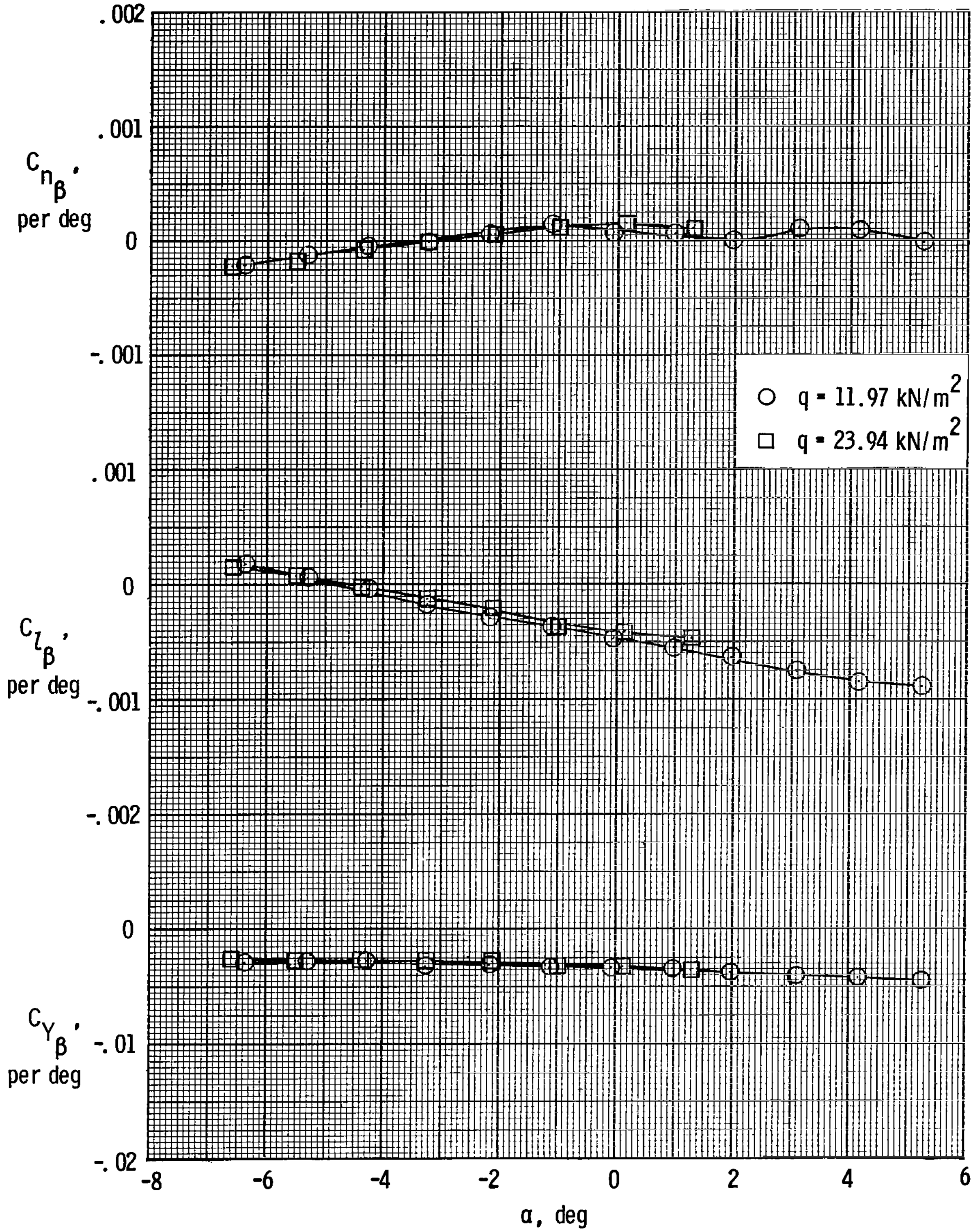

(e) M = 2.7.

Figure 14.- Concluded.

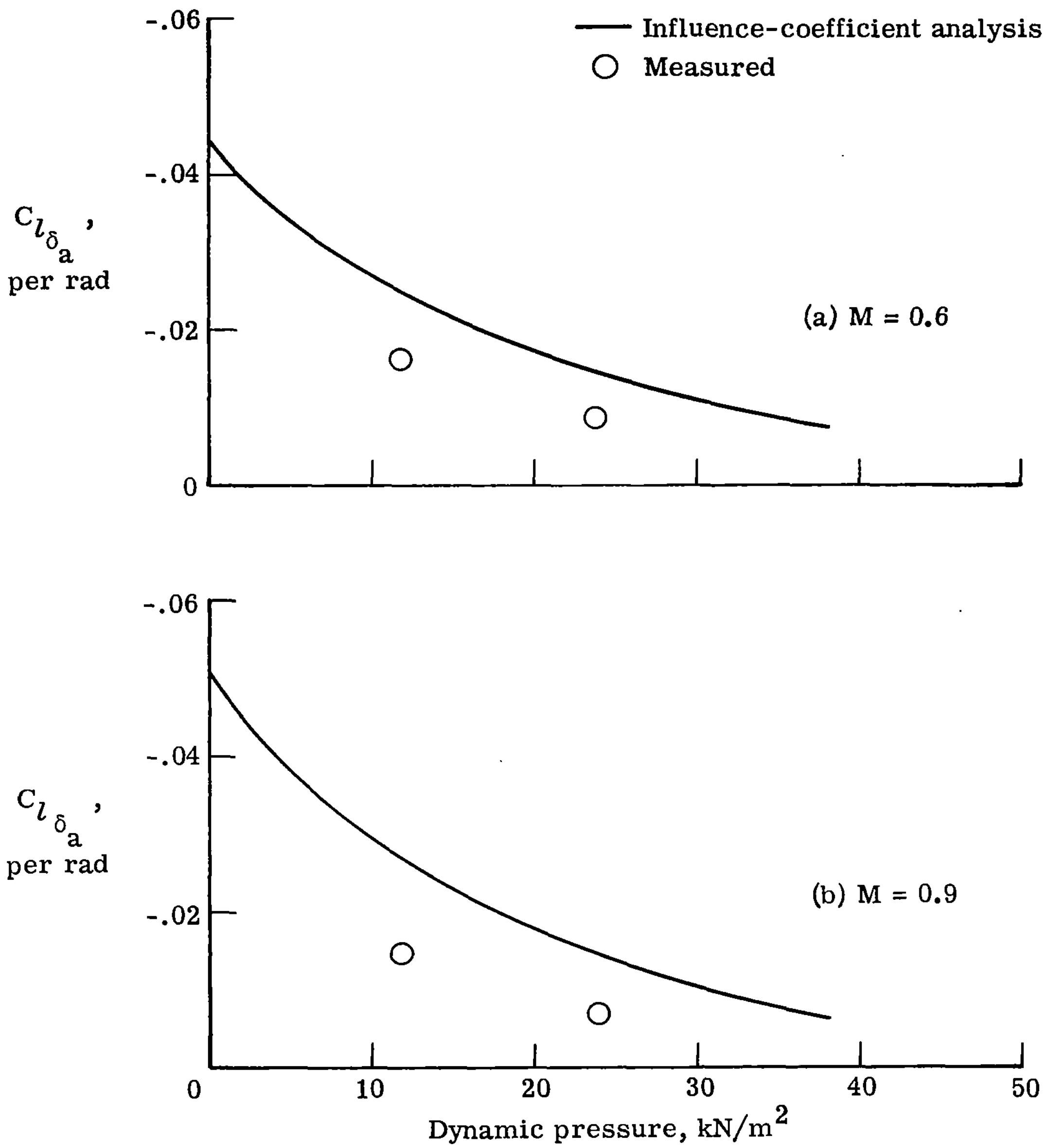

Figure 15.- Effect of dynamic pressure on control-surface effectiveness in roll.

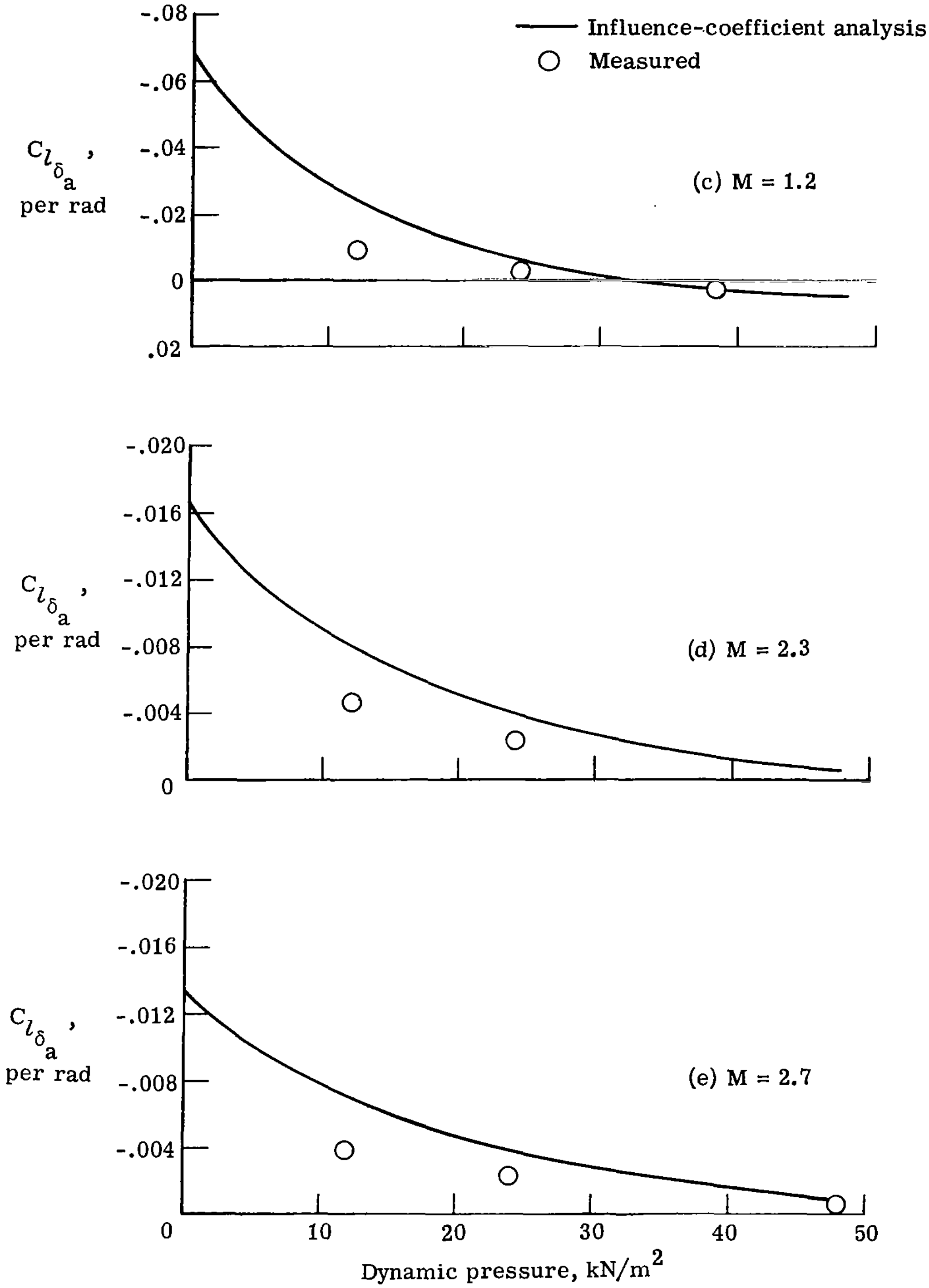

Figure 15.- Concluded.

NASA-Langley, 1972 — 1 L-8105

NATIONAL AERONAUTICS AND SPACE ADMISTRATION
WASHINGTON, D.C. 20546

OFFICIAL BUSINESS
PENALTY FOR PRIVATE USE $300

FIRST CLASS MAIL

POSTAGE AND FEES PAID
NATIONAL AERONAUTICS AND
SPACE ADMINISTRATION

U.S.MAIL

026 001 C1 U 01 720317 S00903DS
DEPT OF THE AIR FORCE
AF WEAPONS LAB (AFSC)
TECH LIBRARY/WLOL/
ATTN: E LOU BOWMAN, CHIEF
KIRTLAND AFB NM 87117

POSTMASTER: If Undeliverable (Section 158 Postal Manual) Do Not Return

---

"The aeronautical and space activities of the United States shall be conducted so as to contribute . . . to the expansion of human knowledge of phenomena in the atmosphere and space. The Administration shall provide for the widest practicable and appropriate dissemination of information concerning its activities and the results thereof."

—NATIONAL AERONAUTICS AND SPACE ACT OF 1958

NASA SCIENTIFIC AND TECHNICAL PUBLICATIONS

TECHNICAL REPORTS: Scientific and technical information considered important, complete, and a lasting contribution to existing knowledge.

TECHNICAL NOTES: Information less broad in scope but nevertheless of importance as a contribution to existing knowledge.

TECHNICAL MEMORANDUMS: Information receiving limited distribution because of preliminary data, security classification, or other reasons.

CONTRACTOR REPORTS: Scientific and technical information generated under a NASA contract or grant and considered an important contribution to existing knowledge.

TECHNICAL TRANSLATIONS: Information published in a foreign language considered to merit NASA distribution in English.

SPECIAL PUBLICATIONS: Information derived from or of value to NASA activities. Publications include conference proceedings, monographs, data compilations, handbooks, sourcebooks, and special bibliographies.

TECHNOLOGY UTILIZATION PUBLICATIONS: Information on technology used by NASA that may be of particular interest in commercial and other non-aerospace applications. Publications include Tech Briefs, Technology Utilization Reports and Technology Surveys.

Details on the availability of these publications may be obtained from:

SCIENTIFIC AND TECHNICAL INFORMATION OFFICE

NATIONAL AERONAUTICS AND SPACE ADMINISTRATION

Washington, D.C. 20546